Evaluation of Sulfidic Materials

in Virginia Highway Corridors

by

Zenah Wilson Orndorff

Dissertation submitted to the Faculty of the

Virginia Polytechnic Institute and State University

in Partial Fulfillment of the requirements for the degree of

Doctor of Philosophy

in

Crop and Soil Environmental Sciences

W. Lee Daniels, Chair
Lucian W. Zelazny
James Craig
Donald Rimstidt
William Carstensen

Sept 10, 2001

Blacksburg, Virginia

Key words: sulfides, highway construction, acid rock drainage, potential acidity, pyrite

Evaluation of Sulfidic Materials in Virginia Highway Corridors

Zenah Wilson Orndorff

(ABSTRACT)

Road construction through sulfidic materials in Virginia has resulted in localized acid rock drainage (ARD) that threatens water quality, fill stability, integrity of building materials, and vegetation management. The objectives of this study were: i) to develop a state-wide sulfide hazard rating map based on characterization of the geologic formations associated with acid roadcuts, ii) to estimate depth to sulfidic sediments in the Coastal Plain based on landscape relationships, and iii) to evaluate potential acidity testing procedures on diverse materials. Geologic formations associated with acid roadcuts were characterized by potential peroxide acidity (PPA) and S content, and grouped into four categories. Listed in order of increasing severity, these formations included: the Tabb Formation (Coastal Plain), the Lynchburg Group of the Ashe Formation (Blue Ridge), the Chesapeake Group and Lower Tertiary deposits (Coastal Plain), the Millboro shale, Marcellus shale, Chatanooga shale and Needmore Formation (Valley and Ridge), and the Quantico Formation (Piedmont). Evaluation of landscape parameters near Richmond, Virginia, indicated that the likelihood of encountering sulfidic materials within a given depth at a specific location was related to elevation and mapped soil types. Elevation and soil map units were assigned to risk classes to indicate the likelihood of encountering sulfides within a depth of 9 m. Comparison of PPA and S content for 296 diverse samples indicated that S may serve as a screening tool to evaluate materials without carbonates. Comparison of PPA and conventional Acid-Base Accounting (ABA) for 14 diverse samples indicated that PPA and ABA were highly correlated, with PPA yielding 0.60 to 0.95X the amount of acidity as ABA. Potential acidity by Soxhlet extraction and PPA were equivalent for 3 of 4 diverse samples. Average acidity and metal contents of leachate from Soxhlet extractors were correlated with acidity and metals of road drainage. Sulfide hazard analysis should be an essential step in the pre-design phase of highway construction and other earth-disturbing activities.

TABLE OF CONTENTS

LIST OF TABLES

LIST OF FIGURES

Acknowledgements

I would like to thank my committee members for the unique contributions that they each provided –Lee Daniels, Lucian Zelazny, Don Rimstidt, Jim Craig, and Bill Carstensen. I also would like to thank Mike Fitch, who served as project manager for the Transportation Research Counsel. I would like to thank the Virginia Department of Transportation and the Transportation Research Council for funding this project, and the Waste Policy Institute and the Association of Women Geoscientists for providing additional support.

The following people provided significant assistance through laboratory/field work, academic discussions, and guidance: Steve Nagle, Ronnie Alls, W.T. Price, Sue Brown, Luis Diaz, Matt Eick, Pat Donovan, Emily Smith, Ryan Reed, Sara Davis, Jody Lambert, Leslie Moore, Brian Jones, Chris Jage, Phil Cobb, Bob Hodges, Bill Henika, Rick Berquist, and Gerrie Johnson. I am deeply grateful for their help.

Finally I would like to thank my family and friends for their support and guidance over the years – my husband (Wil), daughters (TJ and Naomi), parents (Ken and Odette Wilson), brother (Dwight) and all the folks of the VPI Cave Club, the Bat Ranch, and Septapus.

Chapter 1

INTRODUCTION

Acid rock drainage (ARD) develops when sulfidic materials are excavated from below the Earth's surface and are subsequently exposed to water, dissolved oxygen, and atmospheric oxygen (Evangelou, 1995). The sulfides oxidize to form sulfuric acid, which dissolves surrounding materials and generates a highly acidic metalliferous leachate. This leachate poisons aquatic life and vegetation, pollutes streams and lakes, and corrodes construction materials. Visual indicators of ARD include orange iron precipitates in streambeds, black manganese oxide and hydroxide precipitates, white calcium and aluminum precipitates, and white sulfate salt precipitates along stream banks and rocks (Nordstrom, 1982). A specific site may exhibit all, or only some, of the features described above. The degree to which these different symptomatic features occur varies significantly, depending on such factors as the particle size and mineralogy of the sulfidic materials, composition of the host rock and surrounding geologic formations, and availability of water and oxygen. Most commonly, ARD is associated with mining and mineral processing; however, it may result from other earth-disturbing activities such as road construction.

In the case of road construction, ARD presents a number of technical, environmental, and social problems. Technical problems are primarily related to the degradation of construction materials from acid attack (Figure 1.1), weathering of sulfidic fill materials and precipitation of sulfates which compromise structural stability, and the depletion of roadside vegetation (Figure 1.2) which increases erosion and acid runoff. Local surface water quality is threatened as high acidity and elevated levels of heavy metals are detrimental to aquatic life (Figure 1.3). From an aesthetic point of view, ARD diminishes the appearance of roads by killing roadside vegetation and by causing unsightly orange stains on curbs (Figure 1.4). The combination of visible pollution and adverse conditions for aquatic life limits recreational uses of impacted surface waters. Considering these detrimental effects, sulfidic deposits are best avoided when siting a

Figure 1.1. Sulfide-bearing sediments of the Chesapeake Group are exposed along this stretch of I-95 in Spotsylvania County. The stability of this signpost is compromised due to concrete degradation from acid attack. Furthermore, acid conditions (soil pH ~ 2.5) limit vegetative growth, which makes these sites particularly prone to erosion.

Figure 1.2. Mine Road in Stafford County exposes sulfides in the Quantico slate, creating extremely acid conditions that will not support vegetation without intense remediation efforts. Surface soil pH at this site is typically less than 3.0.

Figure 1.3. This acid drainage from the Tabb formation, which was excavated during construction of an industrial park in Hampton, has a pH around 3.0

Figure 1.4. Acid drainage from the Quantico slate in Stafford, Virginia (see also Figure 1.2), has caused extensive iron-staining along curbs and sidewalks through the Hampton Oaks subdivision. Also, concrete etching occurs when acid drainage "dissolves"out the cement, deteriorating the concrete. Homeowners in this neighborhood apply the equivalent of 2 Mg agricultural lime per hectare per month to maintain soil pH above 5.5.

highway corridor or other major earth-disturbing activity. When they cannot be avoided, a mitigation plan should be implemented as soon as sulfidic materials are exposed.

Sulfidic deposits are found in various geologic and geomorphic settings across the state of Virginia. These settings include unconsolidated sulfide-rich sediments in formations of the Coastal Plain, certain slate and phyllite bearing formations in the Piedmont and Blue Ridge, some of the black shales in the Valley and Ridge, and sulfide-rich coal seams in the coalfields of southwest Virginia. In many of these settings, road construction has resulted in localized ARD problems of varying severity. While such problems historically had been considered isolated occurrences, over the past decade the Virginia Department of Transportation (VDOT) has come to recognize these sites as manifestations of the same underlying cause. Due to the broad occurrence and variability of sulfidic materials, future road planning must consider two factors to minimize the effects of ARD. First, boundaries of potential ARD deposits intersecting planned highway corridors must be delineated. In some cases, a slight shift in route or change in profile grade may prevent exposure of sulfides. Second, the potential ARD severity in problem areas must be predicted to determine optimal handling and treatment procedures. When deposits cannot be avoided, advance knowledge of their locations and characteristics will allow for appropriate road design and environmental remediation procedures. With a carefully developed remediation plan in place from the start, detrimental effects may be significantly reduced.

With these problems in mind, this study was designed to assist VDOT, and other groups involved with major earth-disturbing activities, identify and manage potentially acidic soil and geologic materials. Therefore, the specific objectives of this study were:

1) The compilation of a state-wide sulfide hazard rating map.
2) Development of a GIS based procedure for evaluating the risk of encountering sulfidic materials within specific excavation depths in the Coastal Plain.
3) The evaluation of existing potential acidity procedures to determine their applicability to diverse sulfidic materials.

References

Evangelou, V. P. 1995. Pyrite oxidation and its control. CRC Press, New York.

Nordstrom, D. K. 1982. Aqueous pyrite oxidation and the consequent formation of secondary iron minerals. p. 37-56. *In* J. A. Kittrick, D. S. Fanning, and L. R. Hossner (ed.) Acid Sulfate Weathering. Soil. Sci. Soc. Am. Spec. Pub. 10. Soil Sci. Soc. Am. Madison, WI.

Chapter 2

LITERATURE REVIEW

Oxidation of certain sulfide minerals, particularly pyrite, marcasite, and pyrrhotite, produces a highly acidic, metalliferous leachate. This leachate is commonly referred to as acid mine drainage (AMD) since it most commonly occurs when sulfidic materials are exposed from mining operations. Sulfidic materials may be exposed from other earth-disturbing activities, such as highway construction, in which case the leachate is typically referred to as acid drainage (AD) or acid rock drainage (ARD) (Byerly, 1990; Fox et al., 1997). The generation of ARD from road construction presents a number of technical, environmental, and social problems**.** These problems may be minimized with proper planning and application of appropriate remediation procedures. Throughout this document, the term 'sulfide' is used to refer specifically to acid-producing sulfidic minerals. This chapter reviews the pertinent literature related to sulfide formation, sulfide oxidation, acid-sulfate soils, engineering impacts of ARD, and highway planning procedures.

Sulfide Morphology and Formation (Sulfidization)

Acid rock drainage results from the oxidation of certain sulfide minerals, such as pyrite (FeS_2), marcasite (FeS_2), and pyrrhotite ($Fe_{1-x}S$). While ARD can result from pyrite levels as low as 0.5%, studies related to acid-sulfate weathering typically indicate levels of up to 5% (Adams et al., 1999; Byerly and Middleton, 1981; Oborn, 1989; Pons et al., 1982; Quigley and Vogan, 1970; Ritsema et al., 1992) and much higher discrete concentrations may occur (Berube et al., 1986). Pyrite occurs in many forms in a wide variety of geologic setting. It is found as single or clustered euhedral crystals, including cubes, pentagonal dodecahedrons (also called pyritohedrons), octahedrons, and framboids (discussed later in this section). Pyrite also occurs in massive forms such as plant replacements and rock joint coatings. Pyrite forms at high and low temperatures and is found in igneous, metamorphic and sedimentary rocks. Marcasite, a polymorph of pyrite, commonly occurs as radiating, tabular crystals. It is less stable and less common than pyrite. Pyrrhotite rarely occurs in crystal form and is usually present as disseminated, anhedral grains and interstitial masses in igneous and metamorphic rocks.

Comparing the various morphologies, framboidal pyrite is most reactive due to its large surface area (Carrucio et al., 1977).

The formation and accumulation of sulfide minerals, particularly pyrite, are typically referred to as sulfidization or pyritization. In sedimentary environments, sulfidization requires sulfate, sulfate reducing bacteria, organic matter, and iron. These conditions commonly occur in saline, anoxic environments. The actual mechanisms by which pyrite forms in low-temperature settings remain unresolved. Nonetheless, in typical oxygenated marine and marsh conditions, the steps involved in sedimentary pyrite formation may be summarized as follows. A few cm below the water-sediment interface, bacterial reduction of interstitial dissolved sulfate produces H_2S. Organic matter acts as a reducing agent and energy source for the bacteria. The overall process may be represented by the equation:

$$2CH_2O + SO_4^{2-} \rightarrow H_2S + 2HCO_3 \qquad (1)$$

where CH_2O represents organic matter (Berner, 1984). The dissolved sulfide reacts with Fe-minerals to form a series of black, fine-grained metastable Fe-monosulfides including crystalline FeS, mackinawite (Fe_9S_8), and greigite (Fe_3S_4). These minerals are referred to as acid volatile sulfides (AVS's) and later transform to pyrite. Wilkin and Barnes (1997a) suggest that Fe-monosulfide crystals nucleate and grow, then are converted to microcrystals of greigite. The greigite microcrystals aggregate to form framboids, which later are converted to pyrite framboids.

Pyrite framboids are spherical to sub-spherical aggregates of equigranular pyrite microcrystals. The average diameter of framboidal aggregates in sediments is about 5 um, and aggregates greater than 50 um are rare. The pyrite microcrystals are about 0.1 - 1 um in diameter. Within a framboid, microcrystals tend to be uniform in size and shape and are usually arranged in ordered three-dimensional arrays (Wilkin and Barnes, 1997a). Framboidal pyrite is the dominant form of sulfide found in modern anoxic environments, such as marine, lacustrine, and salt-marsh sediments, and analagous sedimentary rocks. Pyrite framboids also occur in hydrothermal veins and other types of ore deposits. The diverse environments in which

framboidal pyrite is found, including documentation of framboid development on the pages of antique books (Garcia-Guinea et al., 1998), suggests that framboid formation does not require a narrow set of physical or chemical conditions (Wilkin and Barnes, 1997a).

Controls in the process of pyrite formation include the availability of dissolved sulfate, the amount and reactivity of organic matter, and the amount and reactivity of Fe minerals. Rate control by sulfate is negligible at concentrations greater than 5 mM (Berner, 1984). Therefore, sulfate concentration does not limit pyrite formation in typical brackish and marine environments, but it does constrain pyrite formation in typical freshwater environments.

The amount and, more importantly, the reactivity of organic matter (OM) deposited in sediment controls the rate of SO_4^{2-} reduction (Berner, 1984). In most marine environments, the input of organic matter occurs as detrital deposits at the sediment surface. Total sediment accumulation rates may affect sulfate reduction rates by their effect on OM reactivity (Goldhaber and Kaplan, 1974). High sediment accumulation rates result in less complexation of organic material and more total organic carbon preserved in buried sediments. Low sediment accumulation rates leave the OM exposed to oxidation losses for longer periods of time. By the time of burial, the OM is less reactive and may constrain bacterial sulfate reduction. In a salt marsh environment the major organic input occurs below the sediment surface as the living and dead portion of roots and rhizomes created in situ with the uppermost sediments. Lord and Church (1983) determined that within the surface zone of marsh sediments (approximately 7 cm) reoxidation of dissolved sulfide to sulfate limited pyritization. The rate of pyrite formation increased rapidly between 7 - 9 cm where the levels of organic matter, sulfide, and reactive iron provided optimal conditions for pyritization. Below 9 cm, pyrite accumulation increased very gradually due to limited amounts of dissolved ferrous iron.

Availability of reactive iron minerals may limit the extent of pyrite formation in various marine environments (Raiswell and Canfield, 1998). Canfield et al. (1992) define two main pools of sediment iron based on estimated half-lives with respect to sulfidization. The rapidly reactive pool consists of iron oxides which dominantly have half-lives of less than one month. The slowly reactive pool is comprised of Fe-bearing silicates with half-lives of greater than 80,000 years. In

the presence of sufficient metabolizable organic matter, the maximum abundance of pyrite in sediments may be controlled by burial flux of Fe-oxides into the sediment. In terrigenous marine sediments deposited under normal oxygenated conditions, Fe is sufficiently abundant and reactive to support pyrite formation. However, in locations removed from sources of terrigenous clays and silts, sediments are dominated by $CaCO_3$ from skeletal debris of marine organisms. These sediments do not supply sufficient amounts of Fe and, even in the presence of abundant OM and H_2S, pyrite formation is low (Berner, 1984).

The previous discussion concentrated on framboidal pyrite formation under normal, oxygenated, marine and salt marsh conditions. Framboidal pyrite also forms under euxinic conditions, which exist in anoxic bottom waters. Euxinic conditions tend towards high OM accumulation, extensive bacterial sulfate reduction, and the build up of H_2S in the sediment and bottom water. Consequently, pyrite formation can occur before and after burial. Suspended framboidal pyrite forms from reactions between ferrous and sulfide species just below the oxic-anoxic interface, which may be several meters above the sediment (Wilkin and Barnes, 1997b). The underlying sediments contain framboids that have settled from the water column along with diagenetic euhedral grains and infilled framboids. The pyrite framboids found in euxinic water columns tend to be smaller and less variable in size than those found in modern sediments under oxic water columns. Size apparently is controlled by residence time near the anoxic-oxic boundary (Wilkin and Barnes, 1997b). Since H_sS may be transported laterally in euxinic environments, pyrite formation may occur at sites with low OM levels. Consequently, pyrite concentrations are not always correlated to organic carbon (OC) as in oxygenated marine environments (Berner, 1984).

Since formation of framboidal pyrite in sediments is favored by certain conditions, the occurrence of framboidal sulfides within a particular rock unit is directly correlated to the paleoenvironment of the stratum. Carrucio et al. (1977) used a sedimentary model based on present-day analogues that categorized paleoenvironments into back-barrier, lower delta plain, upper delta plain, and alluvial sequences. Evaluation of a stratigraphic section in Pennsylvania indicated that framboidal pyrite is most abundant in back-barrier and lower delta plain environments, while upper delta and alluvial plain settings are relatively poor in framboidal

pyrite. Similar results were found within the Appalachian coalfield of eastern Kentucky (Carrucio et al., 1977). Furthermore, the Kentucky study showed that while alluvial-upper delta plain sequences contain some framboidal pyrite, they are also associated with highly buffered alkaline-water systems that neutralize acidity. These authors conclude that the occurrence of framboidal pyrite coupled with the geochemistry of the natural waters - both of which are related to varying paleoenvironments - ultimately control the quality of drainage. They suggest that mapping coals in the context of their depositional environments may assist prediction of acid drainage from specific sites.

Fewer studies have examined the formational mechanisms of pyrite at elevated temperatures although pyrite commonly occurs in hydrothermal deposits. Graham and Ohmoto (1994) investigated pathways for the formation of pyrite at elevated temperatures (150 - 350^{o}C) in the presence or absence of anhydrite from solutions that were either saturated or undersaturated with pyrrhotite. They observed two mechanisms. In the first mechanism, cubic pyrite crystals formed on pyrrhotite surfaces. At higher temperatures and longer run periods, the cubic form was overtaken by cube-octahedral crystals. Pyrite formation was greater in the presence of anhydrite. By the second mechanism, micron-sized cubes of pyrite (framboids) formed on the surface of native liquid S droplets. At higher temperatures and longer run periods pyritohedral crystals formed and engulfed the cubic crystals. These authors conclude that the type of precursor surface, and the specific chemical environment, control pyrite types.

Acid Generation by Sulfide Oxidation (Sulfuricization) and Sulfate Dissolution

Sulfuricization is the process by which sulfidic materials oxidize, sulfuric acid weathers existing minerals, and new mineral phases are formed (Carson et al., 1982). Pyrite oxidation is a complex biogeochemical process affected by physical, chemical, and microbial factors. These factors include temperature, pH, surface area of the sulfides, oxygen concentrations, water saturation, chemical activity of Fe^{3+}, and the presence of iron and sulfur-oxidizing bacteria (Nordstrom and Southam, 1997). Pyrite oxidation is commonly described by the following equations (Evangelou and Zhang, 1995; Nordstrom, 1982; Singer and Stumm, 1970):

$$FeS_{2(s)} + 7/2O_2 + H_2O \rightarrow Fe^{2+} + 2SO_4^{2-} + 2H^+ \quad (2)$$

$$Fe^{2+} + 1/4O_2 + H^+ \rightarrow Fe^{3+} + 1/2H_2O \quad (3)$$

$Fe^{3+} + 3H_2O \rightarrow Fe(OH)_3 + 3H^+$ (4)

$FeS_2 + 14Fe^{3+} + 8H_2O \rightarrow 15Fe^{2+} + 2SO_4^{2-} + 16H^+$ (5)

In equation 2, pyrite is oxidized by O_2 and water to produce dissolved ferrous iron, sulfate, and acidity. The ferrous iron is further oxidized to produce ferric iron (equation 3). The ferric iron may hydrolyze to produce iron hydroxide precipitates and acidity (equation 4), or it may react with pyrite and water to produce ferrous iron, sulfate and acidity (equation 5). The oxidation of pyrite by ferric iron (equation 5) produces the greatest amount of acidity. This reaction is pH dependent since ferric iron becomes increasingly soluble, and less likely to precipitate as iron hydroxide, as pH decreases. Under abiotic, acidic conditions, reaction 3 is slow (half-life ~ 1000 days) while reaction 5 is very fast (half-life ~ 20 - 1000 min.; Nicholson et al., 1988) and consumes ferric iron faster than it can be produced. Therefore, reaction 3 is considered the rate-determining step in pyrite oxidation (Singer and Stumm, 1970). However, iron-oxidizing bacteria such as *Thiobacillus ferrooxidans* and *Leptospirillum ferrooxidans* accelerate the rate of ferric iron oxidation by a factor of up to 10^6 (Singer and Stumm, 1970). These acidophilic bacteria occur in essentially all geologic environments. Consequently, the kinetics of pyrite oxidation are strongly controlled by microbial activity. The optimum temperature and pH for microbial catalysis is 30^0C and pH 3.2 (Nordstrom, 1982). Bacterial activity ceases when O_2 is completely depleted, but resumes with even small increases in O_2 content and reaches a maximum at approximately 1% partial pressure O_2 (Evangelou et al., 1998). Under conditions favorable for bacterial activity, reaction 3 is no longer rate-determining, and pyrite oxidation becomes a rapid self-perpetuating process.

In comparison to pyrite, the oxidation reactions for pyrrhotite are poorly understood (Janzen et al., 2000). Pyrrhotite chemistry is complicated by variable iron deficiency in the crystal structure. The general formula for pyrrhotite is $Fe_{1-x}S$, where x can vary from 0.125 (Fe_7S_8), in the monoclinic form, to 0.0 (FeS), in the hexagonal form, with intermediate hexagonal and orthorhombic structures. Nicholson and Scharer (1994) present a number of possible oxidation reactions. When oxygen is the primary oxidant, the overall reaction may be written as:

$$Fe_{(1-x)}S_{(s)} + (2-0.5x)O_2 + xH_2O \rightarrow (1-x)Fe^{2+} + SO_4^{2-} + 2xH^+ \qquad (6)$$

As indicated by equation 6, one mole of pyrrhotite may produce up to one-quarter mole acidity, depending on the value of x. Therefore, with a typical value of x = 0.1, pyrrhotite oxidation produced only about one-tenth as much acid as pyrite. As with pyrite, subsequent Fe oxidation and hydrolysis may produce additional acidity (equations 3 and 4). If oxidation is not complete, and elemental S is produced, the following acid-consuming reaction may apply:

$$Fe_{(1-x)}S_{(s)} + ((1-x)/2)O_2 + 2(1-x)H^+ \rightarrow (1-x)Fe^{2+} + S^0 + (1-x)H_2O \qquad (7)$$

Under low pH conditions, where Fe^{3+}concentration may be significant in pore water, pyrrhotite may be oxidized by Fe^{3+}:

$$Fe_{1-x}S_{(s)} + (8-2x)Fe^{3+} + 4H_2O \rightarrow (9-3x)Fe^{2+} + SO_4^{2-} + 8H^+ \qquad (8)$$

At atmospheric oxygen saturation, and 22^0C, pyrrhotite oxidation is 20 to 100 times faster than values reported for pyrite oxidation under similar conditions (Nicholson and Scharer, 1994). These authors speculate that instability in the crystal structure due to iron deficiency may accelerate reaction rates. A more recent study (Janzen et al., 2000) determined that pyrrhotite crystal structure and trace metal content do not appear to have a consistent effect on oxidation rates, but that high surface area resulting from extensive fractures along cleavage planes deep into the structure may account for high reactivity. The factors affecting pyrrhotite oxidation are further complicated by the fact that pyrrhotite commonly occurs as intergrowths of hexagonal and monoclinic forms. Although pyrrhotite produces less acidity on a molar basis than pyrite, an abundance of pyrrhotite could have detrimental effects on surrounding ecosystems by creating toxic pulses of metal-rich ARD at much faster rates than pyrite (Fox et al., 1997).

In acid weathering environments, iron-sulfate minerals typically form during sulfide oxidation. For example, as presented by Cravotta (1994), the following reaction describes the formation of romerite by pyrite oxidation:

$$3FeS_2 + 11O_2 + 16H_2O \rightarrow Fe^{2+}Fe_2^{3+}(SO_4)_4 \bullet 14H_2O + 2SO_4^{2-} + 4H^+ \qquad (9)$$

As compared to complete pyrite oxidation by oxygen (equations 2, 3, and 4), only 1/3 of the H^+ is released, while the remaining acidity is "stored" as unhydrolized, partly oxidized iron in the solid phase. Romerite, and other iron-sulfate hydrate minerals, are highly soluble and may function as a significant source of acidity upon dissolution:

$$Fe^{2+}Fe_2^{3+}(SO_4)_4 \bullet 14H_2O \rightarrow 2Fe(OH)_3 + Fe^{2+} + 4\ SO_4^{2-} + 6\ H^+ + 8\ H_2O. \qquad (10)$$

Subsequent iron oxidation and hydrolysis will produce additional acidity (equations 3 and 4). Consequently, iron-sulfate hydrate minerals are important as both sinks and sources of acidity (Cravotta, 1994), and may be partly responsible for increased acidity in drainage, particularly during rainstorm events (Nordstrom, 1982).

Acid Sulfate Soils

Potential, actual, and pseudo acid sulfate soils are soils that could be, are currently being, or have been affected by sulfuricization. Worldwide, 10 to 20 million ha of acid sulfate soils are present in areas with climatic conditions that range from tropical to temperate (Kawalec, 1973; Pons et al., 1982). These soils were originally recognized and studied in coastal environments, where man-made and natural drainage of sulfidic materials has resulted in the rapid development of acidic soils that are unsuitable for agriculture. Acid sulfate soils are also associated with brackish lake sediments, inland valleys subject to influx of sulfate-rich water, dredged materials, mine spoils, and construction sites (Fanning and Fanning, 1989; Pons et al., 1982). Studies regarding mapping of acid sulfate soils, particularly with respect to landforms, are discussed in Chapter 4.

Three idealized stages of sulfuricization are presented by Carson et al. (1982), which correspond to nomenclature for acid sulfate soils presented by Brinkman and Pons (1973). In the first stage, pre-sulfuricization, sulfidic materials are present, and may still be forming, under reducing conditions. In Soil Taxonomy (Soil Survey Staff, 1998), sulfidic materials are defined specifically as "mineral or organic soil materials that have a pH value of more than 3.5, and that, if incubated as a layer 1 cm thick under moist aerobic conditions (field capacity) at room

temperature, show a drop in pH of 0.5 or more units to a pH value of 4.0 or less (1:1 by weight in water or in a minimum of water to permit measurement) within 8 weeks." Sulfidic materials typically occur as drab dark colors, with chroma ≤ 1, and values ≤ 4 (Fanning et al., 1993) and often have a sulfurous odor. Soils containing sulfidic materials with no previous oxidation are called potential acid sulfate soils.

In the second stage of sulfuricization, sulfidic materials are actively oxidizing, producing sulfuric acid and sulfate minerals. Acid sulfate weathering may produce a sulfuric soil horizon which is defined as a horizon that is "15 cm or more thick and is composed of either mineral or organic soil material that has a pH value of 3.5 or less…..and shows evidence that the low pH value is caused by sulfuric acid. The evidence is one or more of the following: i) jarosite concentrations, ii) directly underlying sulfidic materials (defined above), or iii) 0.05 percent or more water soluble sulfate" (Soil Survey Staff , 1998). Jarosite typically has hues of 2.5Y or yellower and chromas of 6 or higher, and commonly occurs in juxtaposition with iron oxides (Fanning et al., 1993). A number of soluble sulfates such as gypsum, jarosite, melanterite, ettringite, bassanite, fibroferrite, rozenite, melanterite, pickeringite, and copiapite may form at or near the surface of active sulfate soils and sulfidic rock exposures (Berube et al., 1986; Nordstrom, 1982; Parnell, 1983). These sulfate precipitates are typically white or yellow, although melanterite can be bluish green. Soils in stage 2 of sulfuricization are called actual acid sulfate soils.

In the third stage, postsulfuricization, sulfides are completely oxidized and the pH is usually above 4. Previous sulfuricization may be indicated by the presence of jarosite, and other sulfate minerals; however, their presence is not required as jarosite does not always form in acid sulfate soils, and sulfate minerals may not be preserved in the profile. Past sulfuricization is also indicated by underlying materials representing stages 1 and/or 2. In some soils, enriched levels of arsenic (Dudas, 1984), transformation of mica to swelling clays (De Kimpe and Miles, 1992), and increased salinization (Mermut and Arshad, 1997) have been attributed to past sulfuricization. Soils in stage 3 of the sulfuricization process are called pseudo acid sulfate soils, or postactive acid sulfate soils (Fanning and Fanning, 1989).

Engineering Impacts of Sulfide Oxidation

Engineering impacts from sulfide oxidation, including degradation of local surface water quality, disintegration of construction materials, and structural damage to buildings, have been documented at a number of locations around the world (Table 2.1). Many studies describe structural damage to buildings resulting from heaving and deterioration of concrete and cement (Berube et al., 1986; Chinchon et al, 1995; Dougherty and Barsotti, 1972; Grattan-Bellew and Eden, 1975; Hawkins and Pinches, 1987; Moum and Rosenquist, 1959; Parizek, 1982; Penner et al., 1970; Quigley and Vogan, 1970). These incidents most commonly result from contact, or close proximity, between the base of a structure and an underlying sulfide-bearing strata. A few studies describe deterioration resulting from the use of sulfidic aggregates (Ayora et al., 1998; Chinchon et al., 1995). One study on an abandoned railroad suggests that heat generated from sulfide oxidation in the underlying fill resulted in thermal expansion and localized deformation of rails (Prokopovich, 1987). Studies on the impact of ARD on highway construction focus mainly on the generation of acid drainage and its effect on local surface waters (Adams et al., 1999: Fox et al., 1997; Igarishi and Oyama, 1999; Mathews and Morgan, 1982; Morgan et al., 1982), Less work has been completed on the deterioration of road materials and related structures upon exposure to acid sulfate weathering (Sahat and Sum, 1990; Vear and Curtis, 1981).

After oxidation, sulfides may convert to numerous different sulfate minerals that may occupy several times the volume of the original sulfides and other minerals from which they form. The forces exerted by this expansive crystal growth can result in heaving which affects overlying structures. Many of the case studies cited in Table 2.1 report that floor heave was detected within a few years after construction. Although gypsum growth generally is acknowledged as the main cause of heave (Berube et al., 1986; Grattan-Bellew and Eden, 1975; Hawkins and Pinches, 1987), some reports speculate on the contribution of other sulfates. A detailed study of biochemical alterations in black shale (Quigley et al., 1973) indicated that while gypsum growth was responsible for heaving reported in two buildings in Ottawa, jarosite only

Table 2.1. Engineering impacts of acid sulfate weathering.

Reference	Location	Materials*	Problems
Adams et al., 1999	Buchanan, Georgia	py bearing schist (Sandy Springs group)	decline in local water quality due to acid drainage
Ayora et al., 1998	Central Pyrenees, Spain	po and py bearing schist	concrete degradation due to formation of expansive sulfates in the aggregate
Berube et.al., 1986	Sainte-Foy, Quebec, Can.	py bearing black shale (Sainte-Foy formation)	concrete floor slab heaved more than 10 cm.
Chinchon et al., 1995	Barcelona, Spain	po and py bearing shales and limestone	concrete degradation due to formation of expansive sulfates in the aggregate
Dougherty and Barsotti, 1972	southwest Pennsylvania	py bearing coals and shales (dominantly the Conemaugh and Monongahela formations)	structural damage due to heaving
Fox et al., 1997	Nova Scotia	po bearing slate	decline in local water quality due to acid drainage
Grattan-Bellew and Eden, 1975	Ottowa, Ontario, Can.	py bearing black shale (Eastview formation)	basement floor heaved up to 6.3 cm sulfate attack on concrete
Hawkins and Pinches, 1987	Cardiff, UK	py bearing black mudstone (Westbury formation)	heaving in the floor slab
Igarishi and Oyama, 1999	central Japan	py bearing rhyolite	acidification of reservoir water
Mathews and Morgan, 1982	N. Carolina, USA	py bearing black shales (Anakeesta formation)	metalliferous, acid leachage destroyed aquatic ecological systems
Miller et al., 1976	Texas	py bearing sediements (Weches and Queen City formations)	Vegetative failure, causing increased erosion, on road banks.
Morgan et al., 1982	N. Carolina & Tenn., USA	py bearing black shales (Anakeesta formation)	metalliferous, acid leachate destroyed aquatic ecological systems
Moum and Rosenquist, 1959	Oslo, Norway	po in slightly metamorphosed shales (alum shales, alum slates)	concrete deterioration due to sulfate attack foundation upheaval
Parizek,1982	Kansas City, Missouri	py bearing black shales (Upper Pennsylanian beds)	building floor heave up to 10 inches mine floor heave up to 8 inches
Penner et al., 1970	Ottowa, Ontario, Can.	py bearing black shale (Billings formation)	basement floor slab cracked by 10.2 cm of differential heave

* py = pyrite; po = pyrrhotite

Table 2.1 (Continued)

Reference	Location	Materials*	Problems
Prokopovich, 1987	Redding, California	massive py ore	thermal expansion and deformation due to heat from oxidation reactions
Pye and Miller, 1990	Derbyshire, UK	py bearing black shale (Namurian shale)	collapse of a shale embankment from volumetric changes due to acid leaching
Quigley and Vogan, 1970	Ottowa, Ontario, Can.	py bearing black shale (Lorraine formation)	interior columns heaved up to 7.6 cm
Sahat and Sum, 1990	Malaysia	py bearing granite, hornfels	disintegration of road aggregates
Swaine, 1986	Liddell, New South Wales	framboidal py in siltstone	rapid weathering of excavated siltstone due to acidity and expansion effects
Van Holst and Westerveld, 1973	The Netherlands	Unspecified sulfides	Corrosion of concrete piles poured in situ (unsatisfactory hardening due to sulfates)
Vear and Curtis, 1981	Derbyshire, UK	py bearing black shale (Namurian shale)	slope instability, landslides, and acid drainage along roadut

* py = pyrite; po = pyrrhotite

acted to fill open voids and cracks and probably did not contribute to heave. Less work exists on the specific role of other sulfates towards heaving. In a somewhat different situation Burkart et al. (1999) identified the formation of ettringite ($Ca_6Al_2(SO_4)OH_{12}$-$26H_2O$) and thaumasite ($Ca_3Si(CO_3)(SO_4)(OH)6$-$12H_2O$) as the cause of sulfate-induced heaving under roads at numerous locations near Dallas, Texas. These roads were constructed on montomorillonitic soils containing gypsum, which formed over pyritic shales. Since untreated montomorillonitic soils are unstable for road subgrade they are conventionally modified with the addition of lime (CaO) or some other cementitious material. In some settings, montmorillonite, gypsum, lime, and water will react to form ettringite and thaumasite. The growth of these minerals resulted in soil expansion and destroyed the pavement subgrade. It should be noted that acid sulfate weathering already occurred naturally in these soils and was not due to exposure of sulfidic materials from construction. This indicates that in some situations acid-sulfate type problems may result without actual exposure of sulfidic materials.

When a structure is built above sulfide-bearing strata, a number of interacting factors contribute to the potential for heave. These factors are described in detail by Dougherty and Barsotti (1972). First, the concentration and extent of sulfide minerals must be large enough to produce an appreciable amount of weathering products. Most studies on damaged structures report pyrite contents in the range of 1 -5% by weight. The lateral extent and variability of sulfide minerals is more difficult to quantify. Second, the floor slab must be relatively close to the sulfide-bearing strata. In a survey of buildings affected by heave in western Pennsylvania, Dougherty and Barsotti (1972) note that there were no known cases of heaving damage where sulfides were at least 3 m below the lowest floor bottom or the lowest footing. Third, the behavior of ground water below the structure plays a significant role. If the sulfide-bearing strata is totally submerged then oxidation and the formation of alteration products will cease. In some cases, deliberate submergence of the shale beneath the basement slab has effectively arrested or prevented heave (Penner et al., 1973). On the other hand, fluctuating ground water levels, by man-made or natural causes, may trigger oxidation. Fourth, the extent and nature of fracturing within the rock affects oxidation by controlling the entry of air and water as well as the amount of exposed surface area. In one study (Quigley et al., 1973) alteration products were restricted to a badly fractured rock zone surrounding a fault into which air could easily diffuse. In addition to

the pre-existing fracture density, removal of overburden may increase fracturing due to stress release. This is noticeable particularly along bedding partings in laminated fissile mudstones and shales. Cracks which induce capillary action may supply moisture to sulfides, and may facilitate the transportation and deposition of sulfates. Fifth, heat from the building may accelerate sulfide weathering by two different mechanisms. The increased warmth enhances bacterial activity, which catalyzes the oxidation process. Also, the heat may dry underlying rock to produce the saturated solutions from which sulfate minerals crystallize. These factors, described above, address some of the site characteristics, which must be evaluated when constructing a structure over sulfide-bearing materials.

In addition to heave, structural damage may result from sulfate and acid attack on cement and concrete. Moum and Rosenqvist (1959) describe how the concrete walls of an underground bomb shelter built in alum shale transformed into unconsolidated debris in about 9 months due to sulfate attack. Similarly, Grattan-Bellew and Eden (1975) describe how sulfate and acid attack deteriorated concrete underlying the basement floor of a church into unconsolidated debris within a few decades. The concrete was lying directly on weathered black shale. Ayora et al. (1998) present a thermodynamic model to predict the progress of acid and sulfate attack in a case study where sulfidic rock was used as an aggregate in concrete. Agreement between their calculations and observations of alteration features suggests that simplified chemical models may be useful in predicting the behavior of acidic alterations. Similarly, Oyama and Chigira (1999) investigated mineral, chemical, and physical properties of soft sedimentary rocks exposed along unlined tunnel walls to quantify the relationship between depth of weathering and time. They developed an equation with parameters of water permeability, air porosity, pyrite content, ferrous iron, and carbon to estimate weathering rates. Structural deterioration also may result from the incorporation of sulfides into construction materials, such as sulfide-rich aggregates in concrete (Chinchon et.al. 1995).

Exposure of sulfidic materials from road construction presents a number of technical, social, and environmental problems. Technical problems are primarily related to the degradation of construction materials, weathering of sulfides exposed along roadcuts or in fill material, and limitation of roadside vegetation, which promotes erosion and continual exposure of fresh

sulfidic materials. First, construction materials such as metal pipe culverts, concrete box structures, and metal guardrails cannot withstand extended exposure to ARD. In some problem areas in Virginia galvanized steel guard rails have a life span of only two to five years (W.L. Daniels, personal communication; see Figure 3.5). At one site near Covington, Virginia, deterioration of local water quality due to acidic fill leaching has necessitated the construction of a discharge treatment facility. Second, rapid weathering may severely disintegrate and decompose road banks resulting in landslides and road closures (Vear and Curtis, 1981). Similarly, difficulties occur when sulfidic materials that are excavated from roadcuts and borrow pits are used as fill materials in road beds. In addition to leaching acid, oxidation of these materials results in volumetric changes which compromise fill stability and may lead to subsidence and pavement buckling (Pye and Miller, 1990). Finally, failure to establish roadside vegetation due to extremely acid soil conditions increases sediments and acid runoff from bare road banks (Miller et al., 1976). These geotechnical problems are a nuisance to highway engineers as well as the general public, as remediation procedures are expensive and disruptive to normal traffic flow. From an aesthetic point of view, ARD diminishes the appearance of roads by killing and preventing roadside vegetation, and by causing unsightly orange stains in culverts and on curbs. This point may seem trivial, however, roadside appearance is an important reflection of the state of Virginia to both residents and visitors. Acid rock drainage from road construction also poses environmental threats to water quality, aquatic life and vegetation. The high acidity and elevated levels of heavy metals are toxic to most plants and detrimental to aquatic life. Adverse community responses of stream organisms to conditions induced by ARD are well-documented (Huckabee et al., 1975; Klapper and Schultz, 1995; Morgan et al, 1982; Nathan and Katz, 1969). Furthermore, the combination of visible pollution and adverse conditions for aquatic life limits recreational uses, such as fishing and swimming in surface waters (Morgan et al., 1982).

Most studies regarding the impact of road construction through sulfidic materials have focused on water quality issues. In 1963, reconstruction of U.S. Highway 441 near Great Smoky Mountains National Park involved cut and fill operations in the Anakeesta formation - a sulfidic shale. The demise of aquatic biota in Beech Flats Creek in the Great Smoky Mountains was attributed to indiscriminate use of pyrite bearing rock as rip rap along the stream embankment

(Huckabee et al., 1975). Acid leachate with high heavy metal concentrations decimated local aquatic life, in some areas reaching up to 8 km from the roadcut and fill (Mathews and Morgan, 1982). Construction beginning in 1965 of the Tellico-Robbinsville Highway between Tennessee and North Carolina, also through the Anakeesta shale, caused a similar decline in water quality. A variety of remediation techniques, including NaOH additions at the headwaters of affected streams, lime additions over selected road embankments and installation of soil blankets were applied in the Tellico Wildlife Management Area in 1978, but all proved to be minimally effective (Morgan et al., 1982). Again, in 1978, disturbance of sulfidic shales during highway construction in southeast Tennessee caused deterioration of culverts, guardrails, and aquatic life. Rehabilitation, which included placement of a sealant barrier and topsoil, revegetation, and addition of alkaline solutions to affected streams, exceeded the original highway cost (Anderson et al., 1991).

Halifax International Airport in Nova Scotia provides another dramatic example of adverse ARD impacts. Construction of the airport between 1955 and 1960 exposed large volumes of sulfide-rich slate of the Halifax formation from the Meguma Group. Since that time, acid drainage has severely impacted surrounding watersheds. Remediation efforts beginning in the early 1980's have included capping of the waste rock pile with clay and topsoil, a water treatment facility, wetlands, and other experimental techniques. Initial remediation costs exceeded over two million dollars, with operation and maintenance costing about $240,000 annually since 1982. Nonetheless, acid drainage from the airport and associated sites continues to be a problem (Zentilli and Fox, 1997; Fox et al., 1997).

Highway Planning

Over the past few decades, increased recognition of the problems associated with acid-sulfate weathering has led other countries, such as Australia and Canada, to develop guidelines for handling sulfidic materials. While specifics may vary, the following principles are universally applied. First, geologic and/or soils mapping is a basic tool for assessing ARD potential in proposed construction areas. Second, where necessary, samples from outcrops and drill cores should be evaluated for potential acidity. Third, measures should be taken to avoid or minimize excavation of acid-producing materials. Fourth, when sulfides cannot be avoided, handling and treatment plans should be clearly defined prior to construction since immediate implementation

of remediation plans is essential to minimizing environmental impacts. Incorporating these steps in the pre-design phase of a project is a worthwhile investment compared to the impact of environmental damage and the expense of mitigation after construction.

In the 1980's, the United States Federal Highway Administration initiated studies on handling acid-producing materials during construction. Guidelines were developed for detecting and evaluating potential ARD problems and for handling acid-producing materials (Byerly, 1990 and 1996). Byerly (1990) developed three sets of guidelines dealing with different stages of construction. The first set pertains to the pre-design stage, which is usually the time period of corridor selection. Figure 2.1, adapted from Byerly (1990), provides an outline of steps utilized in the pre-design phase.

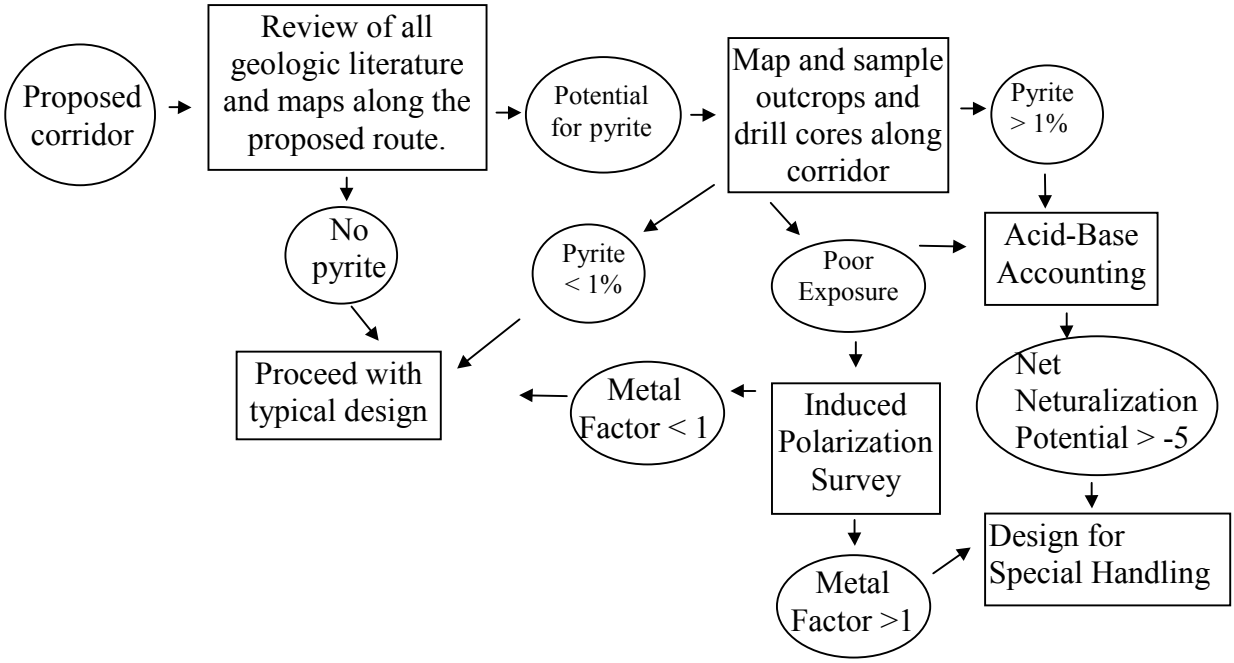

Figure 2.1. Flow-chart for evaluating potentially sulfidic material in the pre-design phase of highway construction (adapted from Byerly, 1990). Metal Factor is based on resistivity and polarizability from an Induced Polarization survey.

The second set of guidelines pertains to the design phase and deals mainly with procedures for handling and disposing acid-producing materials. Byerly's guidelines are based on the use of a modified version of the Federal Highway Administration encapsulation design. (Note: Byerly works primarily with sedimentary and metasedimentary rocks, and not with Coastal Plain sediments.) Actual design plans are site specific, and are controlled by factors such as the nature and volume of acid-producing material, topography, climate, geology and hydrology. Characterization of potential acidity is based on acid-base accounting from the pre-design phase. At this stage, all aspects of disposal should be defined. Disposal sites must be identified, sources of cover material must be identified, hydrologic impacts must be assessed, material transport plans that minimize temporary storage of sulfidic materials must be established, and an encapsulation design should be approved.

The third set of guidelines pertains to the construction phase and discusses the need for continual identification, segregation, handling, and storage of acid-producing materials during construction. All materials should be inspected, at least visually, to verify predictions. Questionable materials should be temporarily stored until laboratory evaluations are completed.

A recent study by Schaeffer and Clawson (1996) indicates that incorporation of the guidelines proposed by Byerly (1996) successfully minimized the impact of acid-producing materials for a site in North Carolina. A program of geologic mapping, petrographic study, and acid-base accounting of rocks along a transmission line in the Blue Ridge Province of southwestern North Carolina was performed to determine the potential for acid drainage from road and tower construction. Available geologic maps were examined for occurrences of rock units identified as having high sulfur content. Detailed geologic mapping was then completed along the transmission line corridor. Representative geologic samples were collected and examined for the presence of pyrite or pyrrhotite. The potential acidity of sulfide-bearing samples was characterized by acid-base accounting. Remediation methods, including mixing lime into the excavated material, encapsulation, and drainage diversion, were developed and implemented during construction. A water-quality program monitored spatial and temporal characteristics of streams in the corridor before, during, and after construction. Three years of water quality monitoring indicated that remediation efforts minimized environmental impact

from construction. No problems related to ARD had been observed along the corridor as of seven years since completion of the study (M. F. Schaeffer, 2000, personal communication).

Additional research has been completed on assessment, management, and remediation of acid sulfate soils from coastal sediments. In particular, New South Wales (NSW), Australia, has made significant progress in addressing the problems of acid sulfate weathering. In 1994, NSW established the Acid Sulfate Soils Management Advisory Committee (ASSMAC) to coordinate an overall government response to acid soil issues. The committee includes representatives from government agencies related to agriculture, conservation, and urban planning, as well as the scientific community and other interested groups. ASSMAC produced an extensive manual with detailed guidelines addressing planning, assessment, management, laboratory methods, drainage, groundwater, and industry (Stone et al., 1998).

Similarly, environmental damage and the high cost of remediation measures led the Nova Scotia Department of the Environment to establish "Sulphide Bearing Materials Disposal Regulations" under the Nova Scotia Environment Act. These regulations outline procedures for notification, screening, sampling, analysis and disposal of acid generating materials. Anyone excavating a stated volume of sulfide-bearing slate must obtain approval, proving that their plans for excavation and disposal of the slate will be consistent with regulations (Environment Act, 1994-95, c.1, s.1).

Exposure of sulfidic materials during highway construction in Virginia has resulted in technical, environmental, and social problems at a number of discrete locations. As indicated by studies discussed above, understanding the geographic distribution of these materials can help prevent their exposure during future highway construction. Publications regarding sulfide occurrence in Virginia are discussed in Chapter 3. When sulfidic materials cannot be avoided, accurate characterization of their acid potential is necessary to establish optimal handling and remediation procedures. Procedures for evaluating the potential acidity of sulfide-bearing materials are discussed in Chapter 5.

References

Adams, C. B., C. A. Klamke, and C. L. Hollabaugh. 1999. Geochemical monitoring of Kiser Creek, near Buchanan, Haralson County, Georgia: the effects of pyrite-rich rocks on the pH, iron, and sulfate content of surface waters. Ga. J. Sci. 57(2):113-122.

Anderson, R., B. Bell, and J. Reynolds. 1991. Induced polarization used for highway planning. Investigations in Geophysics. 4:397-410.

Ayora, C., S. Chinchon, A. Aguado, and F. Guirado. 1998. Weathering of iron sulfides and concrete alteration: thermodynamic model and observations in dams from central pyrenees, Spain. Cement and Concrete Research. 28(9):1223-1235.

Berner, R. A. 1984. Sedimentary pyrite formation: an update. Geochimica et Cosmochimica Acta. 48: 605-615.

Berube, M., J. Locat, P. Gelinas, J. Chagnon, and P. LeFrancois. 1986. Black shale heaving at Sainte-Foy, Quebec, Canada. Can. J. Earth Sci. 23:1774-1781.

Brinkman, R. and L. J. Pons. 1973. Recognition and prediction of acid sulfate soil conditions. p.169-203. *In* H. Dost (ed.) Acid Sulfate Soils. Proc. Int. Symp. on Acid Sulphate Soils, Wageningen, The Netherlands. 13-20 Aug. 1972. Pub. 18 - Vol. I. Int. Inst. For Land Reclamation and Improvement, Wageningen, The Netherlands.

Burkart, B., G. C. Ross, and J. P. Kern. 1999. The role of gypsum in production of sulfate-induced deformation of lime-stabilized soils. Env. Eng. Geosci. (V)2:173-187.

Byerly, D. W. and L. M. Middleton. 1981. Evaluation of the acid drainage potential of certain Precambrian rocks in the Blue Ridge province. p. 174-185. *In* Procedings of the 32nd Annual Highway Geol. Symp. and Field Trip. 6-8 May 1981. Gatlinburg, Tennesseee. Highway Geology Symposium, Atlanta, Ga.

Byerly, D. W. 1990. Guidelines For Handling Excavated Acid-Producing Materials. U.S. Department of Transportation, Federal Highway Administration, DOT FHWA-FL-90-007. Washington, DC.

Byerly, D. W. 1996. Handling acid-producing material during construction. Env. and Eng. Geosci. II(1):49-57.

Canfield, D. E., R. Raiswell, and S. H. Bottrell. 1992. The reactivity of sedimentary iron minerals toward sulfide. Am. J. Sci. 292: 659-683.

Carson, C. D., D. S. Fanning, and J. B. Dixon. 1982. Alfisols and Ultisols with acid sulfate weathering features in Texas. P. 127-146. *In* J. A. Kittrick, D. S. Fanning, and L. R. Hossner (ed.) Acid Sulfate Weathering. Soil Sci. Soc. Am. Spec. Pub. 10, Madison, WI.

Carrucio, F. T., J. C. Ferm, J. Horne, G. Geidel, and B. Baganz. 1977. Paleoenvironment of coal and its relation to drainage quality. US-EPA. EPA-600/7-77-067. Cincinatti, Ohio.

Chinchon, J.S., C. Ayora, A. Aguado, and F. Guirado. 1995. Influence of weathering of iron sulfides contained in aggregates on concrete durability. Cement and Concrete Research. 25(6):1264-1272.

Cravotta, C. A. 1994. Secondary iron-sulfate minerals as sources of sulfate and acidity. p.345-363. *In* C. N. Alpers and D. W. Blowes (ed.) Environmental Geochemistry of Sulfide Oxidation. American Chemistry Society, Washington D.C.

De Kimpe, C. and N. Miles. 1992. Formation of swelling clay minerals by sulfide oxidation in some metamorphic rocks and related soils of Ontario, Canada. Can. J. Soil Sci. 72:263-270.

Dougherty, M. T. and N. J. Barostti. 1972. Structural damage and potentially expansive sulfide minerals. Bull. Assoc. Eng. Geol. v. 9. 2: 105-125.

Dudas, M. J. 1984. Enriched levels of arsenic in post-active acid sulfate soils in Alberta. Soil Sci. Soc. Am. J. 48:1451-1452.

Environment Act S.N.S. 1994-95, c. 1, section 66. Order in Council 95-296 (April 11, 1995), N.S. Reg 57/95.

Evangelou, V. P. and Y. L. Zhang. 1995. A review: pyrite oxidation mechanisms and acid mine drainage prevention. Crit. Rev. Env. Sci. Tech. 25(2):141-199.

Evangelou, V. P., A. K. Seta, and L. M. McDonald. 1998. Acid mine drainage. pp. 1-17. *In* R. A. Meyers (ed.) Encyclopedia of Environmental Analysis and Remediation. John Wiley and Sons, Inc., New York

Fanning, D. S. and M. C. B. Fanning. 1989. Soil morphology, genesis and classification. John Wiley and Sons, Inc., New York.

Fanning, D. S., M. C. Rabenhorst, and J. M. Bingham. 1993. Colors of acid sulfate soils. p.91-108. *In* J. M. Bingham and E. J. Ciolkosz (ed.) Soil color. Soil Sci. Soc. Am. Spec. Pub. No. 31. Madison, WI.

Fox, D., C. Robinson, and M. Zentilli. 1997. Pyrrhotite and associated sulphides and their relationship to acid rock drainage in the Halifax Formation, Meguma Group, Nova Scotia. Atlantic Geology. 33: 87-103.

Garcia-Guinea, J., J. Martinez-Frias, R. Gonzales-Martin, and L. Zamora. 1998. Framboidal pyrite in antique books. Nature (London). 388:6643:631.

Goldhaber, M. B. and I. R. Kaplan. 1974. The Sulfur Cycle. The Sea. 5:569-655.

Graham, U. M. and H. Ohmoto. 1994. Experimental study of formation mechanisms of hydrothermal pyrite. Geochimica et Cosmochimica Acta. 58(10):2187-2202.

Grattan-Bellew, P. E., and W. J. Eden. 1975. Concrete deterioration and floor heave due to biogeochemical weathering of underlying shale. Can. Geotech. J. 12: 323-378.

Hawkins, A. B. and G. M. Pinches. 1987. Cause and significance of heave at Llandough Hospital, Cardiff - a case history of ground floor heave due to gypsum growth. Quart. J. Eng. Geol. 20:41-57.

Huckabee, J. W., C. Goodyear, and R. D. Jones. 1975. Acid rock in the Great Smokies: unanticipated impact on aquatic biota of road construction in regions of sulfide mineralization. Trans. Am. Fish. Soc. 104:677-684.

Igarishi, T. and T. Oyama. 1999. Deterioration of water quality in a reservoir receiving pyrite-bearing rock drainage and its geochemical modeling. Eng. Geol. 55:45-55.

Janzen, M. P., R. V. Nicholson, and J. M. Scharer. 2000. Pyrrhotite reaction kinetics: reaction rates for oxidation by oxygen, ferric iron, and for nonoxidative dissolution. Geochim. et Cosmo. Acta. 64(9):1511-1522.

Kawalec, A. 1973. World distribution of acid sulphate soils. p.293-295. *In* H. Dost (ed.) Acid Sulfate Soils. Proc. Int. Symp. on Acid Sulphate Soils, Wageningen, The Netherlands. 13-20 Aug. 1972. Pub. 18 - Vol. I. Int. Inst. For Land Reclamation and Improvement, Wageningen, The Netherlands.

Klapper, H. and M. Schultze. 1995. Geogenically acidified mining lakes - living conditions and possibilities of restoration. Int. Revue. Ges. Hydrobiol. 80(4):639-653.

Lord, C. J. III and T. M. Church. 1983. The geochemistry of salt marshes: sedimentary ion diffusion, sulfate reduction, and pyritization. Geochimica et Cosmochimica Acta. 47:1381-1391.

Mathews, R. C. Jr., and E. L. Morgan. 1982. Toxicity of Anakeesta Formation leachates to shovel-nosed salamander, Great Smoky Mountains National Park. J. Environ. Qual. 11(1):102-106.

Mermut, A. R. and M. A. Arshad. 1987. Significance of sulfide oxidation in soil salinization in southeastern Saskatchewan, Canada. SSSAJ 51:247-251.

Miller, W. L., C. L. Godfrey, W. G. McGully, and G. W. Thomas. 1976. Formation of soil acidity in carbonaceous soil materials exposed by highway excavation in East Texas. Soil Sci. 121(3):162-169.

Morgan, E. L., W. F. Porak, and J. A. Arway. 1982. Controlling acidic-toxic metal leachates from southern appalachian construction slopes: mitigating stream damage. Trans. Res. Record. 948:10-16.

Moum, J. and I. TH. Rosenqvist. 1959. Sulfate attack on concrete in the Oslo region. J. Am. Con. Inst. 31(3):257- 264.

Nathan, R. R. and M. Katz. 1969. Impact of mine drainage on recreation and stream ecology:appendices E and F to acid mine drainage in Appalachia. ARC-69-3 and ARC 69-25. Appalachian Regional Comm., Washington, D.C.

Nicholson, R. V., R. W. Gillham, and E. J. Reardon. 1988. Pyrite oxidation in carbonate-buffered solution. I. Experimental kinetics. Geochem. Cosmochim. Acta. 52:1077-1085.

Nicholson, R. V. and J. M. Scharer. 1994. Laboratory studies of pyrrhotite oxidation kinetics. p.14-30. *In* C. N. Alpers and D. W. Blowes (ed.) Environmental Geochemistry of Sulfide Oxidation. American Chemistry Society, Washington D.C.

Nordstrom, D. K. 1982. Aqueous pyrite oxidation and the consequent formation of secondary iron minerals. p. 37-56. *In* J. A. Kittrick, D. S. Fanning, and L. R. Hossner (ed.) Acid Sulfate Weathering. Soil Sci. Soc. Am. Spec. Pub. 10, Madison, WI.

Nordstrom, D. K. and G. Southam. 1997. Geomicrobiology of sulfide mineral oxidation. Geomicrobiology. 361-390.

Oborn, I. 1989. Properties and classification of some acid sulfate soils in Sweden. Geoderma. 45:197-219.

Oyama, T. and M. Chigira. 1999. Weathering rate of mudstone and tuff on old unlined tunnel walls. Eng. Geo. 55:15-27.

Parizek. E. J. 1982. Geology and space beneath a city; Kansas City. Rev. in Eng.Geol. 5:63-73.

Parnell, R. A. 1983. Weathering processes and pickeringite formation in a sulfidic schist: a consideration in acid precipitation neutralization studies. Environ. Geol. 4:209-215.

Penner, E., J. E. Gillott, and W. J. Eden. 1970. Investigations of heave in Billings shale by mineralogical and biogeochemical methods. Can. Geo. J. 7: 333-338.

Penner, E. J., W. J. Eden, and J. E. Gillot. 1973. Floor heave due to biochemical weathering of shale. p. 151-158. Vol. 2. Proc. of the 8th Int. Conf. on Soil Mechanics and Foundation Eng., Moscow, U.S.S.R. A. A. Balkema, Boston.

Pons, L. J., N. Van Breemen, and P. M. Driessen. 1982. Physiography of coastal plain sediments and development of potential soil acidity. *In* J. A. Kittrick, D. S. Fanning, and L. R. Hossner (ed.) Acid Sulfate Weathering. Soil Sci. Soc. Am. Spec. Pub. 10, Madison, WI.

Prokopovich, N. P., Engineering impact of oxidation of pyrite. Bull. Assoc. Eng. Geol. 24(1): 140-144.

Pye, K. and J. A. Miller. 1990. Chemical and biochemical weathering of pyritic mudrocks in a shale embankment. Quart. J. of Eng. Geol. 23:365-381.

Quigley, R. M. and R. W. Vogan. 1970. Black shale heaving at Ottowa, Canada. Can. Geo. J. 7: 106-115.

Quigley, R. M, J. E. Zajic, E. McKyes, and R. N. Yong. 1973. Biochemical alteration and heave of black shale; detailed observations and interpretations. Can. J. Earth Sci. 10: 1005-1015.

Raiswell, R. and D. E. Canfield. 1998. Sources of iron for pyrite formation in marine sediments. Am J. Sci. 298: 219-245.

Ritsema, C. J., J. E. Groenenber, and E. B. A. Bisdom. 1992. The transformation of potential into actual acid sulphate soils studied in column experiments. Geoderma. 55:259-271.

Sahat, A. M. and C. W. Sum. 1990. Disintegration of road aggregates along parts of the Gurun-Alor Setar and Ipoh-Changkat Jering highways. Warta Geologi. 16(3):142.

Schaeffer, M. F. and P. A. Clawson. 1996. Identification and treatment of potential acid-producing rocks and water quality monitoring along a transmission line in the Blue Ridge Province, Southwestern North Carolina. Env. and Eng. Geosci.. 2(1): 35-48.

Singer, P. C. and W. Stumm. 1970. Acid mine drainage: rate-determining step. Science. 167: 1121-1123.

Soil Survey Staff. 1998. Keys to Soil Taxonomy. USDA-NRCS. Washington, D.C.

Stone, Y, C. R. Ahern, and B. Blunden. 1998. Acid Sulfate Soils Manual. Acid Sulfate Soil Management Advisory Committee, Wollongbar, NSW, Australia

Swaine, D. J. 1986. The rapid weathering of siltstone. J. and Proc. Royal Soc. of New South Wales. 119: 83-88.

van Holst, A. F. and C. J. W. Westerveld. 1973. Corrosion of concrete foundations in potential acid sulphate soils and subsoils in The Netherlands. p. 373-382. *In* H. Dost (ed.) Acid Sulfate Soils. Proc. Int. Symp. on Acid Sulphate Soils, Wageningen, The Netherlands. 13-20 Aug. 1972. Pub. 18 - Vol. II. Int. Inst. For Land Reclamation and Improvement, Wageningen, The Netherlands.

Vear, A. and C. Curtis. 1981. A quantitative evaluation of pyrite weathering. Earth Surface Processes and Landforms. 6:191-198.

Wilkin, R. T. and H. L. Barnes. 1997a. Formation processes of framboidal pyrite. Geochimica et Cosmochimica Acta. 61:323-339.

Wilkin, R. T. and H. L. Barnes. 1997b. Pyrite formation in an anoxic estuarine basin. Am. J. Sci. 297: 620-650.

Zentilli, M. and D. Fox. 1997. Geology and mineralogy of the Meguma Group and their importance to environmental problems in Nova Scotia. Atlantic Geology. 3(2): 81-85.

Chapter 3

DISTRIBUTION OF SULFIDES IN VIRGINIA: CREATING A STATE-WIDE SULFIDE HAZARD RATING MAP

Introduction

The state of Virginia contains five distinct physiographic provinces. From east to west, these are the Atlantic Coastal Plain, Piedmont, Blue Ridge, Valley and Ridge, and Appalachian Plateau. To the east, the Coastal Plain consists of fluvial and marine sediments. The oldest sediments were deposited unconformably during the Cretaceous Period upon the much older crystalline bedrock of the Piedmont. Overlying Tertiary and Quaternary age sediments dip gently to the east, extending beneath the Chesapeake Bay and Atlantic Ocean. From east to west, the Coastal Plain topography gradually changes from broad, relatively low-lying flat areas to a gently rolling incised landscape. West of the Coastal Plain, the Piedmont province is underlain by Precambrian and Paleozoic igneous and metamorphic rocks, which are folded, faulted, and rife with igneous intrusions. Several remnants of Mesozoic-aged basins are exposed within the Piedmont, and contain sedimentary and volcanic rocks deposited during the early stages of the opening of the Atlantic Ocean. Piedmont topography is characterized by a gently rolling land surface, where long exposure to weathering has eliminated most topographic extremes. Rising abruptly to the west from the Piedmont, the Blue Ridge Province consists of a chain of mountain peaks and uplands of Precambrian and early Cambrian age rocks. The rocks of the Blue Ridge are dominantly igneous and metamorphic, with overlying sedimentary formations exposed along its margins. The oldest bedrock in Virginia crops out in the Blue Ridge, where rocks that are over a billion years old are not uncommon. West of the Blue Ridge, extensively faulted and folded Cambrian through Mississippian aged sedimentary rocks comprise the Valley and Ridge province. Differences in erosional resistance among the tilted rock beds have resulted in the formation of alternating parallel ridges and valleys. The Appalachian Plateau intersects Virginia in only a small region in the extreme southwest part of the state. The Mississipian and Pennsylvanian-aged rock strata are similar to those in the Valley and Ridge, but are relatively non-deformed. In addition, coal is commonly found in beds ranging from a few cm to many m in

thickness. The steep relief in this province has resulted from stream dissection through the horizontal or near-horizontal resistant sandstone-dominated strata.

Sulfidic deposits are found in various geologic and geomorphic settings across the state of Virginia. These settings include unconsolidated sediments in formations of the Coastal Plain, certain slate and phyllite bearing formations in the Piedmont and Blue Ridge, some of the Devonian and Mississippian black shales in the Valley and Ridge, and coal-bearing strata in the coalfields of southwest Virginia. In many of these geologic settings, road construction has resulted in localized acid rock drainage (ARD) that threatens water quality, fill stability, integrity of building materials, and vegetation management. Geologic formations containing microcrystalline sulfide forms, such as pyrite framboids, are particularly problematic because as grain size decreases, the surface area available for acid-producing reactions from a given amount of sulfide increases. Acid rock drainage following construction through formations containing large-grained sulfide crystals has not been documented before this study in Virginia; however, acid drainage does exist in areas where these materials have been mined (Anderson and Robbins, 1998).

Limited references to the aforementioned occurrences of sulfides may be found in the expanded explanation of the Geologic Map of Virginia (Rader and Evans, 1993). Publications describing the occurrence of sulfides in Virginia have typically pertained to mineral prospecting (Conley, 1987; Craig et al., 1977; Hodder and Kazda, 1977; Penick, 1987; Sweet et al., 1989; Young, 1956).; therefore, the documented sulfides are dominantly large-grained. Similarly, for most geologic mapping reports, sulfide occurrence is usually noted only when grains are readily apparent in hand specimens. Only a small part of the state has been covered by large-scale mapping that includes the level of detailed petrographic analyses which is necessary to detect and describe the occurrence of fine-grained, disseminated pyrite (William S.Henika, personal communications). Consequently, the occurrence of fine-grained, disseminated iron sulfides has generally remained undocumented. For example, in geologic mapping northeast of Richmond, Daniels and Onuschak (1974) report that at some locations Miocene transgressive sediments have a sulfurous odor. This is the closest indicator that iron sulfides may be present in these formations, which are now known to extensively contain noticeable levels of framboidal pyrite

(described later in this chapter). Similarly, geologic mapping reports for Hampton (Johnson, 1976) and Suffolk (Coch, 1971) make no mention of sulfides, which are now known to occur in the Tabb formation (described later in this chapter).

Increasing development over the past several years, along with the ever-deepening nature of road cut designs, has resulted in numerous new problem sites throughout the state. The first step in preventing ARD from future road construction is to identify potential acid-producing materials and delineate their boundaries. Sulfide occurrence is a function of geologic setting. If sulfides are identified in numerous rock samples from a specific geologic formation, then the entire formation may be considered as "at risk" for containing sulfides. Therefore, on a statewide scale, delineation of potentially acid materials is best accomplished by identifying the boundaries of sulfide-bearing formations based on the Geologic Map of Virginia. With advance detection, highway corridors could be sited to avoid or minimize exposure of sulfidic materials. When sulfides cannot be avoided, advance knowledge of the nature and extent of these materials will allow for adequate development of remediation procedures.

Materials and Methods

In the fall of 1997, a questionnaire regarding occurrence of acid roadcuts was distributed to all of the Virginia Department of Transportation (VDOT) planning districts (Appendix A). Twenty completed forms were received from around the state by the spring of 1998. All reported sites were visited over the following year. Additional sites were reported later or discovered independently. The location of all sampling sites is indicated in Figure 3.1.

Geologic materials and road drainage grab samples, where available, were collected from all sites. Both fresh and weathered representative samples of lithologies present at each site were obtained using a shovel and immediately sealed in plastic bags. Reduced Coastal Plain sediment samples were stored on dry ice during transport, and placed in a freezer upon arrival at the laboratory. Sample processing is discussed in detail in Chapter 5. Samples of road drainage were collected in 250-ml Nalgene bottles. The bottles were rinsed three times with drainage from the collection site prior to obtaining a sample. Water samples also were collected from a shallow

1. Hampton Roads Center: I-64 and Big Bethel Rd., Hampton
2. I-664 and Rt-17, Suffolk
3. I-664 and Rt-337, Suffolk
4. Otterdam Swamp: north of I-95/Rt-58 intersection, Greensville Co.
5. Near Fort Lee Mil. Res.: N of I-295/Rt-36 intersection, Prince George Co.
6. Proctor's Creek: Rt-288 and Rt-145, Chesterfield Co.
7. Walthall exit: I-95 and Rt- 620, Chesterfield Co.
8. I-295 and Rt-156, Henrico Co.
9. Behind Richmond City Jail
10. E. Main St. and 14th St., Richmond
11. E. Richmond Rd. landfill, Richmond
12. I-295 and Rt-360, Mechanicsville, Hanover Co.
13. Behind Wal-Mart, Mechanicsville, Hanover Co.
14. I-95, milepost 120.5, Spotsylvania County
15. I-95 and Rt-1 bypass, Fredericksburg, Spotsylvania Co.
16. Mine Rd: I-95 and Rt-610.
17. I- 95, milepost 148, Spotsylvania Co.
18. Rt-750 and Rt-735, Floyd Co.
19. Rt-8, between Rt-750 and Rt-705, Floyd Co.
20. I-77, mileposts 21 – 22, Carroll Co.
21. VDOT quarry, Rt-600 bw. Rt-50 and Rt-608, Frederick Co.
22. Rt-250 and Rt-614, Highland Co.
23. I-64, Clifton Forge, Alleghany Co.
24. Numerous sites along Rt-23 near Rt-610, Wise Co.

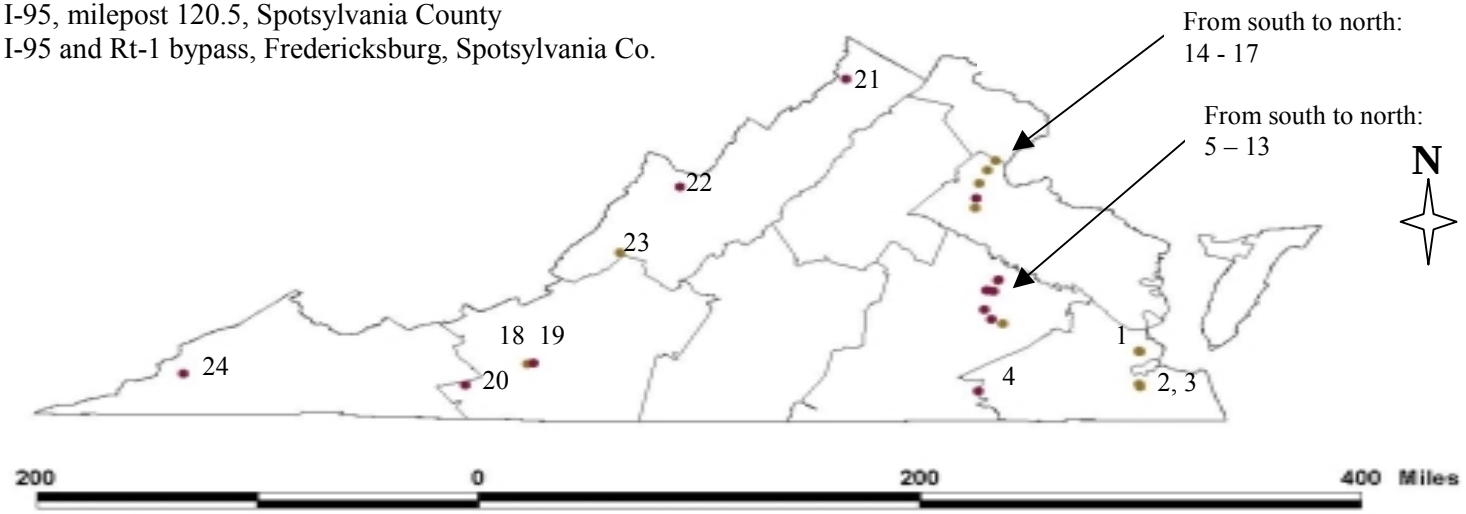

Figure 3.1. Sampling locations from state-wide survey of documented acid-sulfate roadcuts in Virginia with VDOT districts outlined.

well installed at the base of a roadcut along the cloverleaf of Rt-360W to I-295S. The well consisted of three sections. The base, which served as a drainage reservoir, was 36 cm in height and built out of solid PVC pipe. The middle section, through which drainage entered the well, was 66 cm in length and built out of 10-slot PVC pipe. The top section, which prevented entry of surface water, was 38 cm in length and build out of solid PVC pipe. The well was installed so that the top of the middle section lay approximately15 cm beneath the ground surface. The well was evacuated 24 h prior to sample collection. Field descriptions of soil profiles developed in undisturbed material at the top of roadcuts were completed at a number of locations (Appendix B).

The geologic formations and specific rock types at all sites were determined through field observations, personal communications with state geologists, and geologic maps. All geologic samples were tested for potential peroxide acidity (PPA) using the H_2O_2 method of Barnhisel and Harrison (1976), for Total-S using an Elementar Vario Max CNS analyzer, and rated for presence of carbonates by the HCl "fizz test" (Sobek, et al., 1978). Potential acidity procedures are discussed in Chapter 5. Coastal Plain sediments were tested for particle size analysis (PSA) by the pipette method (Gee and Bauder, 1986) and pH in H_2O and KCl using a combination electrode. Surface samples from rock exposures that contained a sufficient amount of soil-sized particles (< 2mm in diameter) also were tested for pH in H_2O and KCl. Water samples were tested for pH and for electrical conductivity (EC) using a Cole-Parmer conductivity meter. Water subsamples were filtered, preserved with HNO_3, and analyzed for Fe, Al, Mn, Cu, Zn, and S concentrations by Inductively Coupled Plasma Emission Spectroscopy (ICPES).

Geologic materials were sampled in detail at two sites to evaluate the heterogeneity of the materials with regards to S levels and PPA. The first site was along the shoulder of the northwest cloverleaf at the interchange of I-295/360 near Mechanicsville. Samples of the Calvert and Eastover Formations of the Chesapeake Group were collected along a grid at horizontal intervals of 4.6 and 9.2 m for 102 m, and at vertical intervals of 1.9 m (starting at 1 m from the base of the roadcut) for 7.3 m (Figure 3.2). The grid was divided into three sections, one central densely sampled area, and two neighboring areas with larger sampling intervals. Surface maps were generated for each section using Excel, and then attached to illustrate the entire sampling area.

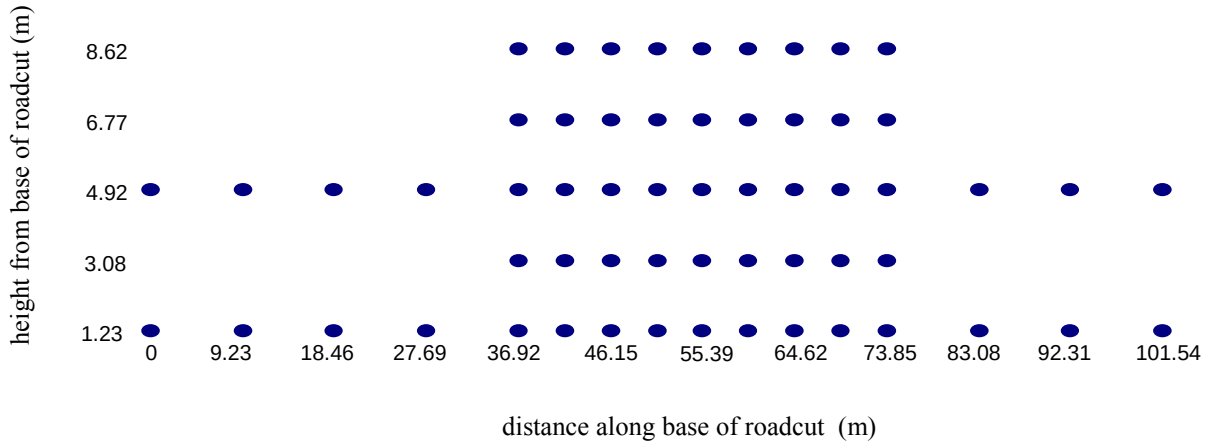

Figure 3.2. Sampling grid for section of roadcut on the shoulder of the cloverleaf from 360W to 295S near Mechanicsville, Virginia.

To approximate depth of weathering for the first few holes, pH was tested at depth intervals of 30 cm using a Hanna conic point combination electrode, inserted directly into moist sediment samples, and a field pH meter. These measurements were used only to estimate pH during field sampling. All reported pH values in this report, unless otherwise indicated, refer to laboratory determined pH. Comparison of field and laboratory pH values is discussed in Chapter 4. The pH of unoxidized sediments typically ranges between 5.5-8.0, whereas the pH of oxidized material is significantly lower. To ensure the material was minimally affected by oxidation, samples were collected below a depth where pH measured 5.5. Samples were collected by augering perpendicular into the exposure and collecting material at approximately 1.4 m. At two locations, samples were collected at 15, 50, 75, and 100 cm into the exposure to characterize depth of weathering. Samples were tested for PPA, total-S, pH in H_2O and KCl, and PSA.

The second detailed sampling site was along Rt-250 in Highland County. Samples of the Millboro shale and Needmore Formation were collected from two sections of the roadcut. Starting at the western extreme of the roadcut, on the shoulder of the westbound lane, samples were collected at a height of 1.5 m from the base of the cut at 6.2 m intervals for 142 m, ending just west of a blanket of riprap. Starting on the eastern edge of the riprap, samples were collected at 15.4 m intervals for 277 m. Samples were tested for PPA and Total-S.

Based on laboratory results for the geologic formations evaluated in this study, and in conjunction with field observations of acid sulfate weathering damage at specific locations, and with consideration of standard vegetation management practices, a sulfide hazard rating scheme was developed with four levels of severity. Ratings are based on the proportion of samples for a given formation with PPA and S values within defined ranges. A state-wide hazard map was produced by i) assigning the appropriate rating to each studied formation, ii) identifying the respective map unit on the Geologic Map of Virginia for each formation, iii) color-coding the four ratings, and iv) applying the code for each formation to its respective map unit on a digital version of the Geologic Map of Virginia using ARCView Geographic Information Systems (GIS) software. An unpublished version of the digital geology map was provided by the Virginia Division of Mines and Mineral Resources (VDMR, 2001). Documented sulfide-bearing formations, not evaluated in this study, are identified on the hazard map with a fifth color code.

Results and Discussion

Locations of documented acid roadcuts, and the geologic formations identified at these sites, are described in Table 3.1 and illustrated in Figure 3.1. All sites exhibited lack of vegetation due to very low pH of surface materials, and numerous sites exhibited iron staining on concrete, deterioration of concrete and metal construction materials (drainage ditches, culverts, and guardrails), iron and aluminum precipitation on streambeds, and sulfate salt efflorescence on roadcut surfaces (Figures 3.3, 3.4, 3.5, 3.6, 3.7, 3.8, 3.9, and 3.10 and see Chapter 1).

Table 3.1. Locations and geologic formations of documented acid roadcuts and excavation sites in Virginia.

City/County	Roadcut location	codes	Geologic formation
Coastal Plain			
Hampton	Hampton Roads Center: I-64 and Big Bethel Rd.	HRC	Tabb, Sedgefield member
Suffolk	I-664 and Rt-17	SUF 1, 2	Tabb, Sedgefield member
Suffolk	I-664 and Rt-337	SUF 3, 4	Tabb, Sedgefield member
Greensville Co.	Otterdam Swamp: north of I-95/Rt-58	ODS	Chesapeake Group
Prince George Co.	Near Fort Lee Mil. Res.: north of I-295/Rt-36 intersection.	FTL	Tertiary marine sediments
Chesterfield Co.	Proctor's Creek: Rt-288 and Rt-145	CHF	Lower Tertiary Deposits
Chesterfield Co.	Walthall exit: I-95 and Rt- 620	WHE	Lower Tertiary Deposits
Henrico Co.	I-295 and Rt-156	HEN	Chesapeake Group
Richmond	Behind Richmond City Jail	JAIL	Chesapeake Group (Calvert)
Richmond	Broad St. and 14th St.	WALL	Chesapeake Group
Richmond	East Richmond Rd. landfill	LF	Chesapeake Group/Lower Tertiary Deposits (Eastover, Calvert, Aquia)
Hanover Co.	I-295 and Rt-360	MCV	Chesapeake Group (Calvert, Eastover)
Hanover Co.	Behind Mechanicsville Wal-Mart	WM	Chesapeake Group
Spotsylvania Co.	I-95, milepost 120.5	SPT	Chesapeake Group/Lower Tertiary Deposits
Spotsylvania Co.	State Farm Insurance: near I-95 and Rt-1 bypass	SFI	Chesapeake Group/Lower Tertiary Deposits
Piedmont			
Stafford Co.	I-95, milepost 148	STF 7	Quantico Formation
Stafford Co.	Mine Rd: I-95 and Rt-610	STF 1-6	Quantico Formation
Blue Ridge			
Floyd Co.	Rt-750 and Rt-735	FL 1-13	Ashe Formation of the Lynchburg Group (Alum phyllite)
Floyd Co.	Rt-8: two roadcuts between Rt-750 and Rt-705	FL 14-22	Ashe Formation of the Lynchburg Group (Alum phyllite)
Carroll Co.	I-77: mileposts 21 - 22	CC	Lynchburg Group of the Ashe Formation
Valley And Ridge			
Frederick Co.	VDOT quarry: Rt-600, bw. Rt-50 and 608	FC	Marcellus shale
Highland Co.	Rt-250 and Rt-614	HC	Millboro, Needmore shales
Clifton Forge	I-64	CF	Millboro shale
Wise Co.	Numerous sites along Rt-23 near Rt-610	WC	Chattanooga shale

Figure 3.3. (a) Exposure of the Tabb formation along I-664 in Suffolk has resulted in extremely acid soil conditions (pH < 3-4), which inhibit the growth of vegetation. (b) Exposure of the Tabb formation during the construction of Hampton Roads Center, in Hampton, has resulted in patchy areas with acid soil conditions (pH 3–5). The water in this sediment pond had a pH of 3.1.

Figure 3.4. Proctor's Creek was redirected due to road construction near the intersection of Rts-288 and 156 in Chesterfield County. The creek was routed into an excavated channel through Lower Tertiary deposits. Extremely acid soil conditions (pH < 2.5), which developed upon oxidation of the sediments, have inhibited vegetation along the stream bank.

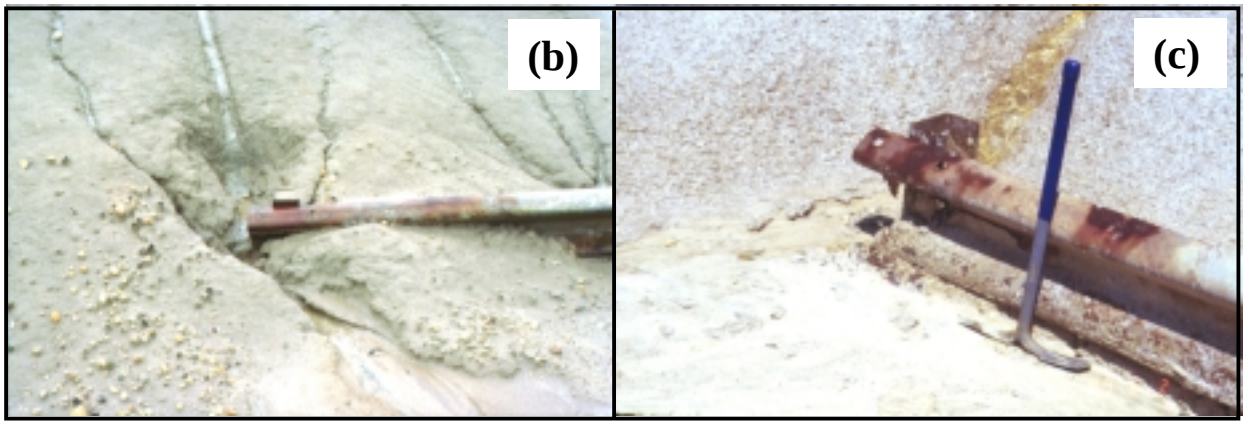

Figure 3.5. (a) This roadcut along the cloverleaf of Rt-360W to I-295S, near Mechanicsville, Virginia, exposes the Eastover and Calvert formations of the Chesapeake Group. Sulfide oxidation has created extremely acid surface soil conditions (pH < 3.5). (b) A few years after construction, erosion began to expose the end of this metal guardrail further, and corrosion is evident. (c) Within 5 years, erosion has removed over 30 cm of sediment and the metal is severely corroded.

Figure 3.6. Acid drainage from the Quantico slate Stafford, Virginia, (see Figure 1.1) has caused extensive iron staining and concrete etching along the curbs and sidewalks of the Hampton Oaks subdivision.

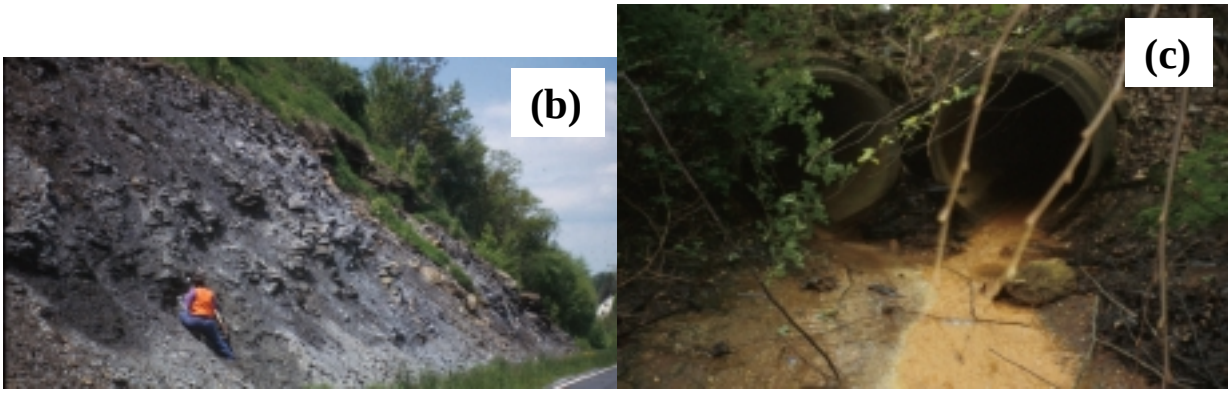

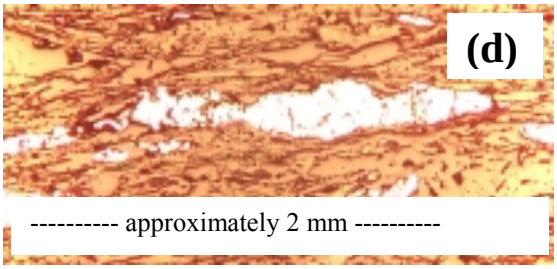

Figure 3.7. (a) This roadcut along I-77 in Carroll County exposes sulfidic rocks within the Lynchburg group of the Ashe formation. Extremely acid surface soil conditions (pH 3.5 – 4.5) inhibit vegetation. (b) This roadcut along Rt-750 in Floyd County also exposes the Lynchburg group. (c) Drainage from the Rt-750 roadcut drains to the culvert on the right, and has consistently had pH values between 2.5 – 4.0. The streambed is coated with iron and aluminum precipitates for at least 30 m downstream of the culvert. (d) Acid drainage from the Rt-750 roadcut is produced from the oxidation of pyrrhotite, which appears as the bright phase in this picture of a polished section using reflected light microscopy.

Figure 3.8. (a) This roadcut along Rt-250 in Highland County exposes the Millboro shale and Needmore formation. Iron staining and concrete etching are evident along the base of the roadcut. (b) The rock pick is leaning against a septarian concretion in the Millboro shale, which contains pyrite veins visible in hand specimens.

Figure 3.9. Acid drainage from the Millboro shale, exposed along I-64 in Clifton Forge, has decimated this stream. The pH of water samples from the downstream end of the culvert has ranged from 2.9 to 7.1. Iron and aluminum precipitates coat the stream bed, and concrete joints within the culvert have been degraded.

Figure 3.10. White sulfate precipitates are evident in fractures in these rocks from the Chattanooga shale, which is exposed along Rt-23 in Wise County.

Coastal Plain

Results from analyses of geologic materials and drainage from acid roadcuts in the Coastal Plain are presented in Tables 3.2 and 3.3. Schematic diagrams of detailed sampling locations are shown in Figures 3.11 and 3.12. Acid sulfate weathering problems in the Coastal Plain primarily result from exposure of unconsolidated Tertiary marine sediments, particularly those mapped as the Chesapeake Group and Lower Tertiary deposits. These sediments occur in drab shades of green, blue and gray, and consist of fine- to coarse-grained, quartzose sand, silt, and clay that is variably shelly, diatomaceous, and glauconitic (Rader and Evans, 1993). Formations of the Chesapeake Group include Chowan River, Yorktown, Eastover, St. Mary's, Choptank, and Calvert. Formations of the Lower Tertiary deposits include Brightseat, Aquia, Marlboro, Nanjemoy, Piney Point, and Chickahominy. Of these formations, the Eastover and Calvert specifically have been identified as being acid-forming at the I-295/360 interchange, behind the Richmond City Jail, and along Proctor's Creek at Rts-288/145. The Eastover, Calvert, and Aquia formations have been identified at the East Richmond Road Landfill (R. Berquist and G. Johnson, personal communication). Although the expanded explanation for the Geologic Map of Virginia describes abundant, finely crystalline iron sulfide only in the Chickahominy Formation, the occurrence of sulfides in many other Tertiary marine formations has been well documented in this study, and in Maryland by Valladares (1998). Reflected light microscopy of polished sections from numerous samples of Tertiary marine sediments indicates that sulfides occur as abundant dispersed framboids, clusters of microcrystals, and small, weathered, subhedral grains of pyrite (Figure 3.13). All forms were present in all samples, and no major differences in morphology or grain size were noted among the samples.

Analysis of samples from twenty-three deep borings (see Chapter 4) throughout an area of approximately 55 square miles northeast of Richmond indicates that completely reduced sediments have pH values ranging from approximately 5.5 – 8.0, PPA values ranging from approximately 30-50 Mg $CaCO_3$/1000 Mg material, and Total-S values ranging from approximately 1.0 – 2.5%. Relatively high S values (> 0.2%) were found at all locations indicating that S occurrence may be ubiquitous in the Chesapeake Group. Sediments containing carbonates have lower PPA values, generally ranging from 0 – 20 Mg $CaCO_3$/1000 Mg material,

Table 3. 2. Characteristics of geologic material from acid roadcuts in the Coastal Plain.

Sample	Depth cm	pH H_2O	pH KCl	PPA*	% Clay	% Silt	% Sand	% S	Fizz test	Sample Description
Tertiary marine sediments										
CHF3	2-20	2.23	2.11	22.7	9	18	73	1.16	0	Creek bank, about 50 ft upstream of culvert.
CHF4	20-60	2.24	2.21	53.6	4	23	73	2.33	0	Below chf3
CHF5	60-120	2.25	2.25	41.7	4	23	73	1.67	0	Below chf4
CHF6	0-20	2.13	2.15	48.2	2	31	67	1.72	0	Creek bank, about 50 ft upstream of culvert.
CHF7	20+	2.18	2.20	46.3	4	19	78	1.75	0	Below chf6
FTL1	0-2.5	4.92	4.12	0.0	18	15	68	0.05	0	Cutslope into wetland off of I-295
FTL1	2.5-28	4.68	3.58	1.9	22	12	66	0.05	0	Same as above
FTL1	28-74	3.78	3.27	62.4	19	24	57	1.20	0	Same as above
FTL1	74-91	3.74	3.35	2.9	21	19	60	0.37	0	Same as above
FTL1	91-124	3.15	2.86	5.4	22	16	62	0.05	0	Same as above
FTL1	124-134	4.10	3.52	3.7	15	21	64	0.05	0	Same as above
FTL1	134-210	4.74	3.46	2.4	26	16	58	2.00	0	Same as above
FTL2	0-15	3.2	3.02	7.4	21	16	64	0.23	0	Median, I-295
FTL2	15-50	3.17	3.01	6.3	22	16	62	0.18	0	Same as above
FTL2	50-70	4.08	3.46	16.2	21	16	63	0.49	0	Same as above
FTL2	70-170	3.56	3.38	11.5	19	16	65	0.34	0	Same as above
FTL2	170-210	3.13	2.88	3.2	15	17	68	0.08	0	Same as above
FTL2	210-280	3.48	3.29	44.6	25	14	61	1.64	0	Same as above
HEN1	2-20	2.60	2.39	11.3	7	15	78	0.50	0	I-295, just N of exit 31A to 156.
HEN2	20+	2.42	2.36	17.8	3	5	92	0.88	0	Material below HEN1
HEN3	2-20	2.73	2.60	5.5	7	11	82	0.20	0	Same cut as HEN1
HEN4	20+	2.51	2.44	16.2	3	7	90	0.68	0	Material below HEN3
JAIL1	0-30	2.89	2.63	28.9	n.d.	n.d.	n.d.	0.80	0	Cut behind jail, S end
JAIL2	0-30	3.04	2.91	n.d.	n.d.	n.d.	n.d.	1.22	0	Cut behind jail, N end
JAIL3	0-30	3.14	3.06	7.7	n.d.	n.d.	n.d.	0.25	0	Behind jail
MCV2	10	2.91	2.46	10.0	30	26	44	0.36	0	Perpendicular boring into roadcut surface
MCV2	50	2.49	2.29	10.0	21	32	47	0.44	0	Same as above
MCV2	75	3.04	2.92	33.6	17	28	55	1.16	0	Same as above
MCV2	100	3.42	3.19	40.1	20	32	49	1.10	0	Same as above
MCV3	0	3.26	2.18	12.5	29	30	41	0.34	0	Same as above
MCV3	15	2.96	2.33	7.53	27	19	54	0.24	0	Same as above
MCV3	50	3.33	3.04	32.6	16	21	63	1.10	0	Same as above
MCV3	75	4.25	3.76	32.1	11	37	52	1.14	0	Same as above
MCV3	100	5.12	4.56	32.6	14	26	60	1.13	0	Same as above
ODS3	0-15	2.72	2.42	12.9	8	44	48	0.41	0	I-95 wetland, about 100 ft from water.
ODS4	15-25	2.29	2.17	22.2	4	30	66	0.89	0	Beneath ODS4
SFI1	0-10	2.86	2.69	12.3	n.d.	n.d.	n.d.	0.45	0	Lot near SFI
SPT1	5-12	2.49	2.25	12.4	n.d.	n.d.	n.d.	0.39	0	Shoulder cut bank, I-95S
SPT1	12-30	2.74	2.22	36.8	13	50	37	0.87	0	Shoulder cut bank, I-95S
SPT1	30-50	2.86	2.38	39.1	45	37	18	1.12	0	Shoulder cut bank, I-95S
SPT2	0-5	2.44	2.02	17.9	11	25	64	0.43	0	Shoulder cut bank, I-95S
SPT3	4-24	2.5	2.25	14.4	10	17	73	0.24	0	Shoulder cut bank, I-95S
SPT3	24-30	n.d.	n.d.	30.6	n.d.	n.d.	n.d.	1.01	0	Shoulder cut bank, I-95S
WAL1	0-20	5.37	4.73	13.7	8	30	62	1.03	0	Retaining wall, Broad and 14th St.
WAL2	0-20	4.69	4.72	13.9	6	22	78	1.01	0	Retaining wall, Broad and 14th Ss.
WHE1	0-10	2.61	2.5	21.6	16	9	75	0.87	0	Walthall exit, I-95

Table 3.2 (continued)

Sample	Depth cm	pH H_2O	pH KCl	PPA*	% Clay	% Silt	% Sand	% S	Fizz test	Sample Description
WHE1	125	3.65	3.07	28.4	10	12	78	1.25	0	Walthall exit, I-95
WHE2	0-10	2.6	2.54	15.3	9	11	80	0.67	0	Walthall exit, I-95
WHE2	125	3.53	3.07	31.3	9	16	74	1.02	0	Walthall exit, I-95
AVERAGE (n=49)		**3.21**	**2.88**	**20.9**				**0.79**		
Tabb Formation										
HRC1	2-8	3.87	3.5	3.0	11	11	78	0.11	0	Bank of lake 1 at HRC
HRC2	8-18	4.14	3.77	0.5	4	5	91	0.05	0	Below HRC1
HRC3	0-18	4.58	3.95	6.0	16	21	63	0.10	0	Bank of lake 2 at HRC
HRC4	18-45	4.25	3.89	2.0	5	10	85	0.04	0	Material below HRC3
HRC5	40-50	4.33	3.38	2.0	16	25	59	0.08	0	Gully leading to lake 2
HRC7	0-15	3.38	3.12	1.5	7	7	86	0.05	0	Stockpiled material
SUF1	10-30	3.32	3.23	4.5	14	20	66	0.17	0	64E near mp 18
SUF2	5-20	3.75	3.48	2.5	13	19	68	0.10	0	64E near mp 18, better vegetated
SUF3	0-15	3.39	3.35	4.0	11	19	70	0.16	0	64E, next exit from SUF1
SUF4	0-15	3.28	3.15	5.5	14	16	70	0.12	0	64E, next exit from SUF1
AVERAGE (n=10)		3.83	3.48	3.2				0.10		

* $MgCaCO_3$/1000 Mg material

Table 3. 3. Water quality data from acid roadcuts in the Coastal Plain (specific locations for MCV samples are shown in Figure 3.11).

Sample	pH	EC	acidity	Fe	Al	Mn	Cu	Zn	S	Sample Description
		mmhos /cm	mg $CaCO_3$/L	mg/L						
Tertiary marine sediments										
CHF1	6.14	0.08	n.d.	n.d.	n.d.	n.d.	n.d.	n.d.	n.d.	Rts-288/145, 200 ft downstream from culvert.
CHF2	6.68	0.07	n.d.	n.d.	n.d.	n.d.	n.d.	n.d.	n.d.	Rts-288 and 145, upstream of culvert.
ODS1	3.93	0.28	n.d.	n.d.	n.d.	n.d.	n.d.	n.d.	n.d.	4ft from edge of water
ODS2	2.93	1.30	n.d.	n.d.	n.d.	n.d.	n.d.	n.d.	n.d.	Puddle near water
MCV1.1	3.16	n.d	226	17.5	12.1	2.1	<0.004	0.3	348	360E /295N, well at base of cut (fall)
MCV2.1	2.71	n.d	350	0.2	0.9	0.2	<0.004	<0.025	32	360E /295N, culvert outlet in cloverleaf (fall)
MCV3.1	2.62	n.d	336	0.9	0.9	0.9	<0.004	<0.025	26	360E /295N, drainage in cloverleaf (fall)
MCV1.2	3.09	n.d	416	13.9	49.5	2.1	<0.004	0.9	298	Same as MCV1.1 (spring)
MCV2.2	3.91	n.d	258	0.2	36.4	1.2	<0.004	0.8	198	Same as MCV2.1 (spring)
MCV3.2	6.91	n.d	14	0.1	0.3	0.8	<0.004	<0.025	34	Same as MCV3.1 (spring)
MCV4	3.60	0.71	n.d.	0.6	17.5	0.8	0.008	0.3	86	Ditch on exit ramp 295S to 360W.
MCV7	6.20	1.48	n.d	n.d	n.d	n.d	n.d	n.d	n.d	Between MCV2 and stream.
MCV8	6.55	0.11	n.d	n.d	n.d	n.d	n.d	n.d	n.d	Stream, base of cloverleaf.
SFI3	3.50	0.50	n.d	0.6	8.3	0.3	<0.004	0.1	41	pond near State Farm Insurance
Tabb Formation										
HRC6	3.05	1.142	n.d.	12.4	15.2	2.4	<0.004	0.6	136	Drainage puddle off of stockpiled material
HRC8	3.09	0.708	n.d.	2.1	7.0	0.5	<0.004	0.3	60	Lake 2
HRC9	4.20	0.498	n.d.	0.1	0.5	0.8	<0.004	0.2	76	Lake 1

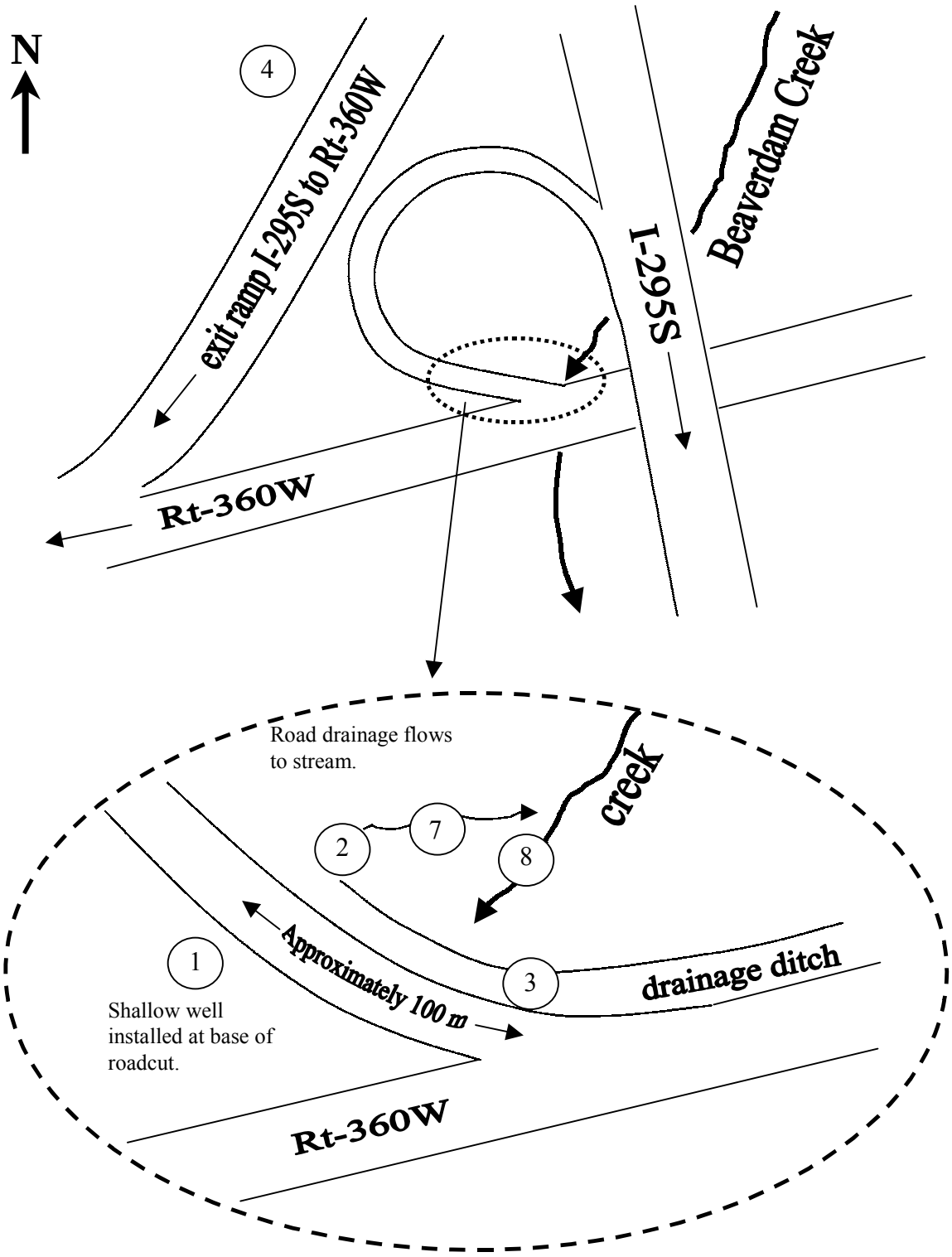

Figure 3.11. Schematic diagram of sampling from shoulder of cloverleaf from 360W to 295S near Mechanicsville. Circled numbers refer to MCV drainage samples described in Table 3.3.

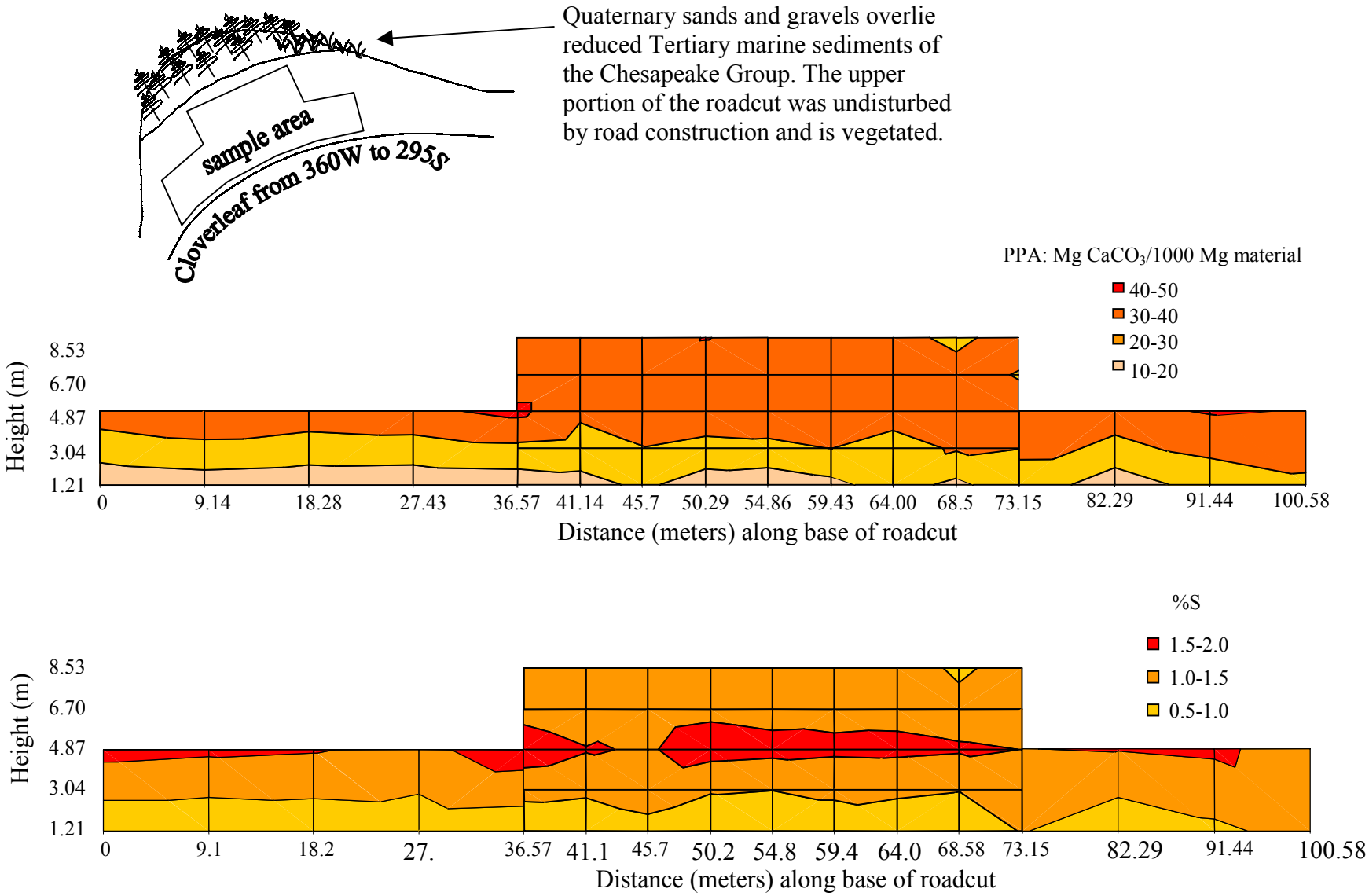

Figure 3.12. Potential peroxide acidity (PPA) values and % S from detailed sampling along the shoulder of the cloverleaf from Rt 360W to I-295S.

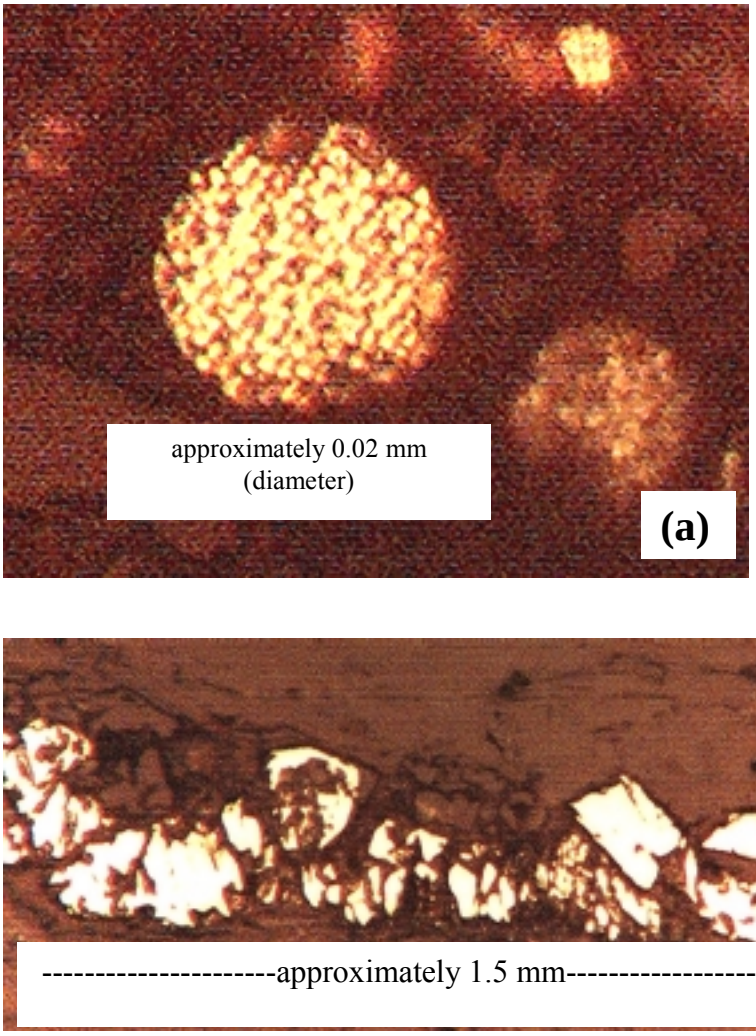

Figure 3.13. (a) Pyrite framboid from the Chatanooga shale in Wise County. (b) Subhedral grains of pyrite in a veinlet from the Millboro Shale in Highland County.

and were found in only few samples from deep borings and not in acid road banks. This suggests one of the following: i) carbonate-bearing layers in the Tertiary marine sediments tend to occur at greater depths, ii) excavation through carbonate-bearing sediments does not result in severe ARD, or iii) carbonates have been leached out of existing roadcuts by acid drainage.

Upon exposure, sulfide oxidation causes pH to decrease rapidly. Weathered materials at the surface of roadcuts through the Chesapeake Group and Lower Tertiary deposits typically appear yellowish-brown, have pH values between 2.5 – 3.5, have PPA values between 10-20 Mg $CaCO_3$/1000 Mg material, and retain less than 1% S. Less oxidized, underlying gray sediments have slightly higher pH values and much higher PPA values, ranging from about 30-50 Mg $CaCO_3$/1000 Mg material. Examples of changes with depth of weathering are best observed in samples MCV2, MCV3, WHE1, and WHE2 (Table 3.2, Figure 3.14). Samples from the I-295/360 interchange which was constructed approximately 20 years ago, indicate that within 50 to 75 cm from the surface the sediments are yellowish-brown in color, have pH values below 3.5, and PPA values below 15 Mg $CaCO_3$/1000 Mg material. Below this upper weathering surface, a transition zone exists for about 75 to 100 cm where the material is grayer with few yellow jarosite mottles and/or red redoximorphic features. Moving down through this zone, pH steadily increases and PPA values are high (> 30 Mg $CaCO_3$/1000 tons material). Below the transition zone, at depths greater than 120 cm, the material is uniformly dark gray, has relatively high pH values (> 5.5), and high PPA values indicating that the material has been minimally affected by oxidation. Qualitative observations during detailed sampling of the roadcut indicated that this sequence was uniform over the entire roadcut.

Sediments from the Calvert and Eastover Formations of the Chesapeake Group, along the shoulder of the cloverleaf from Rt-360E to I-295S, also were sampled in detail. A photograph of the roadcut is shown in Figure 3.5. Sulfide levels across the roadcut (Figure 3.12) are relatively homogenous laterally, but somewhat variable vertically. The S values increase from 0.5-1.0% at the base of the outcrop to 1.0-1.5 for the upper half of the acid portion of the roadcut (non-acid Quaternary sediments overlie parts of the roadcut). A discontinuous band of higher-S material (1.5-2.0%) runs laterally along the middle of the sampling area, approximately 5m up from the base of the roadcut. Similarly, the PPA values increase from 10 –20 Mg $CaCO_3$/1000 Mg

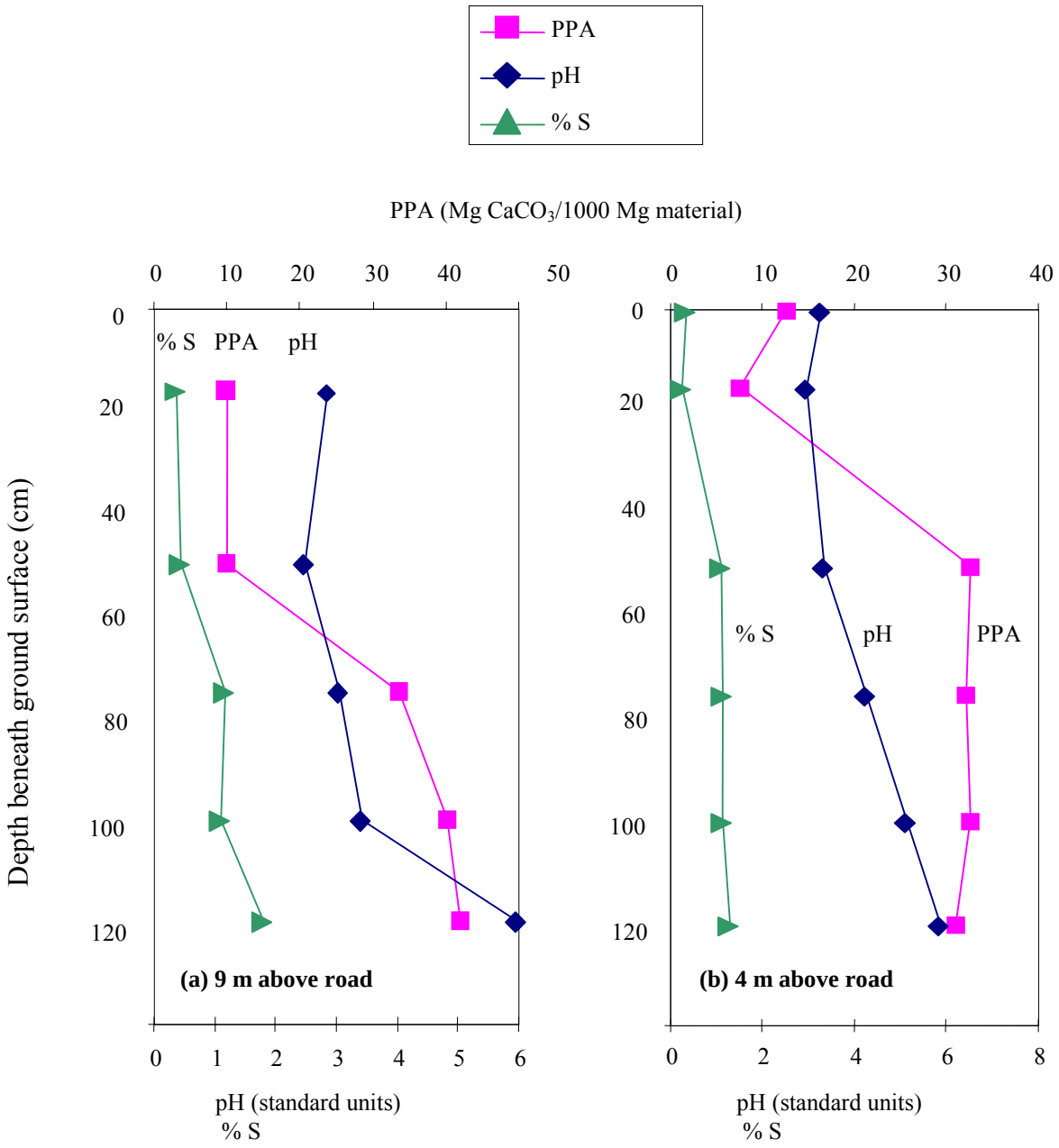

Figure3.14. Profiles showing potential peroxide acidity (PPA), % S, and pH versus depth for shallow borings perpendicular to the roadcut surface along the cloverleaf from 360W to 295S near Mechanicsville, Virginia: (a) approximately 9 m up from base of roadcut, (b) approximately 4 m up from base of roadcut. Values at 120 cm are estimated from detailed sampling (Figure 3.12).

material at the base of the roadcut to 30-40 Mg $CaCO_3$/1000 Mg material for the upper half. A few locations, corresponding to the pockets of high-S material, had values ranging between 40-50 Mg $CaCO_3$/1000 Mg material.

Road drainage, collected at various locations throughout the northwest portion of the I-295/360 interchange, exhibited very low pH (< 4.0) except for one sample (Table 3.3, Figure 3.11). A previous sample collected at the same location did have a low pH. Samples collected from a shallow well installed at the base of the outcrop represent the most concentrated road drainage. These samples exhibited high levels of Fe, Al, Mn, and S. In comparison to EPA effluent limitations for coal-mine drainage (Table 3.4), Fe significantly exceeded the daily maximum load and Mn exceeded the 30-day average load. Samples from the outlet of a culvert on the other side of the road indicate that the drainage is diluted as it flows towards a local stream, although pH is still very low and Al and S values are relatively high. Water samples from Proctor's Creek at Rts-288 and 145 in Chesterfield County have moderate pH values and low EC values, suggesting that ARD from the sediments is sufficiently diluted by channel throughflow, which limits adverse effects on water quality.

Table 3.4. EPA Best Available Technology for Coal Mine Drainage. (40 CFR 434)

Parameter	One Day Maximum	30 Day Average
Total Iron (mg/L)	7	3.5
Total Manganese (mg/L)	4	2
pH	6-9	6-9

Acid sulfate weathering problems are less severe at a few sites that are surficially mapped as the Sedgefield member of the Tabb formation. The Sedgefield member consists of fossiliferous brackish-bay sand, beach and near-shore marine clayey sand, and lagoonal and marsh clay and clayey sand. Reflected light microscopy of a polished section from material collected at Hampton Roads Center (HRC3) revealed few, small, dispersed, subhedral grains of pyrite. The presence of sulfides in this formation is not identified in detailed local geologic mapping of the area (Johnson, 1976) or in the expanded explanation for the Geologic Map of Virginia (Rader and Evans, 1993). Based on this work, and one previous study (Daniels et al., 1995), sulfides appear to occur in discontinuous pockets throughout the Sedgefield member of

the Tabb formation. Alternatively, depending on the thickness of the Tabb at a given location, sulfides may be exposed from the underlying Shirley Formation

Sediment samples, believed to be from the Sedgefield member, collected from two roadcuts in Suffolk, and a construction site in Hampton (Figure 3.3), had pH values ranging from 3.2 – 4.6, PPA values ranging up to 6.00 $MgCaCO_3$/1000 Mg material, and sulfur values less than 0.2%. Previous sampling at Sandy Bottom Nature Park (also known as Chisman Lakes) indicated, with few exceptions, that materials generally had PPA values under 10 Mg $CaCO_3$/1000 Mg material and contained less than 0.2% sulfur (Daniels et al., 1995). Qualitative field observations at the two Suffolk roadcuts indicate that severe soil compaction also may limit vegetation growth. Samples could not be collected from deeper than 0.2m because the material was too compact to penetrate with a shovel. Water samples from two small lakes at Hampton Roads Center (adjacent to Sandy Bottom Nature Park) had low pH values around 3 – 4, moderate EC values, and relatively low metal concentrations (Table 3.3). Water drainage from a stockpile of excavated material at the same site had a very low pH, high EC, and high levels of Fe, Al, Mn and S. In comparison, water samples from two small lakes had slightly higher pH values, and lower EC and metal concentrations.

As a rule of thumb, materials with PPA values below 10 Mg $CaCO_3$/1000 Mg are readily reclaimed with proper management, while materials with PPA values between 10 - 60 require intense reclamation management (Daniels et al., 1995). Considering these guidelines, and the widespread occurrence of S through the Chesapeake Group and Lower Tertiary deposits, exposure of Tertiary marine sediments may be considered highly likely to produce problematic roadside management conditions which require intense reclamation efforts. Exposure of the Sedgefield member of the Tabb formation may be considered likely to produce moderately problematic roadside vegetation management conditions, which could require special reclamation efforts.

Piedmont

Results from analyses of geologic materials and road drainage at acid roadcuts in the Piedmont are presented in Tables 3.5 and 3.6. A schematic diagram of sampling locations is shown in Figure 3.15. Acid roadcuts along I-95 and Mine Road (Rt 610) in Stafford occur in pyritic phyllite and slate of the Quantico Formation. Reflected light microscopy of polished sections from Mine Road (STF1:15-30cm and STF4:1-5cm) revealed the presence of pyrite as corroded subhedral and euhedral grains, along with chalcopyrite and covellite (Figure 3.13, and see Chapter 5). Microcrystalline forms, such as those described for Coastal Plain sediments, were not observed. The PPA values for surface samples ranged from 6 – 22 Mg $CaCO_3$/1000 Mg material, and S values ranged from 0.24 – 1.00%. One sample from relatively unweathered underlying material had a significantly higher PPA value, 99 Mg $CaCO_3$/1000 Mg material, and contained over 3.8% S. Previous analysis of six samples collected by VDOT at Mine Road revealed PPA values ranging from 1 - 85 Mg $CaCO_3$/1000 Mg material. Based on these values, sulfides appear to be unevenly distributed throughout the roadcut; however, more detailed sampling would be necessary to characterize this spatial variability.

Drainage samples collected along the base of Mine Road had very low pH values, and high EC and metal concentrations (Table 3.6). Extensive iron-staining and concrete etching are evident along drainage ditches at the base of this roadcut, and throughout an adjacent neighborhood (Figure 3.6). Nonetheless, one water sample from the vicinity of where road drainage enters a local stream had neutral pH and low EC and metal concentrations, indicating that acid road drainage may be sufficiently diluted so as to limit adverse effects on surface water quality. Neutralization reactions between acid drainage and concrete may also decrease acidity.

Compared to sulfidic sediments of the Coastal Plain, sulfide levels in the Quantico Formation appear to be more variable and occur over a much larger range of S values. With one exception, drainage from this site had lower EC, and higher acidity and metal concentrations, than any other evaluated roadcut. Exposure of the Quantico Formation may be considered highly likely to produce severely problematic roadside management conditions, which require intense reclamation efforts. Roadcut surfaces of the Quantico Formation may be quite steep and generally consist of shallow, rocky, weathered material over bedrock, and rock outcrops, which

are less suited for standard soil remediation methods than the unconsolidated sediments of the Coastal Plain.

Table 3.5. Characterization of geologic materials from acid roadcuts in the Piedmont.

Sample	Depth (cm)	pH H_2O	pH KCl	PPA*	% S	Fizz Test	Sample Description
STF1	0-10	4.23	3.70	11.1	0.66	0	Weathered material, Mine Road
STF1	10-15	2.74	2.22	11.4	0.71	0	Less weathered material, Mine Road
STF1	15-30	n.d.	n.d.	99.0	3.85	0	Least weathered material, Mine Road
STF4	0-5	2.58	2.16	17.5	0.85	0	Weathered material, Mine Road
STF4	5-15	n.d.	n.d.	6.0	0.24	0	Weathered parent material, Mine Road
STF7	0-5	n.d.	n.d.	6.0	0.35	0	Weathered material, cutbank, 95S, mile 148
STF7	5-15	n.d.	n.d.	21.6	1.00	0	Weathered material, cutbank, 95S, mile 148
1	n.d.	n.d.	n.d.	25	n.d.	n.d.	These six samples were analyzed for VDOT in 1994 by the Soil Survey and Mine Land Reclamation Laboratory in the Department of Crop and Soil Environmental Sciences at Virginia Tech.
2	n.d.	n.d.	n.d.	1	n.d.	n.d.	
3	n.d.	n.d.	n.d.	70	n.d.	n.d.	
4	n.d.	n.d.	n.d.	85	n.d.	n.d.	
5	n.d.	n.d.	n.d.	61	n.d.	n.d.	
6	n.d.	n.d.	n.d.	11	n.d.	n.d.	
AVERAGE (n=13, 7)				**32.7**	**1.09**		

*Mg $CaCO_3$/1000 Mg material

Table 3.6. Water quality data from acid roadcuts in the Piedmont.

Sample	pH	EC	acidity	Fe	Al	Mn	Cu	Zn	S	sample
		mmhos/cm	mg $CaCO_3$/L	mg/L						
STF2	2.82	1.67	n.d.	64.1	20.5	4.8	0.1	1.1	228	Mine Road
STF3	2.47	3.19	1465	249.3	46.2	18.0	0.6	3.2	548	Mine Road
STF5	2.74	1.59	n.d.	13.4	24.4	1.4	0.1	0.7	140	Mine Road
STF6	2.49	2.86	n.d.	175.9	32.9	10.1	0.2	2.7	407	Mine Road
STF10	2.61	3.27	n.d.	114.2	66.9	17.4	0.4	3.5	639	Mine Road
STF11	7.14	0.32	n.d.	<0.1	<0.1	0.1	<0.002	<0.004	12	Mine Road
STFn1	2.27	n.d.	2069	494.3	74.9	20.9	0.3	6.6	828	Mine Road
STFf1	2.36	n.d.	1238	91.4	35.8	9.3	0.1	2.7	352	Mine Road
STFn2	2.61	n.d.	990	189.9	34.6	10.2	0.2	2.9	400	Mine Road
STFf2	2.70	n.d.	935	245.2	36.4	11.3	0.2	3.2	431	Mine Road
STF8	4.33	0.37	n.d.	0.5	0.9	0.2	<0.002	0.1	26	Rt-630 exit off I-95N

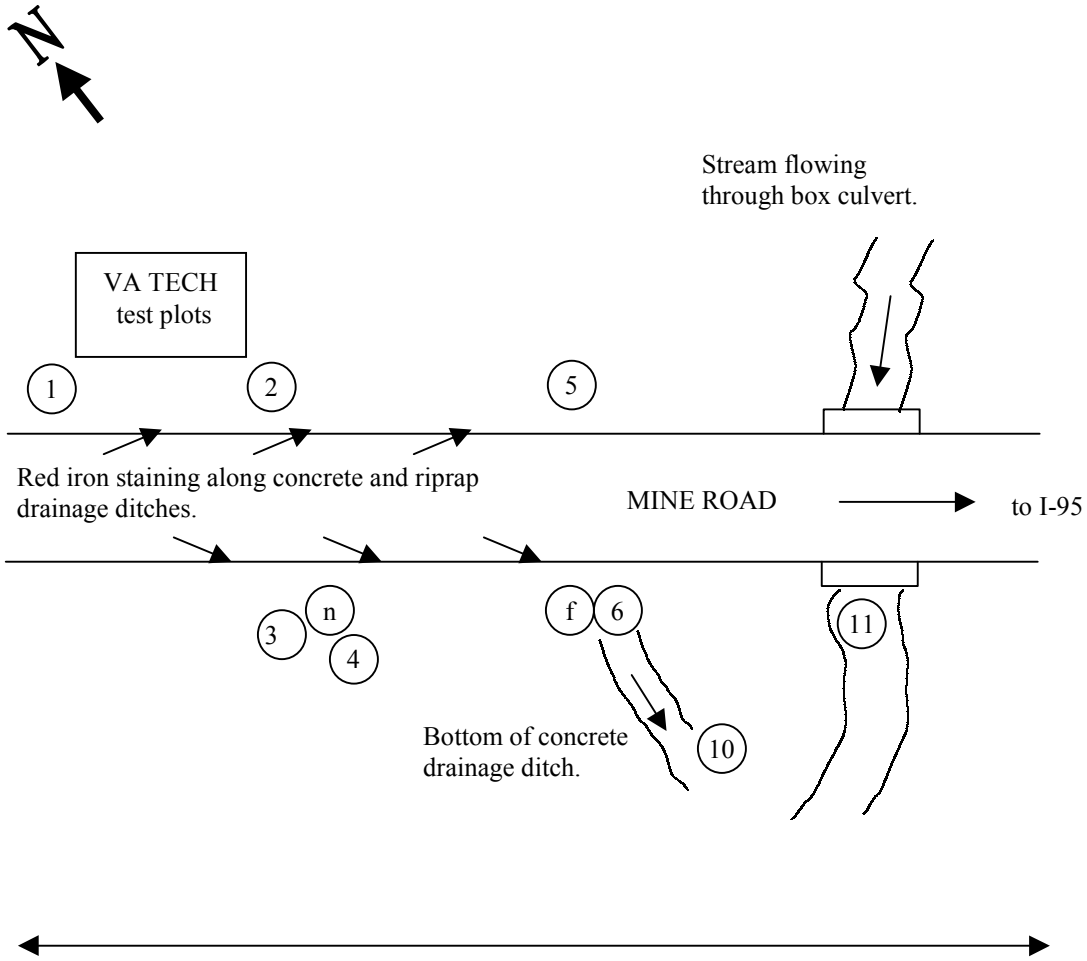

Figure 3.15. Schematic diagram of sampling for Mine Road, Stafford, Virginia. Circled numbers and letters refer to STF samples described in Tables 3.5 and 3.6.

Blue Ridge

Results of analyses for geologic material and road drainage from acid roadcuts in the Blue Ridge are presented in Tables 3.7, 3.8, and 3.9. Schematic diagrams of sampling locations are shown in Figures 3.16 and 3.17. Acid roadcuts along Rt-8 and Rt-750 in Floyd County, and along I-77 in Carroll County, occur in the Ashe Formation of the Lynchburg Group. The rock exposed in Floyd County is mapped locally as the Alum Phyllite (Dietrich, 1959). The Ashe Formation consists of amphibolite, gneiss, schist, and phyllite. The roadcuts in both Floyd and Carroll County are dominantly a steel-gray, fine-grained phyllite with pods of amphibolite and calcsilicate gneiss. Efflorescent sulfate coatings are common on the Floyd County exposures, but minimal along the Carroll County roadcuts. Reflected light microscopy of polished sections from Floyd (FL9, FL19) indicates the presence of polycrystalline, lamellar aggregates of pyrrhotite, small pyrrhotite inclusions within sphalerite, small, subhedral grains of pyrite, and few, scattered, anhedral masses of chalcopyrite (Figure 3.13, and see Chapter 5). Of the sampled roadcuts in Virginia, this was the only occurrence of pyrrhotite, which reacts more rapidly than pyrite but produces less acidity on a molar basis. Polished sections from Carroll County indicate the presence of coarse grains and veinlets of pyrite, anhedral grains of chalcopyrite and sphalerite, and lathes of graphite. The PPA values for Carroll County ranged from 0.93 to 9.26 Mg $CaCO_3$/1000 Mg material and S values ranged from 0.06 – 0.36%. For Floyd County, PPA values ranged from 0.48 – 17.54 Mg $CaCO_3$/1000 Mg and S ranged from 0.05 to 1.93%.

Water drainage from the Rt-750 roadcut has significantly impacted a local stream, and a fish pond on a neighboring property (Figure 3.7). Shortly after the roadwork was completed, a neighboring landowner reported the death of fish in his pond downstream from the road drainage culvert. As indicated in Tables 3.8 and 3.9, and Figure 3.16, water sampling by VDOT over the past fourteen years, in addition to sampling for this study, indicates that water from the source spring upstream of the roadcut has maintained pH values ranging from 5.8 to 7.1 (Paul Johnson, personal communication). Water grab samples from the upstream end of the culvert draining to the fishpond have consistently tested at pH values below 4.0. Three water samples (FL4-1(1) – (3)) from the downstream end of the culvert indicate high levels of Fe, Al, and Mn. Iron and aluminum precipitates heavily coat the streambed for at least 30 m downstream of the culvert.

Table 3.7. Characterization of geologic materials from acid roadcuts in the Blue Ridge.

Sample	Depth (cm)	pH (H_20)	pH (KCl)	PPA	% S	Fizz Test	Sample Description
CC2	0-10	3.54	3.37	6.95	0.28	0	SBL I-77
CC3	0-10	4.42	4.06	1.38	0.25	0	SBL I-77
CC4	0-10	3.91	3.51	0.92	0.06	0	SBL I-77
CC7	0-10	3.90	3.51	1.85	0.09	0	SBL I-77
CC8	10	n.d.	n.d.	9.26	0.41	0	SBL I-77
CC13	0-10	n.d.	n.d.	7.41	0.36	0	NBL I-77
CC15	0-10	3.62	3.24	9.23	0.26	0	NBL I-77
CC16	0-10	n.d.	n.d.	4.62	0.24	0	NBL I-77
CC17	10	n.d.	n.d.	0.93	0.08	0	NBL I-77
AVERAGE				4.72	0.22		
FL1-1	0-10	4.25	3.94	2.35	0.46	0	rt-750
FL1-2	0-10	n.d.	n.d.	6.44	0.20	0	rt-750
FL1-3	0-10	5.03	4.76	0.94	0.29	0	rt-750
FL1-4	0-10	n.d.	n.d.	5.65	0.25	0	Rt-750
FL9	0-10	n.d.	n.d.	17.54	1.93	1	Rt-750
FL10	0-10	n.d.	n.d.	6.92	0.41	0	Rt- 750
FL11	0-10	n.d.	n.d.	0.48	0.09	0	Rt-750
FL13	0-10	n.d.	n.d.	0.50	0.39	0	Rt-750
FL17	0-10	3.21	3.02	3.48	0.24	0	NBL rt-8
FL18	0-10	n.d.	n.d.	4.32	0.05	0	NBL rt- 8
FL19	0-10	3.85	3.41	5.47	0.52	0	NBL rt-8
FL20	10	n.d.	n.d.	4.8	0.04	0	NBL rt-8
AVERAGE				4.9	0.40		

Table 3.8. Water quality data from acid roadcuts in the Blue Ridge (see Figures 3.16 and 3.17 for specific sample locations.)

Sample	pH	EC	acidity	Fe	Al	Mn	Cu	Zn	S	Sample description
		mmhos/ cm	mg $CaCO_3$/ L	mg/L						
CC1	6.90	0.300	n.d.	0.1	<0.03	0.4	<0.1	<0.1	26	I-77S, median
CC6	7.14	0.166	n.d.	<0.1	<0.03	<0.1	<0.1	<0.1	6	I-77S, shoulder
CC12	7.75	0.284	n.d.	<0.1	0.1	0.1	<0.1	<0.1	23	I-77N, shoulder
FL4-1(1)	3.73	0.400	178	2.1	11.7	2.5	<0.1	0.3	72	Culvert, acid roadcut
FL4-2	5.62	0.083	n.d.	1.3	<0.03	0.5	<0.1	0.1	11	Culvert, less acidic material
FL4-3	3.62	0.457	n.d.	1.8	13.6	2.6	<0.1	0.3	81	Sample downstream of culverts
FL5-1	4.10	0.334	n.d.	0.2	10.1	2.0	<0.1	0.3	62	Upstream end of culvert
FL5-2	4.75	0.211	n.d.	0.3	1.3	1.4	<0.1	0.2	34	Between spring and road
FL5-3	7.06	0.167	n.d.	0.1	<0.03	0.1	<0.1	<0.1	3	Head of spring flowing towards culvert.
FL5-4	6.51	0.064	n.d.	0.1	<0.03	<0.1	<0.1	<0.1	1	Head of spring flowing towards culvert.
FL13W	4.71	0.139	n.d.	<0.1	1.1	0.3	<0.1	0.1	20	Rt 8S, culvert
FL14	4.50	0.441	n.d.	1.0	5.4	2.1	<0.1	0.1	68	Rt 8S, ditch
FL15	3.22	1.054	n.d.	39.7	20.1	1.4	<0.1	0.6	182	Rt 8S, ditch
FL16	4.45	0.149	n.d.	0.1	2.3	0.4	<0.1	<0.1	22	Rt 8S, downstream from culvert
FL22	6.72	1.268	n.d.	<0.1	<0.03	0.5	<0.1	<0.1	211	Rt 8N, culvert
FL4-1(2)	2.48	n.d	232	18.1	10.4	4.7	<0.1	0.3	84	Same as FL4-1 (fall)
FL4-1(3)	3.24	n.d	184	6.5	17.3	5.3	<0.1	0.4	97	Same as FL4-1 (spring)

Table 3.9. VDOT sampling of drainage from Rt-750, Floyd County (see Figure 3.16a for locations).

Year	Location 5-3	Location 5-1	Location 4-1	Fishpond
1987	6.8	n.d.	2.8	n.d.
1990	6.2	3.9	3.2	3.2
1994	6.7	4.7	3.9	3.4
1995	5.8	3.4	2.8	2.6

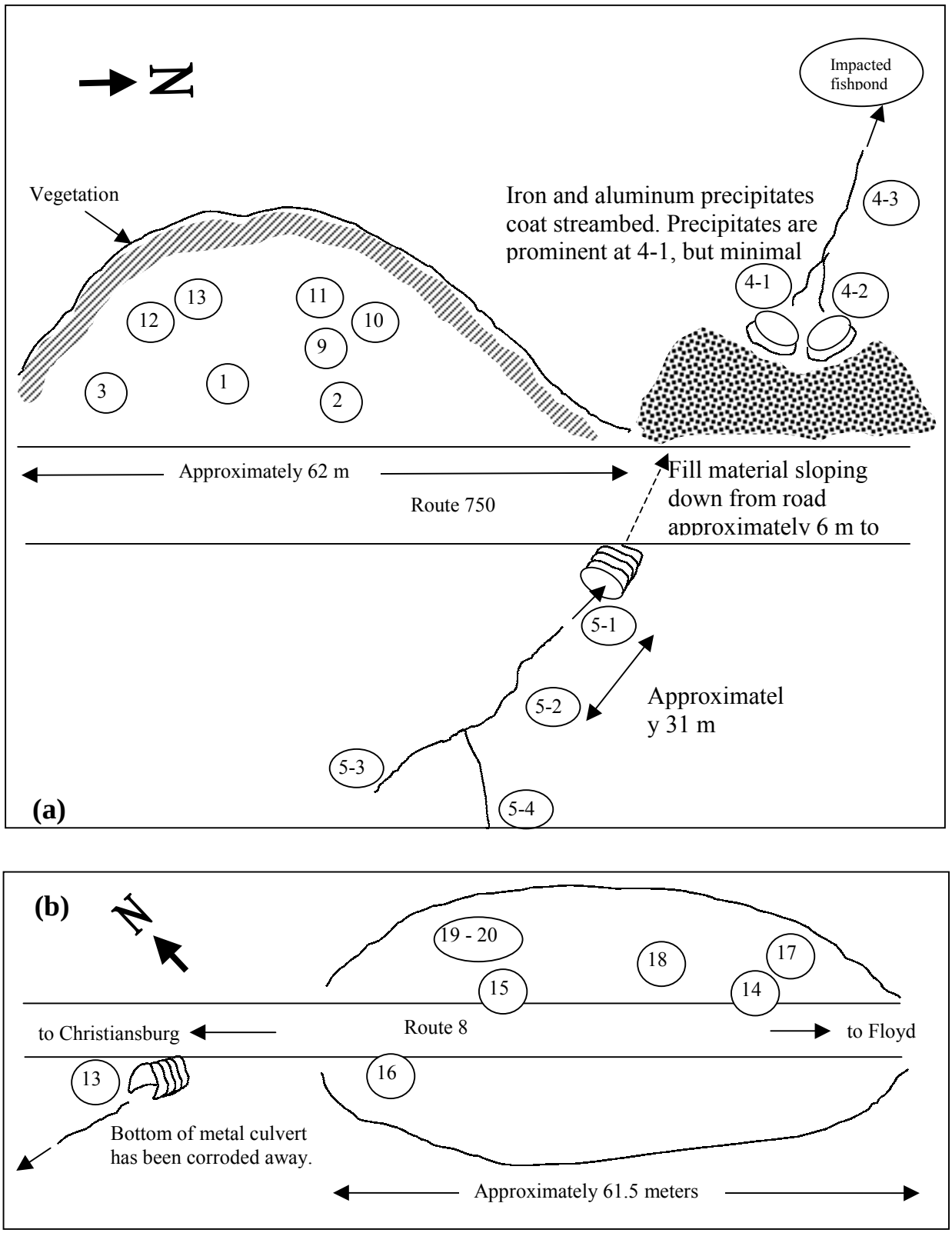

Figure 3.16. Schematic diagrams of sampling from (a) Route 750, and (b) Route 8, Floyd County. Circled numbers refer to FL samples described in Tables 3.7, 3.8, and 3.9.

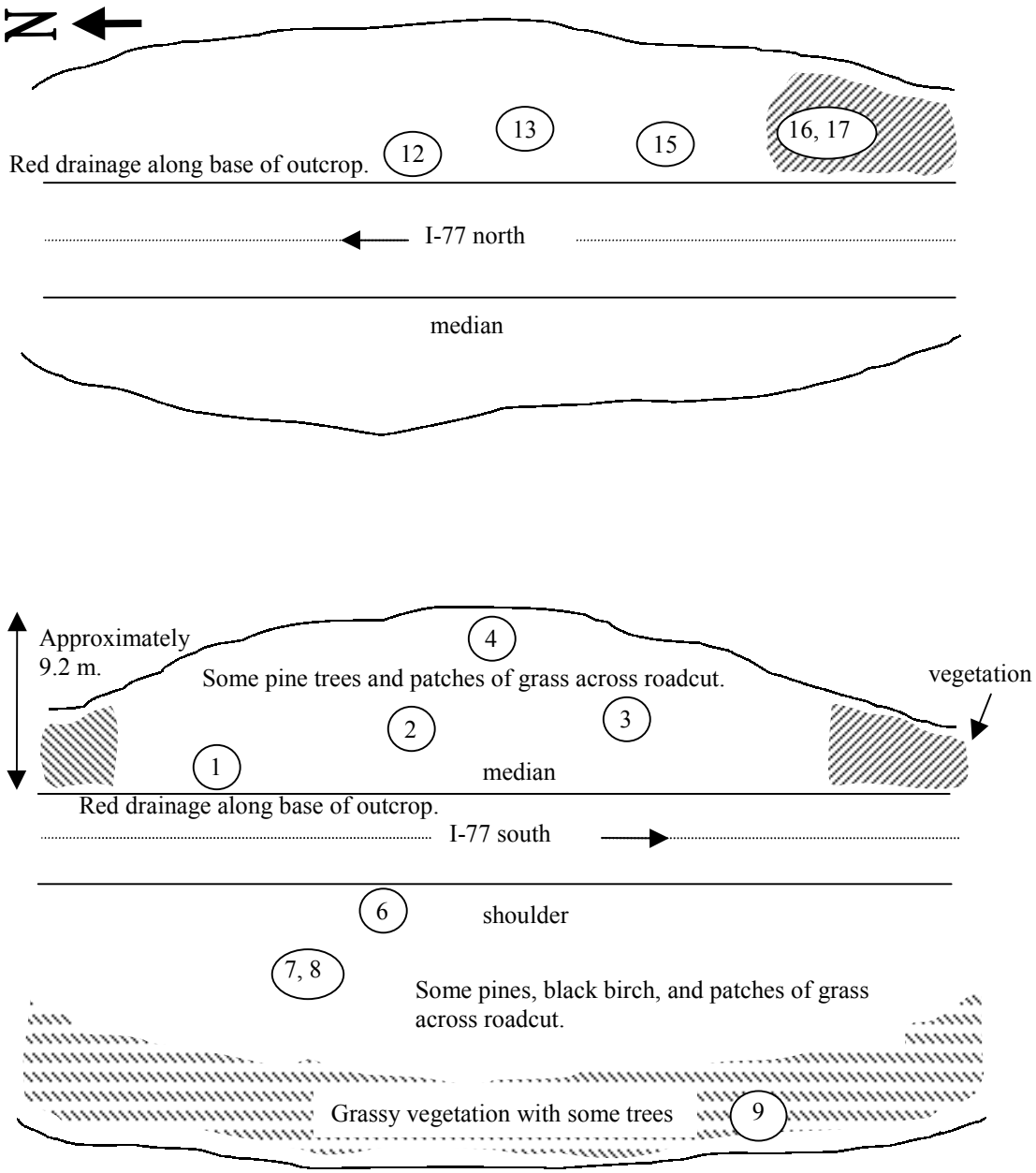

Figure 3.17. Schematic diagram of sampling for I-77 roadcut, Carroll County. Circled numbers refer to CC samples described in Tables 3.7, 3.8, and 3.9.

Along the Rt-8 roadcut in Floyd, iron staining, concrete etching, and deterioration of a metal culvert were evident along the base of the roadcut. Drainage samples from ditches along I-77 in Carroll County had near-neutral pH values and low EC and metal concentrations. An interview with a VDOT environmental manager for the Bristol district revealed that natural drainage "up the mountain" from this site regularly has pH values around 10 (George McCloud, VDOT, personal communication). Local bedrock apparently provides enough alkalinity to neutralize acid drainage.

Compared to materials from the Coastal Plain and the Piedmont, PPA values are much lower for materials from the Ashe Formation. Nonetheless, drainage from this material may have significant adverse effects on local surface water as was seen at Rt-750 in Floyd. Road drainage from Floyd is comparable to drainage from the I-295/360 roadcut; however, stream damage appears more significant at Floyd where concentrated drainage flows directly into a smaller stream. Exposures of phyllitic material from the Ashe Formation may be considered somewhat likely to produce moderate to severe problematic roadside management conditions. As with the Quantico Formation in the Piedmont, roadcut surfaces through the Ashe Formation tend to be quite steep and consist of shallow, rocky, weathered material over bedrock, and rock outcrops, which may not be suited for standard soil remediation methods.

Valley and Ridge

Results from analyses of geologic materials and road drainage from acid roadcuts in the Valley and Ridge are presented in Tables 3.10 and 3.11. Schematic diagrams of some sample locations are shown in Figures 3.18 and 3.19. Acid roadcuts in the Valley and Ridge result from the exposure of Devonian and Mississippian black shales, including the Marcellus shale (northeast of Shenandoah County), the Millboro shale (southwest of Shenandoah County except in extreme southwestern Virginia), the Needmore Formation (occurs with Marcellus and Millboro), and the Chattanooga shale (southwestern Virginia). Reflected light microscopy of polished sections (FC4, CF1-2, HC43, WC4) indicates the presence of pyrite as framboids, clusters of microcrystals, and weathered, anhedral and subhedral grains at all locations (Figure 3.13, and see Chapter 5). The PPA values ranged from 0 to 61 Mg $CaCO_3$/1000 Mg material;

Table 3.10. Characteristics of geologic material from acid roadcuts in the Valley and Ridge.

Sample	PPA	% S	Fizz Test	Sample Description	Geologic Formation
CF1	3.8	0.34	0	Grab sample from cut slope I-64E	Millboro
CF1-2	20.9	0.82	0	More competent rock at same location as CF1	Millboro
FC1	0	0.23	1	Rock from Rts-50 and 600	Marcellus
FC4	59.0	2.12	0	Rock from VDOT quarry, Rt-600	Marcellus
HC1	1.0	0.12	0	Rock, Rt-250W	Needmore
HC2	7.7	0.44	0	Rock, Rt-250W	Needmore
HC4	19.8	0.61	0	Rock, Rt-250W	Needmore
HC10	0	0.02	2	Rock, Rt-250W	Needmore
HC12	0	0.24	0	Rock, Rt-250W	Needmore
HC13	0	0.09	2	Rock, Rt-250W	Needmore
HC14	0	0.01	0	Rock, Rt-250W	Needmore
HC15	11.5	0.43	0	Rock, Rt-250W	Needmore
HC21	10.4	0.24	0	Rock, Rt-250W	Needmore
HC23	1.0	0.04	0	Rock, Rt-250W	Needmore
HC24	1.4	0.06	0	Rock, Rt-250W	Needmore
HC25	2.8	0.04	0	Rock, Rt-250W	Needmore
HC29	52.0	2.31	1	Rock, Rt-250W	Millboro
HC30	18.6	1.33	1	Weathered shale overlying HC29	Millboro
HC31	0	0.32	3	Rock, Rt-250W	Millboro
HC32	0	0.91	2	Weathered shale overlying HC31	Millboro
HC33	0	0.81	3	Rock, Rt-250W	Millboro
HC34	0	0.55	2	Weathered shale overlying HC33	Millboro
HC35	0	0.65	2	Rock, Rt-250W	Millboro
HC37	0	1.40	3	Rock, Rt-250W	Millboro
HC38	0	0.34	3	Weathered shale overlying HC37	Millboro
HC40	0	0.26	3	Weathered shale overlying HC39	Millboro
HC41	0	0.59	3	Rock, Rt-250W	Millboro
HC42	0	0.25	3	Weathered shale overlying HC41	Millboro
HC43	0	1.57	3	Rock, Rt-250W	Millboro
HC44	0	0.44	3	Weathered shale overlying HC43	Millboro
HC45	0	3.28	3	Sample from pyrite seam between HC42 and HC44	Millboro
HC46	0	0.58	3	Rock, Rt-250W	Millboro
HC47	0	0.17	3	Weathered shale overlying HC46	Millboro
HC48	0	0.16	0	Rock, Rt-250W	Millboro
HC50	1.4	0.07	0	Rock, Rt-250W	Millboro
HC52	1.4	0.05	0	Rock, Rt-250W	Millboro
HC56	0	0.04	2	Soil	Millboro
HC57	2.3	0.09	0	Rock, Rt-250W	Millboro
HC58	34.7	1.42	0	Rock, Rt-250W	Millboro
HC59	18.4	0.81	0	Weathered shale overlying HC58	Millboro
HC60	31.5	1.37	0	Rock, Rt-250W	Millboro
HC62	26.2	1.35	1	Weathered shale overlying HC61	Millboro
WC3	20.3	0.85	0	Grab sample from up on roadcut above WC1	Chattanooga
WC4	60.2	1.98	0	Rock from site WC3	Chattanooga
WC7	36.0	1.11	0	Rocks at base of roadcut	Chattanooga
WC8	34.4	1.42	0	Rocks at top of outcrop	Chattanooga
WC9	61.2	2.55	0	Weathered shale, roadcut about 1 mi W of WC8	Chattanooga
WC10	42.4	1.58	0	Weathered shale, roadcut about 1 mi W of WC9	Chattanooga
AVERAGE (n = 49)	**12.1**	**0.75**			

Table 3.11. Water quality data from acid roadcuts in the Valley and Ridge (see Figures 3.18 and 3.19).

Sample	pH	EC	Fe	Al	Mn	Cu	Zn	S	Sample location
		mmhos/cm	mg/L						
HC2	6.37	1.177	<0.1	0.1	4.2	<0.1	<0.1	160	Sedimentation pond near Rt-250
HC2.2	6.69	1.100	<0.1	0.1	3.6	<0.1	<0.1	139	Stream past sedimentation pond near Rt-250
HC63	6.18	0.781	0.80	0.1	0.5	<0.1	<0.1	106	Drainage ditch along Rt-250 W
CF2-1	5.28	0.194	<0.1	0.1	0.9	<0.1	0.2	30	Mouth of box culvert under I-64
CF2-2	6.03	0.620	0.3	0.1	2.8	<0.1	0.4	93	Drain to right of box culvert under I-64
CF2-3	3.74	4.520	9.5	254.5	44.8	<0.1	10.4	1278	Drain in box culvert under I-64
CF6	6.63	0.072	<0.1	0.2	0.5	<0.1	<0.1	7	Upstream end of box culvert under I-64
CFc1	2.67	n.d.	59	162.5	38.5	<0.1	8.3	1011	Drain in box culvert under I-64 (fall)
CFc2	3.90	n.d.	12.7	156.7	31.6	<0.1	6.6	830	Drain in box culvert under I-64 (spring)
CFs1	2.74	n.d.	14.1	36.2	10.3	<0.1	2.0	300	Mouth of box culvert under I-64 (fall)
CFs2	7.10	n.d.	0.1	0.4	0.2	<0.1	<0.1	9	Mouth of box culvert under I-64 (spring)

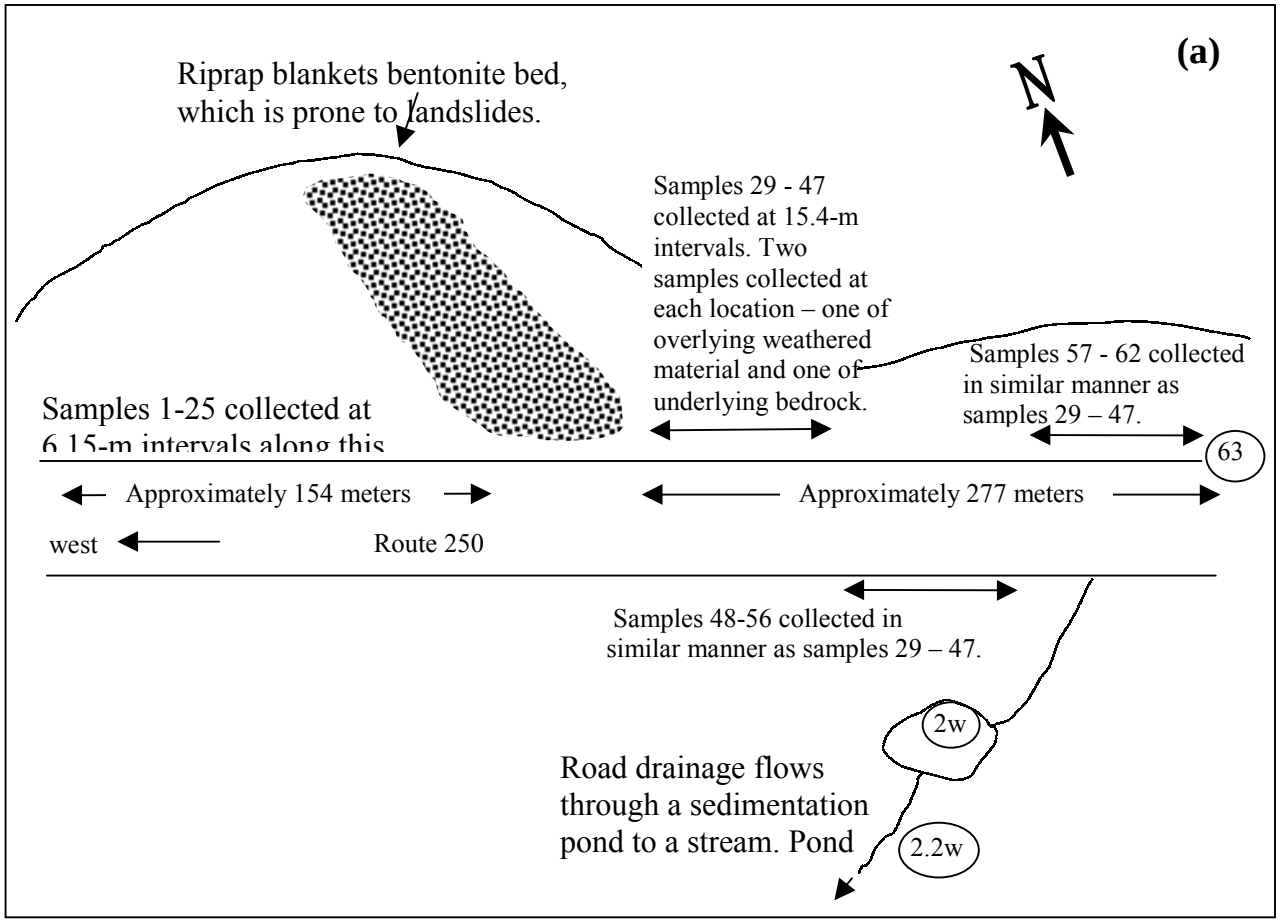

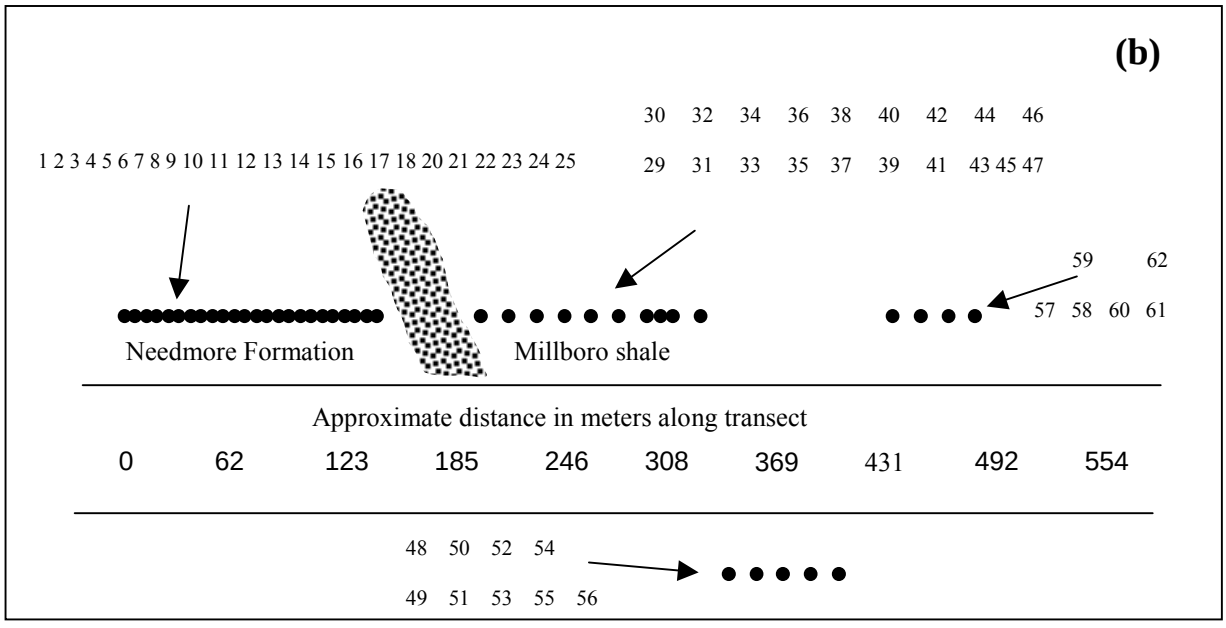

Figure 3.18 (a) Schematic diagram of sampling from Route 250, Highland County. Circled numbers refer to HC samples described in Tables 3.10 and 3.11. (b) Specific sample locations: bullets indicate sample sites and numbers refer to samples described in Table 3.10.

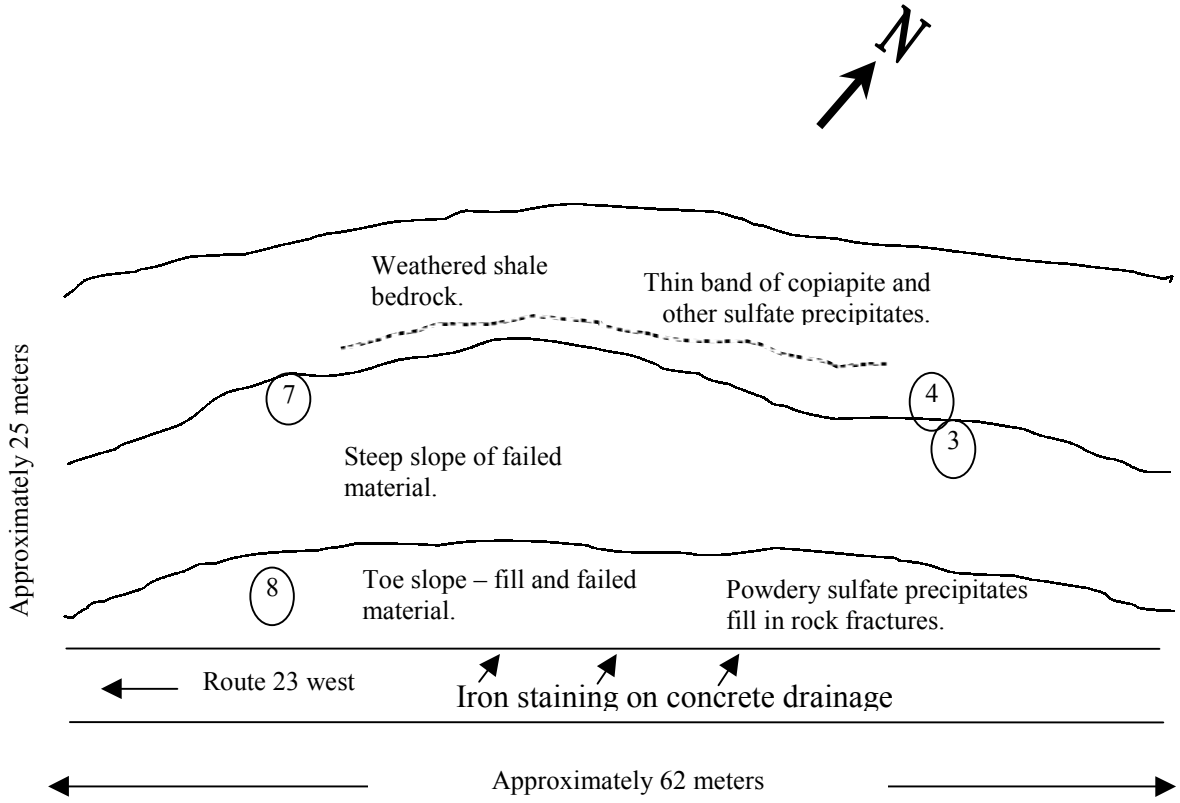

Figure 3.19. Schematic diagram of sampling from Route 23, Wise County. Circled numbers refer to WC samples described in Tables 3.10 and 3.11

however, numerous samples contained $CaCO_3$ as indicated by the fizz test. All of the carbonate-bearing samples, except one, came from the Rt-250 roadcut in Highland County. One carbonate-bearing sample was collected from Frederick County. The S values ranged from 0.0 to 3.3%. Analysis from detailed sampling along 500 meters of the Rt-250 roadcut in Highland County indicates that sulfide occurrence is not laterally homogenous (Table 3.10 and Figure 3.18). Differences of up to 2% S were noted for samples within 15 m of each other, and variation did not seem to appear to be systematic. Locally occurring pyritic seams and septarian concretions (Figure 3.8), evident along this roadcut, account for discrete high-S occurrences. Similarly, calcium carbonate appeared sporadically as secondary vein fillings and as a fine-grained cementing agent, at varying concentrations, throughout the exposure.

Water drainage from I-64 in Clifton Forge has significantly impacted a local stream (Figure 3.9). One water sample, upstream from the roadcut, revealed near-neutral pH, low EC, and low metal concentrations (Table 3.11). Water from a drain inside the culvert, representing the most concentrated drainage, had very low pH, high acidity, high EC, and very high metal concentrations. Water samples from the downstream end of the box culvert have variable pH values and correspondingly variable metal concentrations. Iron and aluminum precipitates heavily coat the bed of the stream, which appears to be biologically dead for at least 0.5 km downstream of the roadcut. Water drainage from a drainage ditch along Rt-250, and from a nearby sedimentation pond and stream, have moderate to near-neutral pH values, but high EC values. Overall, metal values are low except for high Mn values at the sedimentation pond and the stream. Drainage from this site is partially neutralized by calcium carbonate, which occurs throughout the roadcut both in veins and fine-grained particles as indicated by the fizz test. Nonetheless, iron-staining and concrete etching was evident along a drainage ditch at the base of the road, and Fe-flocculation was significant in the sedimentation pond. Although drainage was not present at the Rt-23 roadcut in Wise County at the time of sampling, iron-staining, concrete etching, and deterioration of a metal guardrail were evident in a drainage ditch along the base of the roadcut.

Sulfide levels in materials sampled from Devonian and Mississippian black shales appear to be more variable than other evaluated sulfidic materials. Overall, for samples that do not

contain carbonates, PPA and S values tend to be slightly higher than those for reduced Tertiary marine sediments, but lower than those for the Quantico Formation. Carbonates may appear sporadically and at various concentrations, causing PPA values to drop significantly despite high S values. Although the Chattanooga and Marcellus shales tested higher than the Millboro shale and Needmore Formation, more exposures would need to be evaluated to make definitive statements regarding their relative differences. Drainage from the I-64 roadcut at Clifton Forge had higher acidity and metal concentrations than any other studied roadcut. This drainage has significantly affected local surface water quality. Exposures of the Marcellus, Millboro, and Chattanooga shales, and the Needmore Formation, may be considered somewhat likely to produce severely problematic roadside management conditions.

Appalachian Plateau

The Appalachian Plateau geologic region of Virginia was not sampled in this study due to the relatively large research base associated with potential acidity in Appalachian coal mining environments (Sobek et al., 2000). In Virginia, the vast majority of strata within the Pennsylvanian system exposed to potential road-building excavation are fluvial-deltaic facies that are generally low in pyritic-S. Many of the massive sandstones that dominate the Lee, Norton and Wise formations contain secondary carbonate cementing agents (Howard et al., 1988) which offset the relatively minor amounts of sulfides found in most geologic sections. Significant accumulations of sulfides do occur in coal seams throughout the region; however, these seams are relatively thin (< 3 m) and are always completely removed and marketed during road corridor development. Several relatively thin sections of overburden in Virginia (e.g. the Standiford seam interburden of the middle Wise formation) do generate rock spoils with significant (> 10 Mg/1000 Mg) levels of potential acidity, but these intervals represent less than 10% of the entire geologic section. Detailed reviews of procedures for evaluating southwest Virginia mine spoils and coal-like materials for potential acidity and revegetation potential are given by Daniels and Zipper (1997) and Daniels et al. (1995).

Construction of a State-wide Sulfide Hazard Rating Map

The impact of acid drainage resulting from the exposure of sulfidic materials during road construction depends on many variables, including the relative volume of ARD moving to surface stream flow, the flow rate of local surface waters, and the neutralizing capacity of surrounding geologic materials. Although materials may be rated based on characteristics related to S content, PPA, and rock drainage quality, the true risk of environmental impact will depend on site-specific conditions. For example, the materials at acid roadcuts in Floyd County and Carroll County are relatively similar; however, environmental impact is significantly greater in Floyd County due to specific site conditions such as lack of abundant neutralizing materials and direct drainage of ARD into a small stream. Similar comparisons may be made between the Rt-250 cut in Highland County and the I-64 cut in Clifton Forge. With this in mind, the following scheme was developed to assess geologic materials with general ratings in terms of sulfide hazard. Materials are rated into four classes based on PPA and S values:

1) Materials for which 90% of samples tested less than 10 Mg $CaCO_3$/1000 Mg material and contained less than 0.5% S.
2) Materials for which 90% of samples tested less than 10 Mg $CaCO_3$/1000 Mg material and more than 10% of the samples tested greater than 0.5% S.
3) Materials for which more than 10% of samples tested greater than 10 Mg $CaCO_3$/1000 Mg material and less than 10% of samples tested greater than 60 Mg $CaCO_3$/1000 Mg material.
4) Materials for which more than 10% of the samples tested greater than 60 Mg $CaCO_3$/1000 Mg material.

The class boundaries were determined with consideration of standard remediation methods and the observed properties of a wide range of sulfidic materials. Application of these ratings to the geologic materials evaluated in this study is shown in Table 3.12. Again it should be emphasized that these ratings are based strictly on the acid-producing potential of a particular material, whereas actual acid production and severity of impact will depend on site conditions.

In addition to the materials evaluated for this study, sulfides have been documented in numerous other geologic formations in Virginia (Rader and Evans, 1993; Penick, 1987; J. Peper – personal communication). In many cases the sulfides occur as large crystals, which generally

are considered non-hazardous to road construction due to their minimal surface area that limits oxidation reactions. Nonetheless, these formations should be noted and may require evaluation. This is not intended to be an exhaustive list of pyrite-bearing formations. As previously discussed, the most problematic forms of pyrite such as framboids are rarely noted in general rock descriptions since they are not evident in hand specimens. In the Appalachian Plateau and Valley and Ridge, additional pyrite-bearing map units include igneous rocks (p), Bluefield Formation (Mbf), and Price Formation (Mpr), and Edinburg Formation (Oeln). In the Blue Ridge and Piedmont, additional pyrite-bearing map units include the Everona Limestone (Ꞓev), assorted formations of the Lynchburg group including Charlottesville Formation (Zch), Monumental Mills Formation (Zmm), graphitic phyllite and metasiltone (Zlg), metgrawacke (Zlm), and banded marble (Ꞓzac), metabasalt of the Catoctin Formation (ꞒZc), felsic volcanic and volcaniclastic rocks (Zav), border gneiss (Ybr), Accotink Schist (Ꞓza), Rich Acres Formation (Ꞓra), Diana Mills Complex (PzZdm), diorite and hornblendite of the Green Springs Pluton (PzZgs), Shelton Formation (Ost), members of the Arvonia Formation including slate and porphyroblastic schist (Oa), kyanite quartzite and schist (Obq), Buffards Formation (Obf), and Columbia pluton (Ocg), Chopawamsic Formation (Ꞓcv), kyanite schist of the central Piedmont (ks), Petersburg granite (Mpg). In the Coastal Plain, an additional pyrite-bearing map unit is the Shirley Formation (Qsh). The geographic extent of sulfide-bearing geologic materials is shown in Figure 3.20 and Plate 1 (hard copy on file at Newman library).

Table 3.12. Sulfide Hazard Rating for Evaluated Geologic Materials.

Geologic Map Unit	Sulfide Hazard Rating
Tabb Formation – Sedgefield Member	1
Wise, Kanawha, Norton, New River, Lee and Pocahontas Formations	1
Ashe Formation of the Lynchburg Group	2
Chesapeake Group	3
Lower Tertiary deposits	3
Marcellus shale and Needmore Formation	3
Millboro shale and Needmore Formation	3
Quantico Formation	4
Chattanooga Shale	4

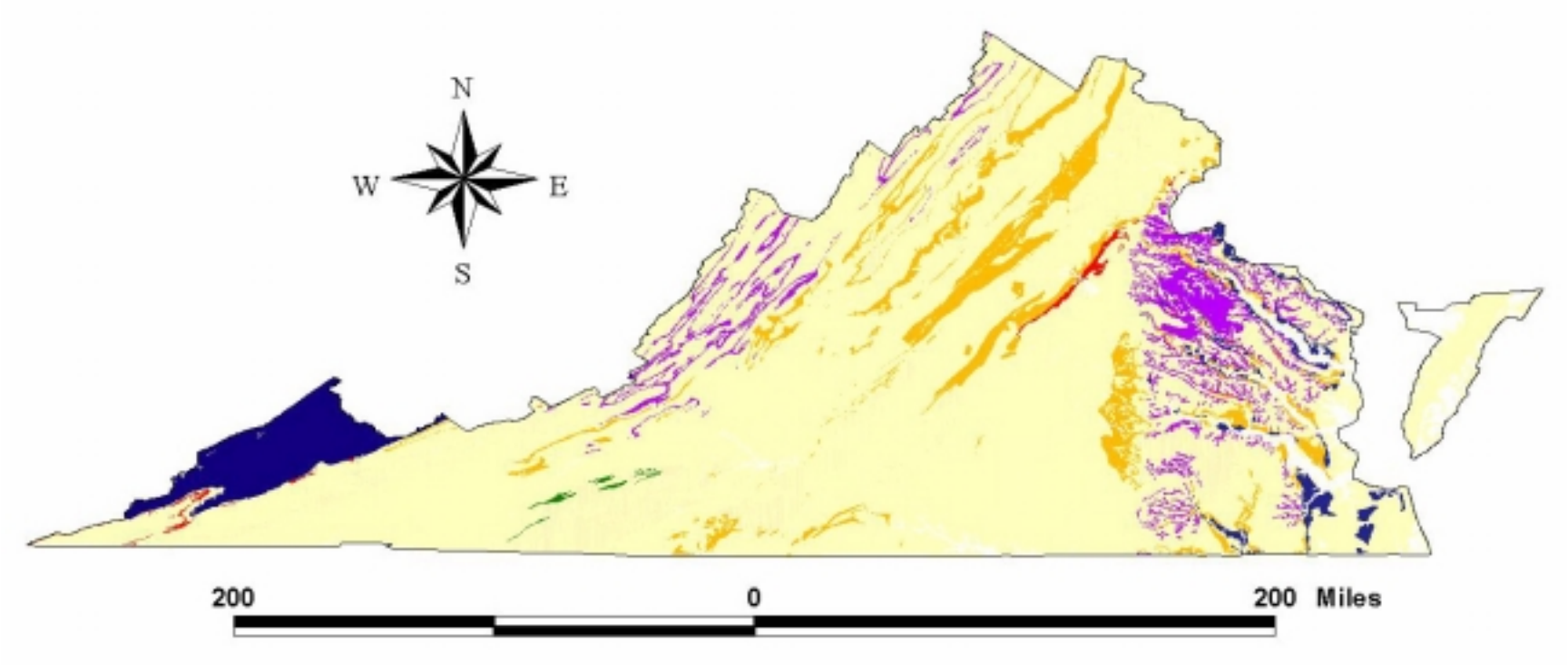

Figure 3.20. Geographic extent and hazard ratings for sulfide-bearing geologic materials in Virginia.

Conclusions

Exposure of sulfidic material from road construction has resulted in localized ARD problems that adversely affect water quality, fill stability, integrity of building materials, and vegetation management throughout Virginia. Geologic materials that were identified at documented acid roadcuts, listed from highest to lowest acid-producing potential, include: the Quantico Formation, Chattanooga shale, Tertiary marine sediments of the Chesapeake Group and Lower Tertiary deposits, Devonian black shales including the Millboro, Marcellus, and Needmore Formation, the Ashe Formation of the Lynchburg Group, and the Sedgefield member of the Tabb Formation. In most cases, except for the Tertiary marine deposits, sulfide distribution was not uniform over the extent of the studied roadcuts. Consequently, proper spatial sampling is critical to adequately characterize the range of S and PPA values that may occur along a roadcut.

In addition to acid-producing potential of the geologic material, the actual impact of ARD at a given location depends on site-specific conditions such as drainage design, proximity and volume of surface water, and the presence of neutralizing material. All documented sites had limited vegetation due to acidity. Most sites exhibited degradation of concrete and metal construction materials. In all cases where drainage was present, the most concentrated forms had very low pH and high EC and metal concentrations, which would not comply with EPA discharge standards for mine effluent. Sites where road drainage is directly channeled into relatively small local streams, such as Rt-750 in Floyd County and I-64 in Clifton Forge, had more significant adverse impacts on local water quality than sites where drainage flowed along ditches before entering relatively larger streams, such as at Mine Road in Stafford and the I-295/Rt-360 interchange at Mechanicsville.

Of the approximately 126,000 km^2 of land area in Virginia, sulfide-bearing geologic map units evaluated in this study make up about 9,000 km^2, or 7% of the land area. The greatest risk of encountering sulfidic materials is in the Coastal Plain, where over 20% of the land area is surficially mapped as the Chesapeake Group, Lower Tertiary deposits, or the Tabb Formation. The Shirley Formation, which is known to contain sulfides, but was not evaluated, adds another

5%. The next greatest risk is in the Valley and Ridge, where approximately 5% of the land area is mapped as the Marcellus, Millboro, Needmore, or Chattanooga shales, and 6% is mapped as numerous coal-bearing strata. Other formations which are known to contain sulfides, but which were not evaluated, add another 4%. The lowest risk exists in the Blue Ridge and Piedmont, where less than 1% of the area is mapped as the Quantico Formation or the Lynchburg Group; however, an additional 8% of the area has documented sulfide occurrences. Theoretically, over 50 km of a highway corridor that crosses the entire state could potentially intersect sulfidic map units. Acid rock drainage will not always occur where sulfidic materials are mapped; at the same time, these tabulations do not take into account areas that are not mapped as being “at risk”, but where sulfidic materials occur within common excavation depths.

References

Anderson, J. E., and E. I. Robbins. 1998. Spectral reflectance and detection of iron-oxide precipitates associated with acidic mine drainage. Photogrammetric Eng. and Remote Sensing. 64(12):1201-1208.

Barnhisel, R. I. And J. Harrison. 1976. Estimating lime requirement by a modified hydrogen peroxide potential acidity method. (Unpublished method for KY Agr. Ex. Sta., Soil Testing Laboratory) Lexington, KY.

Coch, N. K. 1971. Geology of the Newport News, South and Bowers Hill Quadrangles, Virginia. Va. Div. Mineral Resources. Report of Investigations 28. Charlottesville.

Conley, J. F. 1987. Relationships of structure to massive sulfides in the Chopawamsic Formation of central Virginia. p. 19-33. *In* Contributions to Virginia geology-V. Vir. Div. Mineral Resources. Pub. 74. Charlottesville.

Craig, J. R., D. K. Henry, and J. W. Miller. 1977. Comparison of massive sulfide mineralogy at Gossan Lead with the Cofer property, Mineral, Louisa County, Virginia. . Vir. Div. Mineral Resources. Virginia Mineral. 23(3):28.

Daniels, P. A. Jr., and E. Onuschak, Jr. 1974. Geology of the Studley, Yellow Tavern, Richmond, and Seven Pines quadrangles, Virginia. Vir. Div. of Mineral Resources. Report of Investigations 38. Charlottesville.

Daniels, W. L., M. Genthner, R.Whittecar, B. Hodges, and S. Nagle. 1995. Hydrogeology and soils of the Chisman Lakes gravel pit wetlands mitigation site. Field trip guide for VAPPS workshop, 10 – 11 August, 1995. Dept. of Crop and Soil Env. Sci., Virginia Tech, Blacksburg.

Daniels, W.L. and C.E. Zipper. 1997. Creation and Management of Productive Mine Soils. Reclamation Guidelines for Surface Mined Land in Southwest Virginia. Virginia Coop. Ext. Pub. 460-121, Virginia Tech, Blacksburg.

Dietrich, R. V. 1959. Geology and mineral resources of Floyd County of the Blue Ridge Upland, Southwestern Virginia. Bulletin of the Virginia Polytechnic Institute, Engineering Experiment Station Series. No. 134. Blacksburg.

Gee, G. W. and J. W. Bauder. 1986. Particle-size analysis. P. 383-411. *In* A. Klute (ed.) Methods of soil analysis. Part I. 2nd ed. Agron. Monogr. 9. ASA and SSSA. Madison, WI.

Hodder, R. W. and R. F. Kazda. 1977. Case history in massive sulphide exploration in the Virginia Piedmont from airborne geophysics through drilling. Vir. Div. Mineral Resources. Virginia Minerals. 23(2):29.

Howard, J. L., D. F. Amos, and W. L. Daniels. 1988. Phosphorus and potassium relationships in southwestern Virginia mine spoils. J. Environ. Qual. 17(4) 695-671.

Johnson, G. H. 1976. Geology of the Mulberry Island, Newport News North and Hampton Quadrangles, Virginia. Vir. Div. Mineral Resources. Report of Investigations 41. Charlottesville.

Penick, D. A. Jr. 1987. Pyrite and other minerals from Barger's Quarry near Lexington. VDMR Virginia Minerals. 33(2):13-17.

Rader, E. K. and N. H. Evans (eds.). 1993. Geologic map of Virginia – expanded explanation. Vir. Div. Mineral Resources. Charlottesville.

Sobek, A.A., W.A. Schuller, J.R. Freeman, and R.M. Smith. 1978. Field and laboratory methods applicable to overburden and minespoils. U.S. E.P.A. Report EPA-600/2-78-054. Cincinnati.

Sweet, P., R. S. Good, J. A. Lovett, E. V. M. Campbell, G. O. Wilkes, and L. L. Meyers. 1989. Copper, lead, and zinc resources in Virginia. Vir. Div. Mineral Resources. Pub. 93. Charlottesville.

U.S. Code of Federal Regulations, 1995. Title 40-Protection of Environment, Ch. 1-Environmental Protection Agency, Subchapter N-Effluent Guidelines and Standards, Part 434-Coal Mining Point Source Category BPT, BAT, BCT Limitations and New Source Performance Standards, US General Services Administration. Washington, D.C.

Virginia Division of Mineral Resources, 2001, Unpublished digital geologic map of Virginia.

Valladeres, T. M. 1998. Estimating depth to sulfide-bearing sediments in the Maryland Coastal Plain: a pedo-geomorphic modeling approach. M.S. Thesis. Univ. Maryland, College Park.

Young, R. S. 1956. Sulfides in Virginia. Vir. Div. Mineral Resources. Virginia Minerals. 2(1):1-7.

Chapter 4

PREDICTING DEPTH TO SULFIDIC SEDIMENTS IN THE COASTAL PLAIN

Introduction

Over the past few decades, exposure of sulfidic materials from development in coastal areas throughout the world has resulted in environmental degradation and has produced negative engineering impacts (Dent and Pons, 1995; Prokopovich, 1986, Stone et al., 1998; Valladares, 1998, van Holst and Westerveld, 1973). These problems are described in detail in Chapter 2. Recognition of acid sulfate soils, and depth to unoxidized sulfidic materials, prior to land development is essential for minimizing environmental impacts. In upland settings, traditional soil survey techniques do not always provide sufficient information as sulfidic materials usually occur deeper than standard sampling depths (1.5 m), but within routine construction excavation depths. A few studies (Lin and Melville, 1994; Lin et al., 1995; Madsen et al., 1985; Madsen and Jensen, 1988; Valladares, 1998) focus on developing models that can be used locally to predict the occurrence of acid sulfate soils using soil-landscape relationships.

Lin and Melville (1994) examined acid sulfate soil-landscape relationships in the Pearl River Delta of Southern China. The study area was a fluvial-dominated, estuarine-deltaic plain of the South China coast. They determined that acid sulfate soils frequently occurred within narrow zones surrounding rocky hills, which were previously bedrock islands. As bedrock islands, they provided zones of slow sedimentation, which allowed the establishment of mangrove vegetation. The vegetation produced large amounts of organic matter that enhanced pyrite formation. In the adjacent seaward tidal flats, more rapid sedimentation prevented the establishment of mangrove communities, which limited pyrite formation. Lin et al. (1995) subsequently examined soil landscape relationships in a tide-dominated estuarine system in eastern Australia. Pyrite accumulation in this floodplain was more significant than in the Pearl River Delta, supporting the claim (Pons et al., 1982) that tidal action favors the enrichment of pyrite in sediments.

Madsen et al. (1985) present a method for mapping potentially acid sulfate soils in Jutland, Denmark. Although the investigation area was 29,000 km^2, the authors reduced the sampling area to wetlands (marine and non-marine) since pyrite is stable only under reducing

conditions. Over 14,000 samples from almost 8000 soil profiles (augered to 2.5 m), evenly distributed through the approximately 6000 km^2 of wetland areas, were collected. Identification of acid sulfate material was based on incubation pH for carbonate-free samples and acid-base accounting for carbonate-containing samples. The wetlands were divided into eight natural landform regions and assigned to one of four classes depending on the number of potentially acid sulfate profiles to total number of profiles examined in the wetland region. Madsen and Jensen (1988) then examined the distribution of potentially acid sulfate soils in relation to landforms and geology and determined that differences were explained by geologic substratum. The two main sources for development of potentially acid sulfate soils included marine and brackish environments in tidal marsh areas, and high influx of SO_4 and Fe in groundwater from pyrite-containing Tertiary and glacial sediments into non-marine moorlands.

The study by Valladares (1998) is of particular interest because it examines the relationship between depth to sulfide-bearing sediments and landscape parameters in Anne Arundel County, Maryland – an upland setting very similar to that of Virginia's inner Coastal Plain. Three main geologic settings were evaluated – areas covered by Upper Cretaceous, Tertiary, and Pleistocene deposits. For two or three locations within each geologic setting, deep borings were made along transects. Ground elevation and depth to sulfidic sediments were determined for each sample location along these transects. An example of these transects is illustrated in Figure 4.1. For each geologic setting, the transect data were combined to develop regression models that predict depth to sulfidic materials using point relief (the difference in elevation between a given point and the lowest point in the landscape unit). Valladares determined that 75% to more than 90% of the variability in depth to sulfides could be attributed to point relief. The predictive models were applied to the entire county, using digital elevation models to derive point relief, and geologic maps. An example of this application is also illustrated in Figure 4.1. Overall, Valladares concluded that the surface of sulfide-bearing strata generally followed trends in the landscape surface, but occurred relatively deeper at summit locations than at toeslopes. This difference is presumably a function of water table depth, since

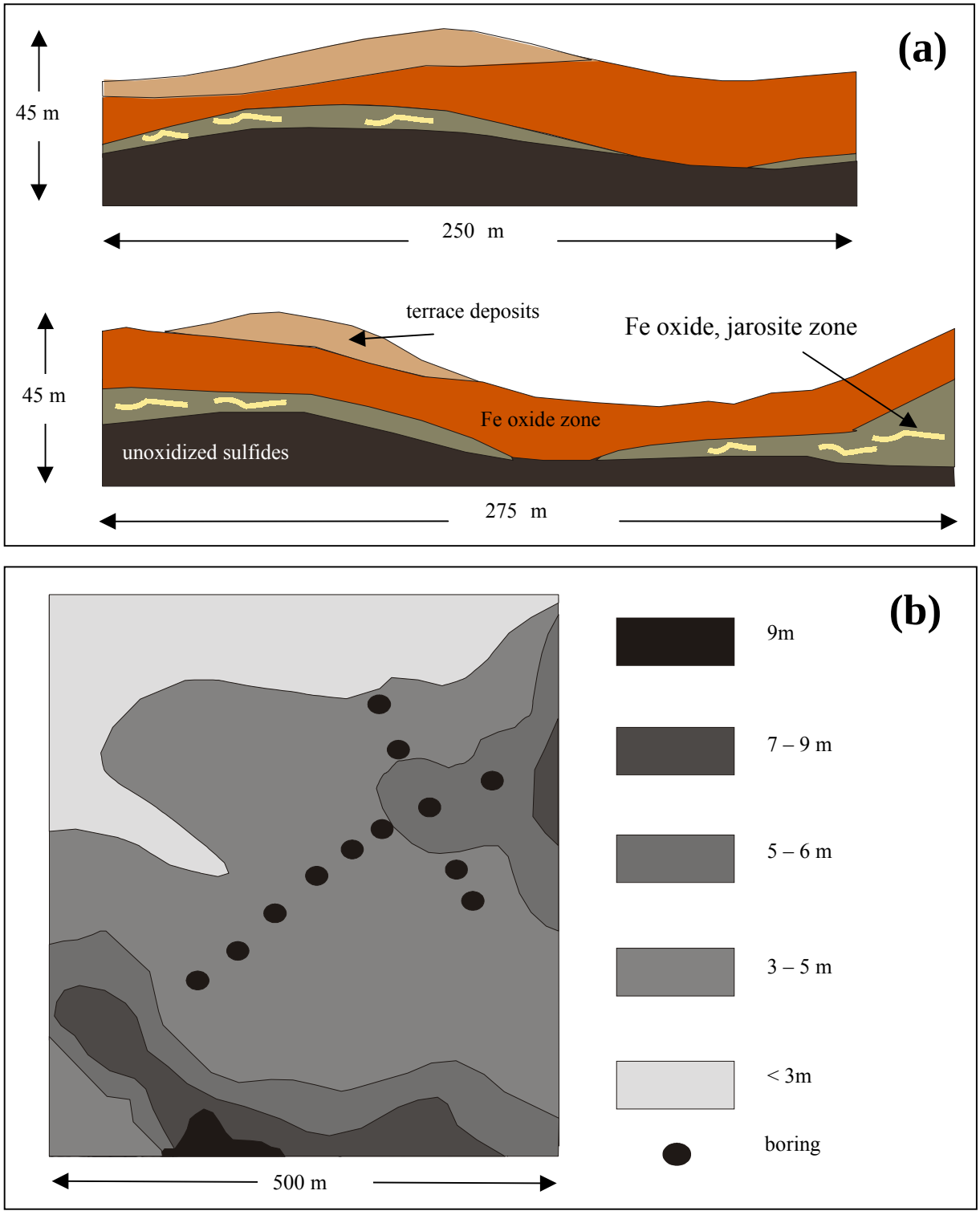

Figure 4.1 (a) Cross-section of transects from Brandy Farms, Anne Arundel County, Maryland used to develop regression model for predicting depth ot unoxidized sulfides based on point relief in Upper Cretaceous materials. (b) Location of transect borings and application of regression model to small area. Figures are redrawn from Valladares (1998).

shallower water tables occur at lower landscape positions. In most cases, sulfides were encountered within 15 m at higher elevations (up to 52 m), and within 2 to 3 m at lower elevations (< 35 m).

Problems associated with acid sulfate weathering are increasingly being recognized in the Coastal Plain province of Virginia. Over the past few decades, numerous roadcuts producing acid rock drainage have been documented (Chapter 3). The depth at which sulfide-bearing sediments occur in this region is highly variable, ranging from approximately 3 m to over 30 m. Information regarding the likelihood of encountering sulfide-bearing sediments along a planned highway corridor can help minimize the negative impacts that result from exposure of these materials. A slight shift in route or change in profile grade may prevent or reduce exposure of sulfides. Furthermore, when deposits cannot be avoided, advance knowledge of their locations and characteristics will allow for appropriate road design and remediation procedures. Therefore, the objectives of this study were (1) to evaluate field relationships between depth to sulfide-bearing sediments and landscape parameters, and (2) to test models for predicting depth to sulfides.

Description of Study Area

The study area (Figure 4.2) encompasses the intersection of Hanover County with the Studley and Seven Pines United States Geological Survey (USGS) 7.5 minute topographic quadrangles, along with small areas of surrounding quadrangles to the east (Manquin and Quinton) and west (Yellow Tavern and Richmond). This area was selected based on proximity to extensive acid roadcuts at the interchange of US-360 and I-295 at Mechanicsville and our assumption of associated regional geologic and geomorphic conditions. Elevation ranges from approximately 6 m to over 62 m above sea level. The topography is characterized as a broad, moderately dissected upland that regionally slopes eastward at approximately 1.7 m per km. The area is drained by two northwest to southeast running rivers - the Pamunkey River to the north and the Chickahominy River to the south. Three main landforms exist in this region: broad, gently rolling uplands, incised valleys along drainages, and broad level floodplains along the two major rivers.

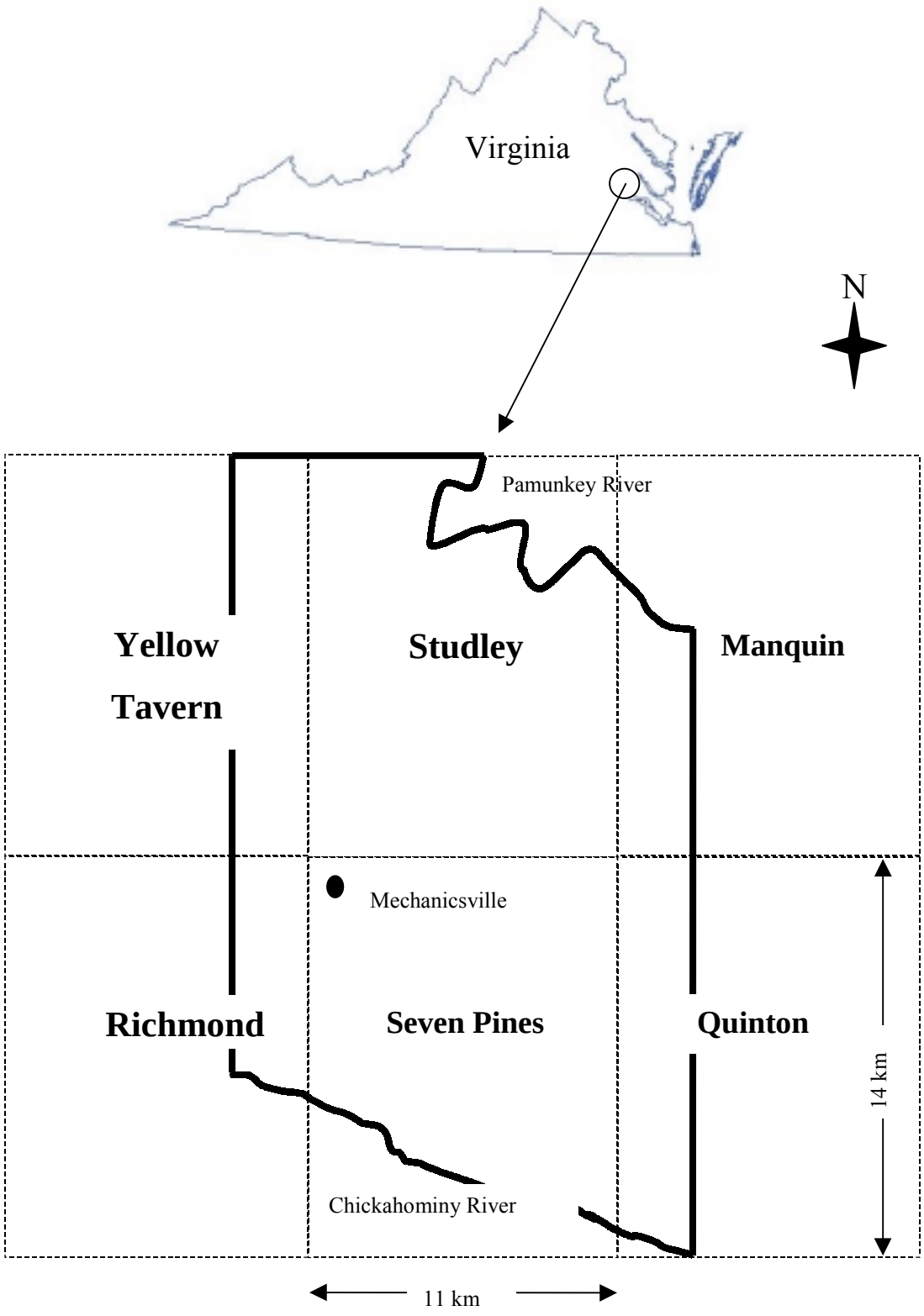

Figure 4.2. Location of study area outlined in bold with USGS 7.5 minute topographic quadrangles identified and outlined with dashed line.

Detailed descriptions of geology in the study area are provided by Daniels and Onuschak (1974) and Ward (1984). Basement rocks, including the Petersburg granite and Triassic red-beds underlie a wedge of Coastal Plain sediments at depths ranging from approximately 62 to 215 m. Cretaceous age sediments of the Potomac Formation, which overlie the basement rock, were deposited in a fluvial setting and are generally brightly colored and heterogeneous in character and extent. Lower Tertiary marine deposits, which overlie the Cretaceous sediments, include the Pamunkey Group and the Old Church Formation. The Pamunkey Group includes the following formations from youngest to oldest: Chickahominy, Piney Point, Nanjemoy, Marlboro, Aquia, and Brightseat. Tertiary marine and estuarine sediments of the Chesapeake Group, which unconformably overlie the Lower Tertiary deposits, include the following formations from youngest to oldest: Chowan River, Yorktown, Eastover, St. Mary's, Choptank and Calvert. Within the study area, the sedimentary record typically includes the following formations, from youngest to oldest: Yorktown, Eastover, Choptank, Calvert, Nanjemoy, Marlboro Clay, and Aquia (Rick Berquist, personal communication). The Lower Tertiary deposits (Nanjemoy and older) are described as drab grayish-green, glauconitic clayey silt and quartz sand, with some fossiliferous layers. The Marlboro Clay is a light-gray to pinkish-gray kaolinitic clay, and may be interlaminated with very fine-grained glauconite. The Lower Tertiary deposits outcrop at very few locations along streams in the northeast section of the study area. Daniels and Onuschak (1974) group the Calvert formation and younger transgressive sediments (now mapped as the Eastover and Yorktown formations) into a clayey silt (cs) map unit, which is described as drab, gray, green, and blue marine sediments. Carbonate-bearing beds are occasionally encountered in some formations, and consequently all drably colored marine sediments are known locally as "the blue marl". The cs unit is exposed in relatively small areas along most streams throughout the study area, and in larger areas along the floodplains of the Pamunkey and Chickahominy Rivers. Where overlain by Quaternary sediments, the surface of the cs unit is believed to somewhat parallel the surface topography. The maximum elevation of the cs unit is estimated to be about 55 m, near the western margin of the study area, and dips gently eastward to an elevation of about 43 m; however, ancient and present-day streams have incised the unit to much lower elevations. Although little information exists on sulfide occurrence in these sediments, pyrite has been documented in most of the formations of the Lower Tertiary deposits and the Chesapeake Group in Virginia (see Chapter 3) and Maryland (Valladares, 1998). Overlying the

Chesapeake group, Tertiary and Quaternary age fluvial sands and gravels blanket most of the study area except where removed by stream incision. These oxidized sediments range in color from buff to red, and in particle size from clays to boulders. The maximum thickness of these sediments is approximately 30 m.

Detailed information on soils in the study area is provided by the Soil Survey of Hanover County, Virginia (Hodges et al., 1980). The flood plains and terraces along the two major rivers are mapped as the Pamunkey-Dogue-Forestdale association, which consists of deep, well-drained, moderately well-drained, and poorly drained soils with loamy or clayey subsoil. Pamunkey soils are found mainly along the Pamunkey River and are typically strongly acid to neutral. The Dogue and Forestdale soils are found on terraces and low-lying upland areas along the Chickahominy. The Dogue soil is typically extremely to strongly acid, while the Forestdale is very strongly to medium acid. Other soils found in this association include: Altavista, Tarboro, Chewacla, Fork, Myatt Variant, Wahee, and Wehadkee series, and Fluvaquents, Hydraquents, and Udifluvents. The uplands between the Chickahominy and Pamunkey Rivers are mapped as the Norfok-Orangeburg-Faceville association and the Udults-Ochrepts-Suffolk association. These associations consist of deep, moderately-well drained to excessively drained soils with sandy, loamy, and clayey subsoils, which are typically very strongly to strongly acid. Other series found in these associations include: Atlee, Bourne, Caroline, Dunbar, Duplin, Goldsboro, Kempsville, Kenansville, Masada, Suffolk, and Varina soils.

Materials and Methods

Regional depth to reduced sulfide-bearing marine sediments (hereafter referred to as depth-rs) was determined from water well logs provided by the Hanover County Health Department. Depth-rs was determined based on distinct color changes between the overlying oxidized sands and gravels and the reduced sediments. Oxidized materials are typically described as red, yellow, or brown. Underlying reduced materials are typically described as gray, blue, or green. In some cases the boundary was identified at a specific depth, but often it was identified as occurring within a depth interval. For example, the data may be recorded as ‘14 – 34 ft: red sand to blue clay’. In such cases, the mean depth (i.e. 24 ft) was used as depth-rs. Well locations

were determined from parcel plats provided with the well logs. Only well logs that clearly marked both the location of the well, and depth-rs, were used. This data set consisted of 408 well logs. The utility of basing a predictive model on existing groundwater well logs is that such data are readily available, and can be used in other areas to construct similar hazard rating maps at relatively low cost. Also, the economics of this study clearly would not have supported such an extensive drilling program. Twenty-three detailed borings were drilled by personnel from the Department of Crop and Soil Environmental Sciences throughout the study area for use as validation points to test the accuracy of interpretations from the well logs and to assess the frequency of S occurrence. Samples from within the first 30 cm of reduced sediments were collected from these detailed borings, analyzed for %S using an Elementar Vario Max CNS analyzer, and rated for presence of calcium carbonate by the HCl fizz test (Sobek et al., 1978). Detailed descriptions and laboratory analyses including Munsell color, particle size analysis, pH, potential peroxide acidity (PPA), and %S were completed for three profiles. A digital map of Hanover County streams, and spatial data transfer standard digital elevation maps (SDTS DEM's) with 30 m horizontal resolution for the 7.5 minute quadrangles, were obtained from the USGS. A digital tax parcel map was provided by the Hanover County Planning Office, and a digital soils map for Hanover County was obtained from the United States Department of Agriculture. The USGS 7.5 minute geologic maps for this area were digitized in-house. Digital maps were analyzed using ARCView geographic information systems (GIS) software to determine elevation, slope, distance to streams, surficial geology and soils for all data points. Three approaches were used to predict depth-rs. The first approach used regression analysis to evaluate relationships between depth-rs and landscape variables, including elevation, slope, distance to streams, and surficial geology, to develop a predictive model. Secondly, interpolation was used to calculate a depth-rs surface based on depth-rs from the well logs. The data were randomly divided into two sets of points. The first set of points, which included approximately three-fourths of the total data set, was used to generate an interpolated surface in ARCView using the default options of inverse distance weighting on the twelve nearest neighbor points. The remaining well points were used to evaluate the accuracy of the predicted values. This approach was repeated three times. Finally, a third procedure was developed which created probability maps to indicate the likelihood of encountering reduced sediments within a given depth for defined elevation groups. The procedure used two risk factors – one based on elevation

and one based on soil type. The data were divided into seven elevation classes. For each class, the depth-rs data were summarized with descriptive statistics, including the relative proportion of data points with depth-rs less than 5, 9 and 13 m. Elevation risk factors were designated and quantified, as indicated in parenthesis, for each elevation class based on the proportion of wells with depth-rs below the specified depth. Risk factors were assigned in the following manner: i) > 50% is a very high risk (4), ii) 26 – 50% is a high risk (3), iii) 11 – 25% is a moderate risk (2), and iv) ≤ 10% is a low risk (1). The data also were divided based on soil map unit. For each map unit the depth-rs data were summarized with descriptive statistics. For soil map units containing at least 5 well data points, the relative proportion of wells with depth-rs less than 9 m was calculated and used to assign soil risk factors as follows: i) > 25% is a high risk (3), ii) 11 – 25% is a moderate risk (2), and iii) ≤ 10% is a low risk (1). For soil map units with fewer than 5 data points, soil risk factors were designated based on mean depth-rs as follows: i) ≤ 9 m is a high risk (3), ii) 10 to 19 m is a moderate risk (2), and iii) ≥ 20 m is a low risk (1). A final compiled map was generated to indicate the two risk factors using DEM's and the digital soil map.

Results and Discussion

Regression analysis of depth to reduced sediments and landscape parameters

Geographic distribution of the well logs is shown in Figure 4.3. Cross-sections (Figures 4.4, 4.5, and 4.6) illustrate that the surface of reduced Tertiary sediments tends to parallel surface topography. In these cross-sections, the dashed lines represent generalized surface topography and the surface of reduced Tertiary sediments as interpolated from the well log data. The bold line illustrates more detailed surface topography as interpolated from numerous points along the transects, and shows that surface topography is actually much more variable than indicated by only the well logs. Despite the apparent relationship between surface topography and the surface of reduced Tertiary sediments, a plot of depth-rs versus elevation for all data points (Figure 4.7) indicated that variability increased significantly with increasing elevation and shallow depth-rs values (< 4 m) occurred at all elevations. Regression analysis of depth-rs versus elevation was not significant ($R^2 = 0.22$). Regression using various combinations of elevation, slope, distance to streams, and geology did not improve results (Table 4.1). Despite repeated efforts, a model could not be developed by regression analysis to adequately predict depth-rs using landscape variables.

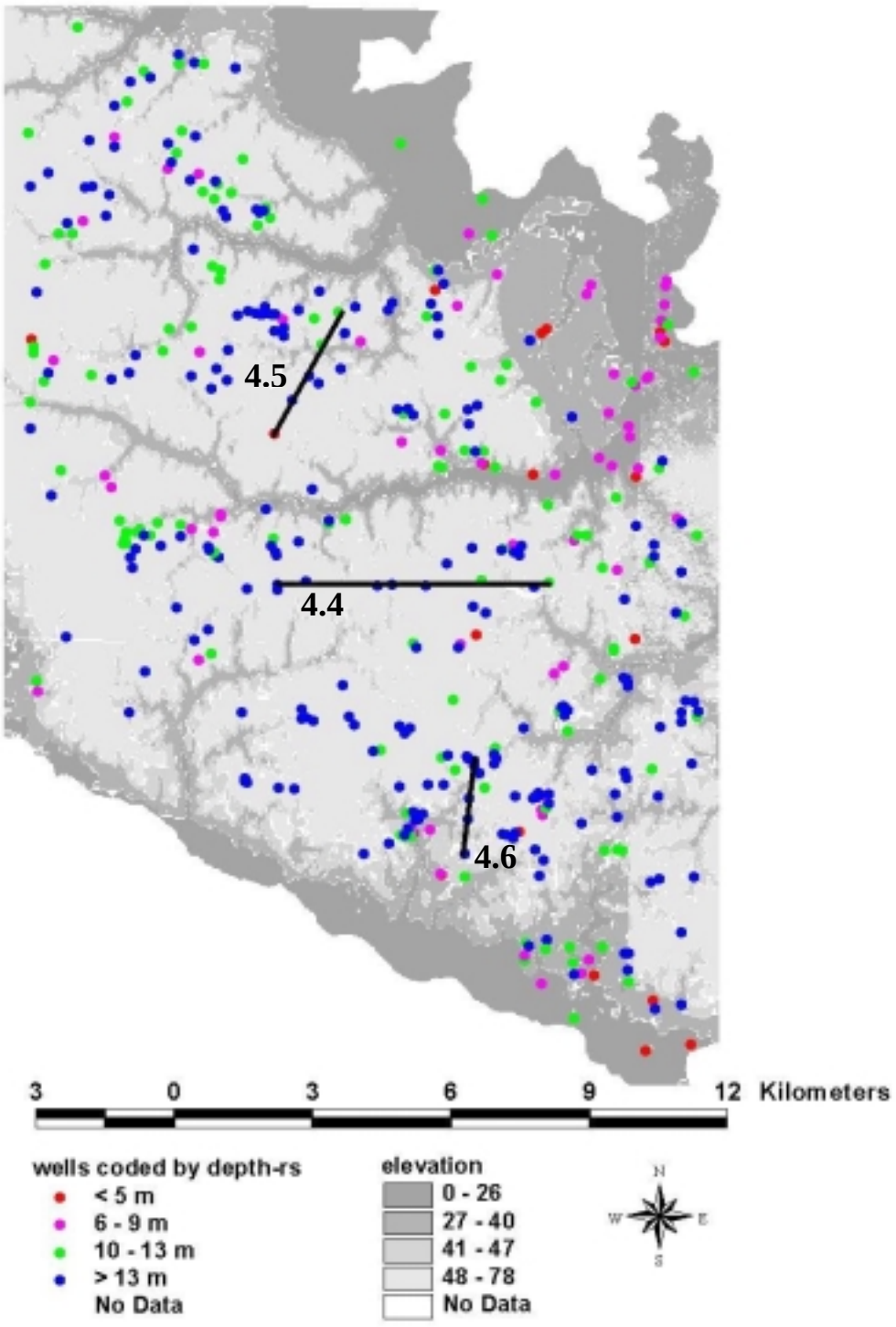

Figure 4.3. Elevation, geographic distribution, and depth-rs of 408 well logs in the study area near Mechanicsville, Virginia (see Figure 4.2). Black lines indicate locations of transects for Figures 4.4, 4.5, and 4.6.

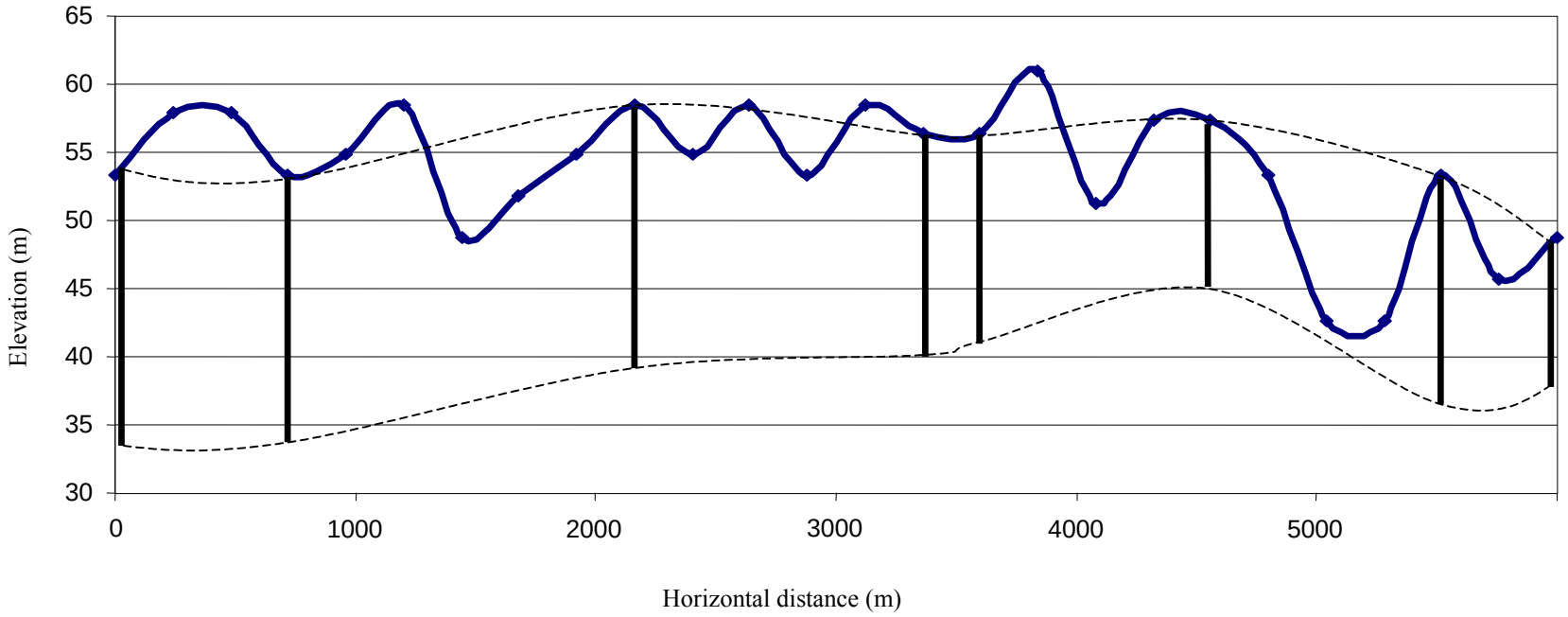

Figure 4.4. Cross section from transect 1 (see Figure 4.3). The dark horizontal line represents surface topography and the dark vertical lines show depth to reduced sediments as indicated by wells along the transect. The dashed lines represent interpolated surface topography, and the boundary between oxidized and reduced sediments, as indicated by the wells. (Vertical exaggeration is 57X.)

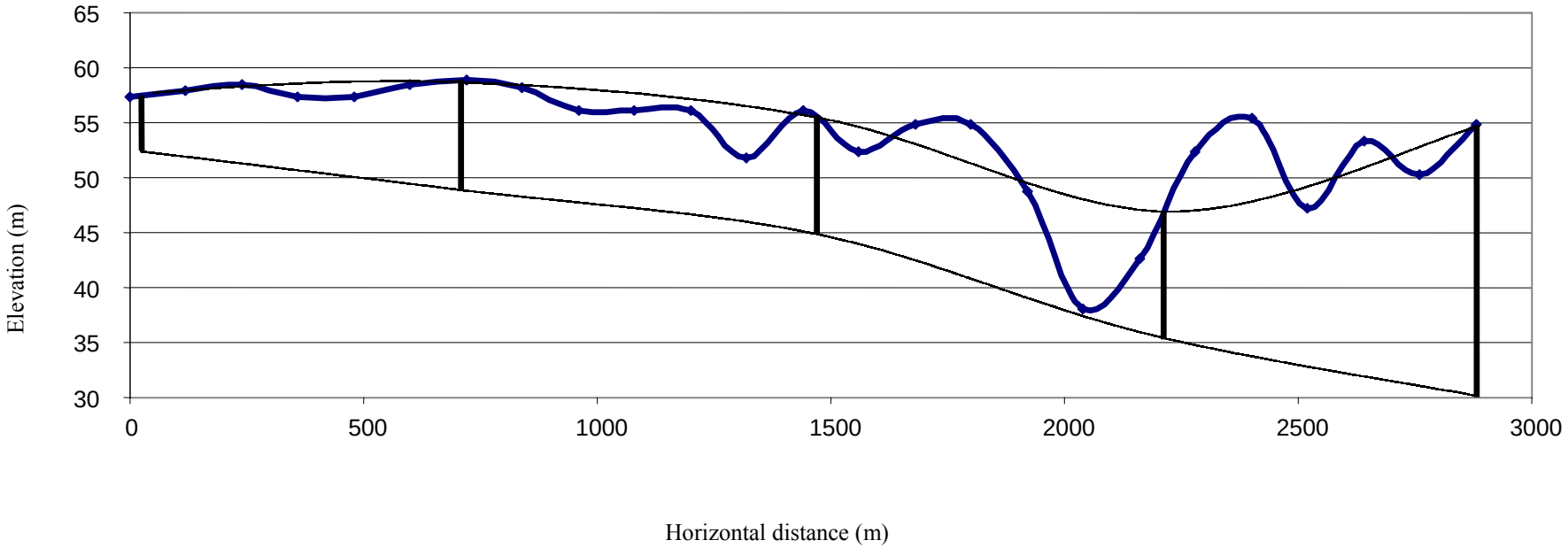

Figure 4.5. Cross section from transect 2 (see Figure 4.3). The dark horizontal line represents surface topography and the dark vertical lines show depth to reduced sediments as indicated by wells along the transect. The dashed lines represent interpolated surface topography, and the boundary between oxidized and reduced sediments, as indicated by the wells. (Vertical exaggeration is 23X)

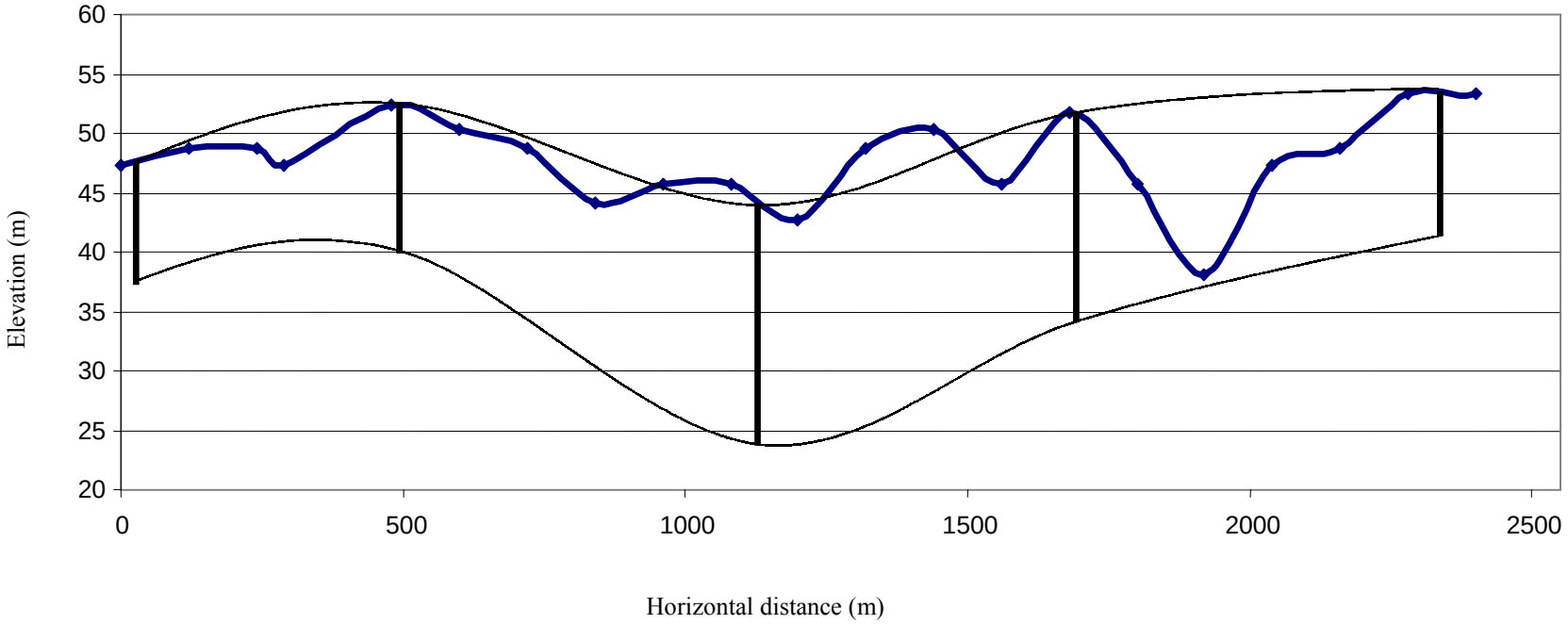

Figure 4.6. Cross section from transect 3 (see Figure 4.3). The dark horizontal line represents surface topography and the dark vertical lines show depth to reduced sediments as indicated by wells along the transect. The dashed lines represent interpolated surface topography, and the boundary between oxidized and reduced sediments, as indicated by the wells.(Vertical exaggeration is 21X.)

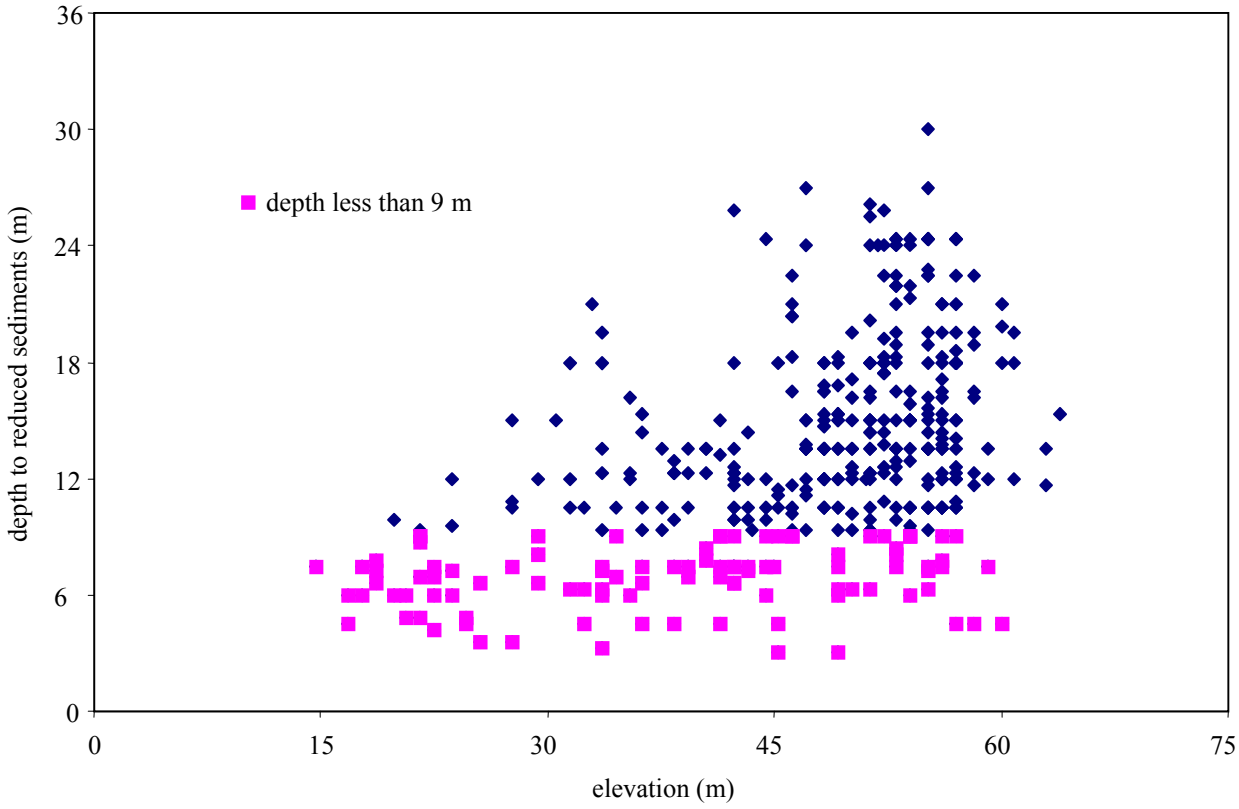

Figure 4.7. Scatterplot of depth to reduced sediments (depth-rs) versus elevation for all well logs in the study area. Points with depth-rs < 9 m are highlighted in pink.

Table 4.1 Coefficients of determination (R^2) from simple and multiple regression analyses of depth to reduced sediments against selected landscape variables.

Variable	Data set	R^2
elevation	all wells	0.22
slope	all wells	0.02
distance to nearest stream	all wells	0.02
Elevation/slope/distance to nearest stream	all wells	0.23
elevation	Wells from areas surficially mapped as Tertiary sediments	0.03
Elevation/slope/distance to nearest stream	Wells from areas surficially mapped as Tertiary sediments	0.23
elevation	Wells from areas surficially mapped as Cretaceous sand and gravel	0.13
elevation	Wells from areas surficially mapped as alluvium	0.15

A number of factors may help explain these poor results. Depth-rs is mainly controlled by two variables: depth of sediments overlying the sulfidic strata and depth of weathering within that strata. Where Tertiary marine sediments are surficially exposed, depth-rs is a function of weathering, and is largely affected by hydrology. Surface features such as elevation, slope, and distance to streams should be related to depth-rs. However, as indicated in Table 1, these factors alone could not be used to predict depth-rs. Underlying factors, such as textural changes between layers, may affect hydrology in locations that otherwise seem similar. Furthermore, local topographic features, such as intermittent streams or depressions, which are not apparent at the available map scale, may help explain discrepancies between seemingly similar locations.

Where Tertiary marine sediments occur in the subsurface, depth-rs is determined more by depth of sediments overlying the sulfidic strata than by hydrology. This depth is a function of the depositional, structural, and erosional features that control the thickness of overlying Quaternary

sediments, and may be further complicated by geologic factors such as lateral variation in sedimentary facies during deposition, the shallow dip of Coastal Plain sediments to the southeast, and the occurrence of normal faults. Consequently, the variables that control depth-rs over the entire study area may be too complex for regression analysis to allow approximations, let alone precise predictions, of depth-rs.

To avoid excavation of sulfidic materials it is most important to be able to identify locations where depth-rs is most likely to be shallow. Figures 4.3 and 4.7 indicate that sites with shallow depth-rs are dispersed throughout the study area and occur over the full range of elevations. Shallow depth-rs is expected at lower elevations because overlying Quaternary sediments have been removed and the water table occurs at shallower depths; however, shallow depth-rs is more difficult to explain for higher elevations. Sorting the data identified twelve high-elevation wells with depth-rs less than 7 m. These wells were not geographically clustered, and they occurred at various elevations (45 m – 61 m), stream proximities (175 – 720 m) and slopes (1 – 15%). While these data do not explain the shallow depth-rs values, site visits could reveal local conditions that help account for these occurrences. Furthermore, features such as soil types, which are controlled by the same factors that influence depth-rs, may provide useful indicators for estimating depth-rs. The application of soils data is discussed later in this chapter.

Finally, while it is impossible to assess the true extent of data error, a number of possible sources may contribute to the poor regression results. For example, three issues must be considered with the use of DEM's. First, most of these maps have a vertical accuracy of 7.5 m root-mean-square error. Given the relatively low elevations through the study area, such error could significantly impact elevation determinations. Furthermore, the SDTS DEM's, released prior to January 1, 2001, have positional errors resulting from the use of incorrect origins used to calculate the coordinate grid for each 7.5-minute quadrangle. The positional error does not exceed the spatial resolution of the DEM, in this case 30 m, and would likely have a trivial impact for the majority of data points in this study. Nonetheless, in some cases a slight positional shift could result in a relatively large elevation difference that could affect results. Finally, at the time this study was completed, DEM's for the study area were available only at 30 m resolution. Use of finer resolution DEM's, which are currently being created, may improve results by

providing for more accurate elevation data. While use of digital maps and GIS allows for rapid data analyses, the data available at the time of this study may not be suitable for the level of precision required to accurately evaluate depth-rs as a function of landscape variables.

Other sources of data error may arise from the precision and accuracy of the well logs. The boundary between reduced sediments and overlying materials is quite distinct, so it is unlikely that the well logs were misinterpreted. However, while some logs identified the boundary at a specific depth, others identified the boundary as occurring within a depth interval, usually around 6 m. When the boundary was identified within an interval, depth-rs was assigned the mean depth value for that interval. This could result in an error of a few meters from the true value. Furthermore, the accuracy with which these logs are recorded is unknown, and may vary among well drillers. Nonetheless, it seems likely that errors would be more significant with increasing depth. Consequently, error in the well logs does not account for the unexpected shallow depth-rs occurrences at higher elevations. For most of the logs, the well location was clearly indicated on a parcel plat. In most cases, elevation changes were minimal in the vicinity of the well location, so precise location of the well was not critical. However, in some cases, even a slight positional change resulted in a significant elevation difference. Therefore, mislocation of some wells may have resulted in inaccurate elevation determinations. Unlike the study by Valladares (1998), depth to sulfidic sediments in the Virginia study area could not be predicted precisely by regression analysis using landscape parameters. This may be explained by three main differences between these two studies. First, the geologic settings differ in a way that may allow depth to sulfides to be predicted by landscape parameters in the region of the Maryland study, but not in the Virginia study. This is due to the variable thickness of Quaternary sediments that blanket most of the Virginia study area, but are almost non-existent in the Maryland study area. Where these sediments do occur in the Maryland landscape studied they tend to exist as a relatively thin layer (less than 4 m deep). Therefore, depth-rs in Valladares' study area is dominantly controlled by weathering and hydrology, which may be explained by landscape parameters that are easy to quantify, such as point relief. In contrast, depth-rs in the Virginia study area was more difficult to predict due to various controls over depth to sulfidic strata as previously described. Second, Valladares observed depth-rs from his own deep borings, and determined elevation by surveying transects in the field. These data should be more accurate

than that obtained from the well logs and DEM's used in this study. Finally, the Valladares study was based on detailed observations from a few locations, and validation data were obtained from the same location as the data used to derive the predictive models. My study was based on observations dispersed throughout a larger study area. The factors that control weathering and hydrology are likely to be more uniform at a specific location than for a much larger area. Consequently, relationships should be more predictable for a small area than for a large area. To evaluate the application of predictive models based on data from a few specific locations, validation data should be collected from outside the study sites.

Interpolation of depth to reduced sediments

For a second approach to predicting depth to reduced sediments, depth-rs values were interpolated to generate a depth-rs surface. The interpolation procedure was repeated three times using randomly selected subsets of the well data. Regression analysis of the interpolated depth-rs values and the known depth-rs values for the remaining well points indicated poor results for all three trials (r^2 = 0.19, 0.19, and 0.24). In each case, the root-mean-square error was approximately 5 m with a standard deviation of 4 m. Interpolation cannot adequately predict depth-rs because the surface of the sulfide-bearing strata is too variable and some areas are not adequately represented with well data. While some regions of the study area have dense clusters of data points, such as where new housing developments have been constructed, other regions yield few data points. In particular, because these are drinking water wells, they are generally located at a distance from creeks and rivers and so those areas are poorly represented. Furthermore, well log data have been kept on file at the Health Department only for the past few decades. The existence of numerous old farms throughout the study area results in relatively large regions without data. Considering the significant landscape changes that may exist between data points depth-rs is too variable to be accurately interpolated with the density and distribution of available sample points for this study area.

Probability mapping of depth to reduced sediments based on general elevation classes

Although regression analyses and interpolation could not provide accurate means for predicting depth-rs, evaluation of the data did reveal a few generalizations. Most importantly, depth-rs values increase with increasing elevation, and shallow depth-rs values are found over the entire elevation range, although they are less frequent at higher elevations. To provide general estimates of depth-rs, the data were grouped into seven elevation classes and depth-rs values were summarized by descriptive statistics. The results are provided in Table 4.2 and illustrated in Figure 4.8. Overall, the data may be divided into three groups based on mean values. Mean depth-rs was 7 m, at elevations below 26 m, 10 - 12 m at elevations between 27 - 47 m, and 15 m at elevations greater than 48 m. Standard deviation increased noticeably above 26 m, indicating that depth-rs is much more variable at moderate to high elevations.

The three groups coincide with the three main landforms present in the study area. Elevations below 27 m are found primarily in floodplains, and to a lesser extent in drainages. Depth-rs is consistently shallow at lower elevations for two reasons. First, the floodplain landforms, which dominantly occur at low elevations in the study area, have naturally exposed Tertiary marine sediments at the surface, although a thin layer of alluvium covers some areas. Second, floodplains have high water tables that prevent oxidation of these sediments. Therefore, sulfidic sediments are maintained in a reducing environment at relatively shallow depth. Elevations between 27 – 46 m typically occur within the incised valleys surrounding drainages. Within this setting, Tertiary marine sediments may be naturally exposed at the surface, or they may be covered by a thin layer of alluvium or a variably thick layer of Quaternary sands and gravels. These geological differences, in combination with variable water table depths, result in a higher range of depth-rs values than for the floodplain landscapes. For a large extent of the study area, the 150 ft (46 m) contour line marks a distinct break between upland topography and incised drainage slopes. Elevations greater than 47 m typically occur in the broad, gently rolling uplands. In this landscape, a variably thick layer of Quaternary sands and gravel overlies the Tertiary marine sediments. This blanket of material, in combination with various possible structural and micro-relief features previously discussed, result in the highest mean and range of depth-rs values.

Table 4.2. Descriptive statistics summarizing depth to reduced sediments (depth-rs) from well log data for seven elevation classes in the study area.

elevation (m)	n*	mean depth-rs(m)	median depth-rs (m)	standard deviation (m)	min depth-rs(m)	max depth-rs (m)
< 20	8	7	7	1	5	8
20 - 26	22	7	7	2	4	12
27 - 33	17	10	11	4	4	18
34 – 40	39	11	11	4	3	21
41 - 47	65	12	11	5	3	26
48 - 54	133	15	14	5	3	27
> 55	124	15	15	5	5	30

***** number of wells

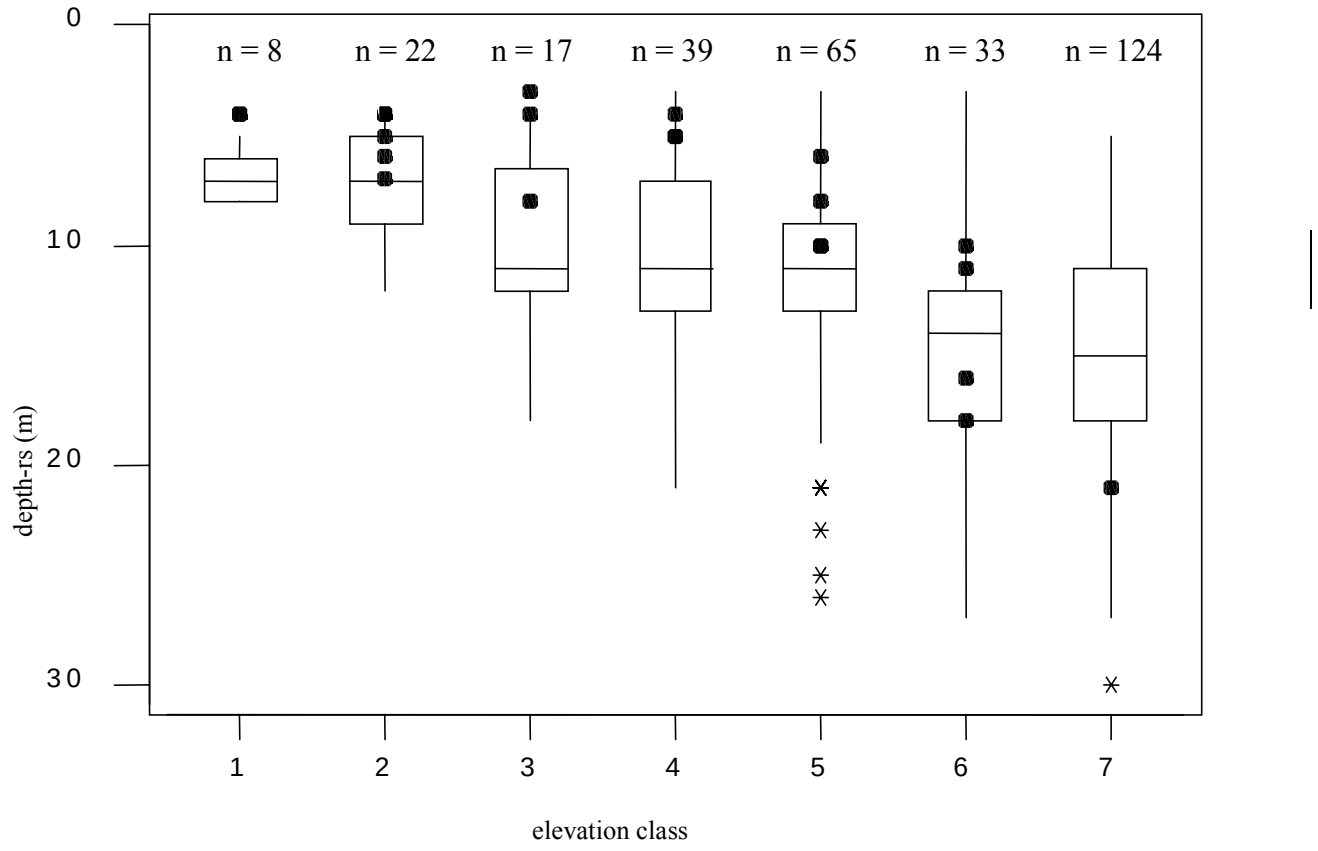

Figure 4.8. Boxplot of depth to reduced sediments for elevation classes. Asterisks indicate outliers from the well log data. Bullet markers indicate validation drill holes.

Summarizing the data in the manner described above provides predictive ranges for depth-rs using elevation to represent related landforms. To evaluate the accuracy of these ranges, 23 deep borings were made at ten sites dispersed throughout the study area. Data from these borings are shown in Table 4.3 and Figure 4.8. For one high-elevation point, reduced sediments were not encountered before reaching the maximum drill depth of 20 m. Depth-rs for this hole was assigned a value of 21 m to represent the minimum value at which reduced materials would be likely to occur. For each of the validation points, depth-rs fell within the depth-rs ranges defined for each elevation class, as indicated in Figure 4.8. However, at lower elevations the validation points tended to lie within the shallow end of the depth-rs range, while at higher elevations the validation points were mostly within or beyond the deep end of the range. The apparent overprediction of depth-rs by the well log data for lower elevations may be due in part to inadequate distribution of the validation points. The twelve lowest elevation validation points, which represent the three lowest elevation classes and part of class 4, were located in areas where Tertiary marine sediments were exposed at the surface, or overlain by only a thin layer of alluvium or terrace deposits. Most of the well log data for elevation classes 1 and 2 were from similar geological settings. Class 1 had only 1 validation point, which lay at the extreme shallow end of the depth-rs values. For class 2, the validation points span over half of the depth-rs range defined by the well log data. As elevation increases, the well logs are increasingly located in areas overlain by Quaternary deposits. Therefore, for elevation classes 3 and 4, overlying Quaternary sediments will result in greater depth-rs values for the well logs than for the validation points. More uniform distribution of validation data over the different geologies may have resulted in closer agreement between the well log data and the validation data. For the remaining elevation classes, well log data and validation data were from areas where reduced sediments are generally overlain by Quaternary deposits. Validation points for elevation classes 5 and 6 were mostly within the average range of depth-rs values. Class 7 had only 1 validation point, which lay within the deep end of depth-rs values. Overall, agreement of the validation points with the defined depth-rs ranges supports the use of the summarized well log data for providing general estimates of depth-rs based on elevation.

In the study area, and surrounding regions, most highway construction tends to involve excavation to depths of less than 9 m. For each elevation class, the relative proportion of data

Table 4.3. Elevation, depth to reduced sediments (depth-rs), percent S at depth-rs, for 23 deep borings used as validation points.

sample	elevation (m)	depth-rs (m)	%S
vdawk1	29	3	0.8
vdawr2	19	4	0.7
vdawr1	27	4	1.4
vdawk2	27	4	0.8
vdatot2	32	4	1.2
vdamcv10	35	4	1.4
vdaecw2	12	4	2.7
gas	25	4	1.3
vdatot3	41	5	0.7
vdabcw3	20	5	1.1
vdaph1	41	5	0.6
vdamcv7	43	6	1.4
vdaecw1	22	6	2.1
vdabcw1	23	7	0.9
vdapeas1	47	8	0.7
vdabcw2	30	8	2.6
wm2	47	10	1.1
vdatot1	47	10	0.6
vdatot4	52	10	0.6
vdacp1	50	11	0.5
vdalfr	55	16	0.6
vdapc	55	18	0.9
vdavl1	57	21	n.d.

with depth-rs less than 9 m indicates the likelihood of encountering sulfidic materials within common excavation depths. This process may be repeated with the data set for any depth of interest. For example, for each elevation class the data were evaluated to determine the proportion of wells with depth-rs less than 5, 9, and 13 m. The results are presented in Table 4.4. Elevation risk factors were designated based on the proportion of wells with depth-rs below the specified depth for each elevation class as follows: i) greater than 50% is a very high risk (4), ii) 26-50% is a high risk (3), iii) 11-25% is a moderate risk (2), and iv) less than 11% is a low risk (1). As shown in Table 4.4, elevations below 26 m have a very high probability of encountering reduced sediments within 9 m. The probability is high between elevations of 27 – 40 m, moderate for elevations between 41 – 47 m, and low for elevations above 47 m.

Table 4.4. Proportion of well logs for each elevation class with depth to reduced sediments (depth-rs) less than 5, 9, and 13 m, and associated risk factor designations.

			depth-rs < 5 m			depth-rs < 9 m			depth-rs < 13 m		
elevation class	elevation (m)	n	n5*	n5/n	risk**	n9*	n9/n	risk	n13*	n13/n	risk
1	< 20	8	0	0.00	l (1)	8	1.00	vh (4)	8	1.00	vh (4)
2	20 - 26	22	2	0.09	l (1)	15	0.68	vh (4)	22	1.00	vh (4)
3	27 - 33	17	1	0.06	l (1)	7	0.41	h (3)	14	0.82	vh (4)
4	34 – 40	39	1	0.03	l (1)	14	0.36	h (3)	29	0.74	vh (4)
5	41 - 47	65	1	0.02	l (1)	15	0.23	m (2)	48	0.74	vh (4)
6	48 - 54	133	1	0.01	l (1)	9	0.07	l (1)	45	0.34	h (3)
7	> 55	124	0	0	l (1)	10	0.08	l (1)	45	0.36	h (3)

*n5, n9, and n13 = number of wells with depth-rs less than 5 m, 9 m, and 13 m, respectively
**risk assessment: l = low probability of encountering sulfidic sediments, m= moderate probability, h = high probability, vh = very high probability. Value in parenthesis indicates quantification of risk.

Probability mapping of depth to reduced sediments – soils

Soils data may provide additional information for predicting general depth-rs values. Soil development results from the interaction of five factors – parent material, time, climate, organisms, and relief. Locally, areas that are mapped with similar soil series likely have experienced the same relative influence of these factors. Furthermore, to some extent, the factors that control soil formation may affect depth-rs. For example, depth-rs values should be shallowest where Tertiary marine sediments are naturally exposed at the ground surface, and depth-rs is primarily a function of the weathering profile. Specific soil types that form over Tertiary marine sediments may be associated with shallow depth-rs, and therefore can be used as an indicator. Similarly, certain soils that form over Quaternary sands and gravels may indicate deeper depth-rs values by reflecting the presence of this material overlying sulfidic sediments.

To evaluate the relationship between soil map units and depth-rs in the study area, the well log data were summarized to indicate the number of wells in each represented soil map unit, along with the minimum, maximum, and average depth-rs for those wells. The proportion of wells with depth-rs less than 9 m was calculated for map units represented by at least 5 data points. The results are presented in Table 4.5. Thirty-seven map units were represented by the well log data. For map units with 5 or more data points, soil risk was designated in a manner similar to elevation risk based on the proportion of wells with depth-rs less than or equal to 9 m. A number of map units contained few data points and additional data would be necessary to

Table 4.5. Soil map units represented by the well log data. For each map unit the dominant soil series, total number or wells, minimum, mean, and maximum depth to reduced sediments (depth-rs) values, and associated soil risk designations are identified.

	dominant soil series	n*	minimum depth-rs (m)	mean depth-rs (m)	maximum depth-rs (m)	n9/n**	soil risk
46	Myatt Variant	1	4	4	4	n.d	h (3)
8	Augusta	1	5	5	5	n.d	h (3)
30	Forestdale	1	6	6	6	n.d	h (3)
43	Kenansville Variant	1	6	6	6	n.d	h (3)
70B	Udults-Ochrepts	1	7	7	7	n.d	h (3)
70F	Udults-Ochrepts	1	9	9	9	n.d	h (3)
65B	Turbeville	1	17	17	17	n.d	m (2)
2	Altavista	1	18	18	18	n.d	m (2)
10B	Bourne	1	20	20	20	n.d	l (1)
40A	Kempsville-Bourne	1	24	24	24	n.d	l (1)
12D2	Caroline	2	7	10	14	n.d	m (2)
63C	Suffolk	2	22	23	24	n.d	l (1)
55B	Pamunkey	3	7	9	12	n.d	h (3)
63A	Suffolk	3	9	13	19	n.d	m (2)
28	Fluvaquents	4	5	7	14	n.d	h (3)
23	Dogue	4	6	8	11	n.d	h (3)
13B2	Caroline-Dogue	5	5	14	25	0.20	m (2)
69D	Udults	5	11	13	16	0.00	l (1)
25A	Duplin	6	5	17	25	0.17	m (2)
25B	Duplin	6	9	16	21	0.00	l (1)
39C	Kempsville	6	9	13	21	0.00	l (1)
34B	Goldsboro	6	9	14	17	0.00	l (1)
69C	Udults	7	6	10	16	0.29	h (3)
50A	Orangeburg-Faceville	8	5	15	25	0.12	m (2)
41	Kenansville	10	8	17	30	0.10	l (1)
13C2	Caroline-Dogue	16	6	14	24	0.25	m (2)
49B	Orangeburg	16	10	15	25	0.00	l (1)
70E	Udults-Ochrepts	17	5	11	26	0.53	h (3)
39B	Kempsville	17	8	12	18	0.18	l (1)
70C	Udults-Ochrepts	19	3	10	18	0.37	h (3)
54B	Pamunkey	19	5	10	20	0.50	h (3)
47A	Norfolk	27	7	14	23	0.11	m (2)
50B	Orangeburg-Faceville	30	8	16	27	0.07	l (1)
70D	Udults-Ochrepts	34	5	10	18	0.38	h (3)
40B	Kempsville-Bourne	37	5	14	25	0.08	m (2)
63B	Suffolk	42	5	14	26	0.12	m (2)
47B	Norfolk	46	3	15	27	0.11	m (2)

* n = number of wells

** n9/n = proportion of wells with depth-rs < 9 m.

accurately assess these units. Nonetheless, soil risk factors based on mean depth-rs were assigned to help illustrate the interpretive process. Map units with a high risk factor included 46, 8, 30, 43, 70B, 70F, 54B, 69C, 70C, 70D, and 70E. Map units with a moderate risk included 65B, 2, 12D2, 63A, and 13B2, 13C2, 25A, 39B, 40B, 47A, 47B, 50A, and 63B. Map units with a low risk included 10B, 40A, 63C, 25B, 34B, 39C, 41, 49B, 50B, and 69C.

Finally, two sets of data points were used to evaluate risk assessments based on elevation and soil type. The first set consisted of the previously described validation points. The second set consisted of 35 well logs provided in Daniels and Onuschak (1974). These well logs included engineering test borings, public water wells, and Virginia Department of Mineral Resources test borings. In the following discussion these two sets of data are referred to collectively as the test points. As described above, and indicated in Table 4.6, each test point was assigned an elevation risk factor and a soils risk factor for encountering depth-rs at less than or equal to 9 m. Three test points occurred in soil map units which were not previously represented by the well log data. These points, indicated in Table 4.6, were assigned soil risk factors based on comparison of the map unit descriptions with the map units listed in Table 4.4. An overall risk was assigned by multiplying the elevation and soil risk factors. Overall risk values of 1 or 2 indicate that the most severe risk is moderate for only one factor, and therefore suggest a relatively low probability of encountering depth-rs within 9 m. Overall risk factors of 3 or higher indicate that at minimum either one factor has a high risk, or both factors have moderate risks, and therefore suggest a relatively high probability of encountering depth-rs within 9 m.

Of the 58 test points, 20 had depth-rs less than 9 m. Of these 20 points, 18 (90%) were accurately assigned high overall risk factors of at least 3. The 2 points with low overall risk values had borderline depth-rs values of 7 and 8 m. Of the 38 points with depth-rs greater than or equal to 9 m, 34 (89%) were accurately assigned low overall risk factors of 1 or 2. Of the 4 points with high overall risk values, 3 had borderline values of 9 or 10 m. These results demonstrate that use of the elevation risk factor, in conjunction with the soil risk factor, can successfully predict if depth-rs is less than 9 m. The interpretations presented in Table 4.4 and 4.5 were applied to DEM's and soils maps using ARCView to generate a risk map (Figures 4.9 and Plate 2 – hard copy on file in Newman library).

Table 4.6. Test points used to evaluate the application of elevation risk and soil risk for predicting depth to reduced sediments (depth-rs).

well ID	soil map unit	depth-rs (m)	elevation (m)	elevation risk*	soil risk*	Overall risk (elevation risk X soil risk)
vdawk1	23	3	29	h (3)	h (3)**	9
1799	70D	3	50	l (1)	h (3)	3
vdawr2	28	4	19	vh (4)	h (3)**	12
vdawr1	63B	4	27	h (3)	m (2)	6
vdawk2	23	4	27	h (3)	h (3)**	9
vdatot2	28	4	32	h (3)	h (3)**	9
vdamcv10	70E	4	35	h (3)	h (3)	9
vdaecw2	22	4	12	vh (4)	h (3)***	12
gas	8	4	25	vh (4)	h (3)**	12
2237	69C	5	43	m (2)	h (3)	6
vdatot3	70E	5	41	m (2)	h (3)	6
vdabcw3	64B	5	20	vh (4)	m (2)***	8
vdaph1	63B	5	41	m (2)	m (2)	4
vdamcv7	70E	6	43	m (2)	h (3)	6
vdaecw1	70D	6	22	vh (4)	h (3)	12
vdabcw1	2	7	23	vh (4)	h (3)**	12
3901	40B	7	54	l (1)	m (2)	2
3087	70E	8	48	l (1)	h (3)	3
vdapeas1	41	8	47	m (2)	l (1)	2
vdabcw2	39B	8	30	h (3)	m (2)	6
3900	40A	9	17	vh (4)	l (1)**	4
3638	41	9	49	l (1)	l (1)	1
1842	50B	9	46	m (2)	l (1)	2
2573	50B	9	50	l (1)	l (1)	1
1800	70B	9	50	l (1)	h (3)**	3
2197	47B	9	56	l (1)	m (2)	2
wm2	63A	10	47	m (2)	m (2)**	4
vdatot1	70C	10	47	m (2)	h (3)	6
vdatot4	63B	10	52	l (1)	m (2)	2
2841	47A	10	55	l (1)	m (2)	2
vdacp1	63B	11	50	l (1)	m (2)	2
2349	39B	12	49	l (1)	m (2)	2
1662	63B	12	50	l (1)	m (2)	2
199	40B	12	52	l (1)	m (2)	2
493	50B	13	46	m (2)	l (1)	2
3068	40B	14	50	l (1)	m (2)	2
1770	41	14	57	l (1)	l (1)	1
969	63C	15	58	l (1)	l (1)**	1
2224	63A	15	52	l (1)	m (2)**	2
2417	64B	15	52	l (1)	m (2)***	2
1948	41	15	53	l (1)	l (1)	1
1301	47B	15	53	l (1)	m (2)	2
590	63B	15	57	l (1)	m (2)	2
3638	40B	15	57	l (1)	m (2)	2
1791	70E	15	61	l (1)	h (3)	3
vdalfr	50B	16	55	l (1)	l (1)	1
338	50A	16	50	l (1)	m (2)	2
vdapc	50B	18	55	l (1)	l (1)	1
749	63A	18	53	l (1)	m (2)**	2
2800	50B	18	53	l (1)	l (1)	1
3546	47A	18	59	l (1)	m (2)	2
2501	63A	20	49	l (1)	m (2)**	2
2617	63B	21	56	l (1)	m (2)	2
vdavl1	50A	21	57	l (1)	m (2)	2
3904	63B	21	52	l (1)	m (2)	2
3782	50B	26	51	l (1)	l (1)	1
750	50B	27	53	l (1)	l (1)	1
3401	50B	34	52	l (1)	l (1)	1

* h = high, m = moderate, h = high, vh = very high

** soil risk factor based on fewer than 5 data points

*** soil risk factor based on assessment of soil map unit description

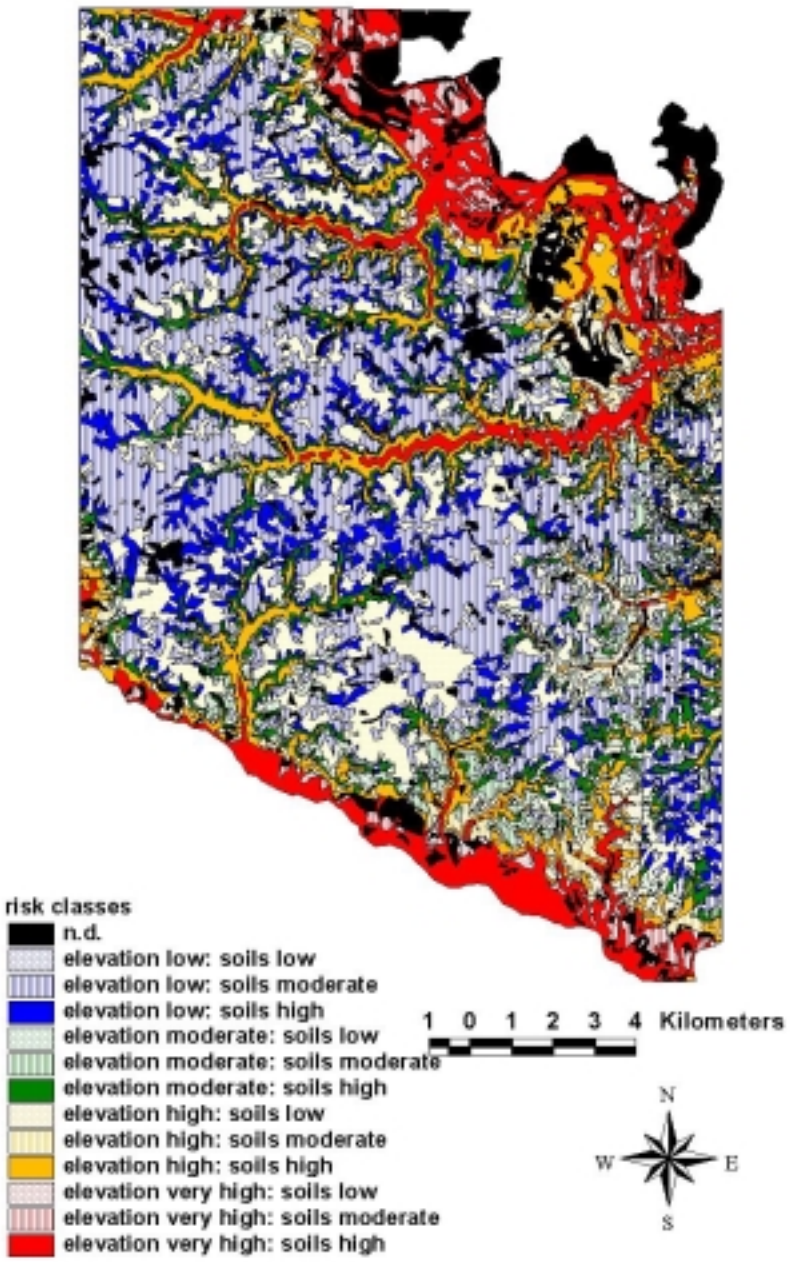

Figure 4.9. Risk map, based on elevation and mapped soil type, for encountering reduced sediments within a depth of 9 m for study area near Mechanicsville, VA (see Figure 4.2).

that may be used to evaluate the likelihood of encountering reduced sediments within 9 m for specific locations. By evaluating the well log data with respect to a specified depth-rs, and appropriately re-assigning risk factors, this process could be repeated for other depth-rs values. These elevation and soil risk factors are specific to the study area, and should not be extrapolated beyond its boundaries. However, this method of risk assessment could be applied to other areas in the Coastal Plain, where the data are available.

Exposure of reduced Tertiary sediments is problematic only if the material contains high levels of S (> 0.2%). Therefore, the deep borings were used to evaluate the large-scale lateral distribution of S in reduced Tertiary sediments. From each boring, a sample was collected from the upper 30 cm of reduced sediments and evaluated for %S and presence of calcium carbonate. Previous work indicated that %S is highly correlated with potential peroxide acidity for samples that do not contain calcium carbonate (see Chapter 3). All samples had relatively high S values (Table 4.3), and none of the samples contained $CaCO_3$, indicating that exposure of reduced Tertiary sediments would always present a high risk of acid production.

Weathering Profiles

Weathering of sulfidic sediments, either naturally or after disturbance, produces two distinct zones in the soil column. The upper zone is an oxidized, or partially oxidized, layer that contains iron oxides, may contain yellow jarosite, and has a low pH (< 4). The lower zone is the unoxidized, sulfidic layer that appears as a drab, dark color and has a higher pH (> 5.5). To illustrate the weathering profiles typically found in the study area, detailed characterizations of three borings are shown in Figures 4.10, 4.11, and 4.12. Although these sites have been disturbed, all three profiles are from locations where Tertiary sediments naturally occur at the surface. The profile in Figure 4.10 is from a cut site with about 2 m of fill material that was emplaced after construction of a cellular phone tower. The profile in Figure 4.11 is from a cut site, where at least 4 m of material have been removed and no fill has been emplaced. This site represents the most disturbed profile in the sense that the natural upper weathering zone has been removed and the existing upper oxidized zone has formed since reduced sediments were exposed at the ground surface (less than 15 years). The profile in Figure 4.12, which was only minimally disturbed, appeared to have been graded then covered with a small amount of fill material. This

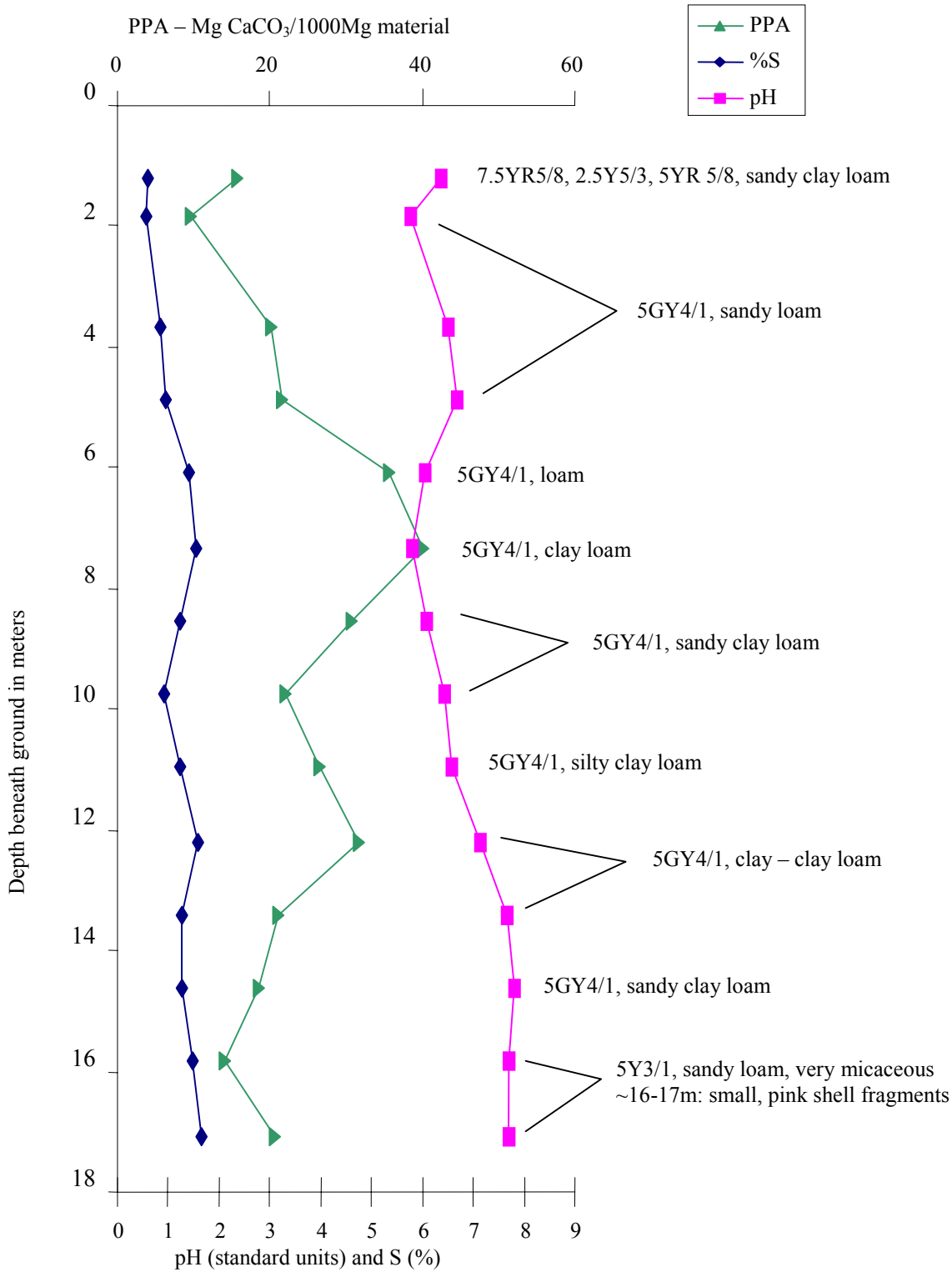

Figure 4. 10. Profile showing potential peroxide acidity (PPA), %S, and pH versus depth, with Munsell colors and sediment textures noted, for a deep boring behind Brook Hill Communications on Power Road and I-295, Henrico County, Virginia.

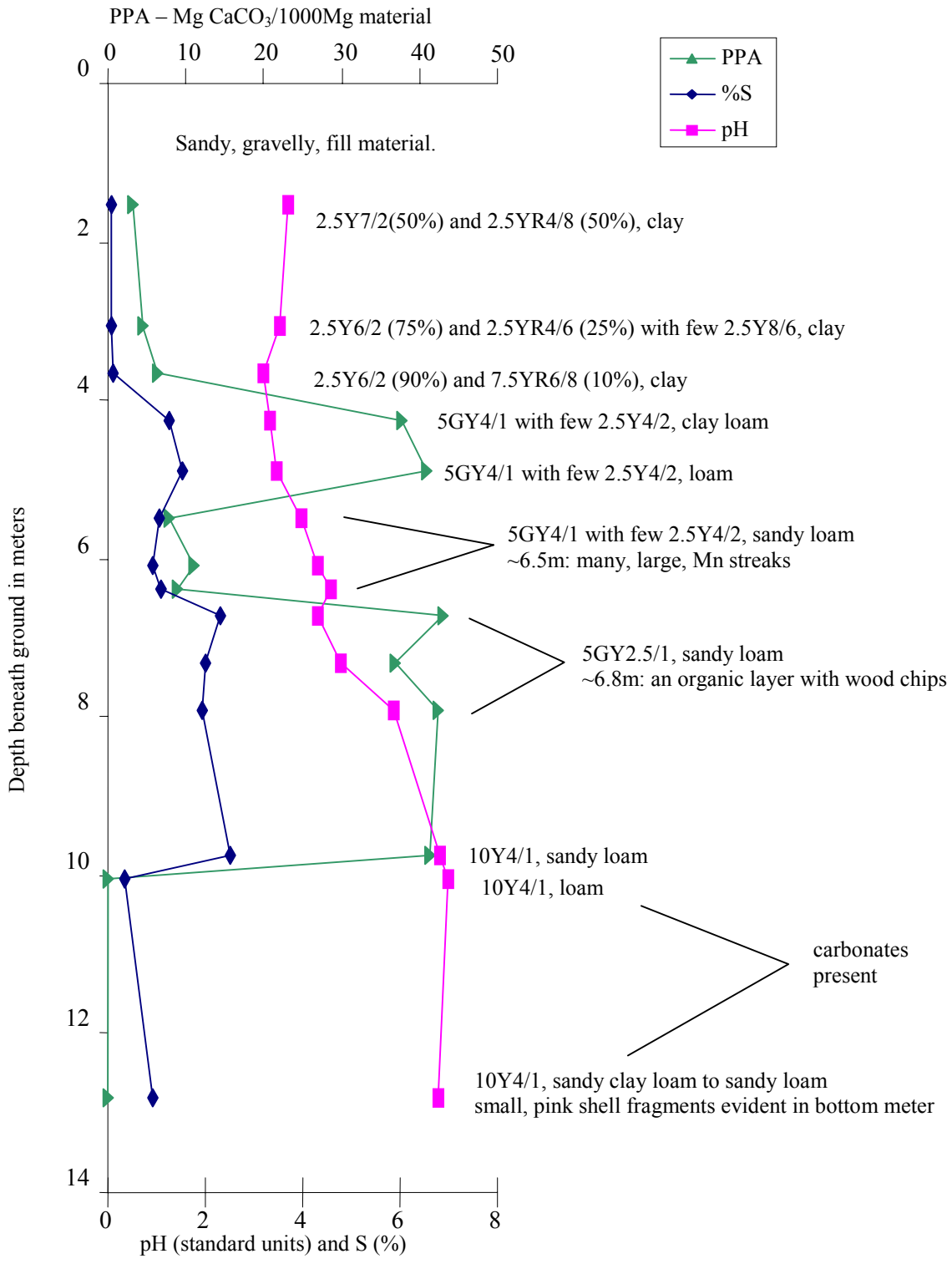

Figure 4.11. Profile showing potential peroxide acidity (PPA), %S, and pH versus depth, with Munsell colors and sediment textures noted, for a deep boring at the intersection of Rts-156 and 630, Hanover County, Virginia.

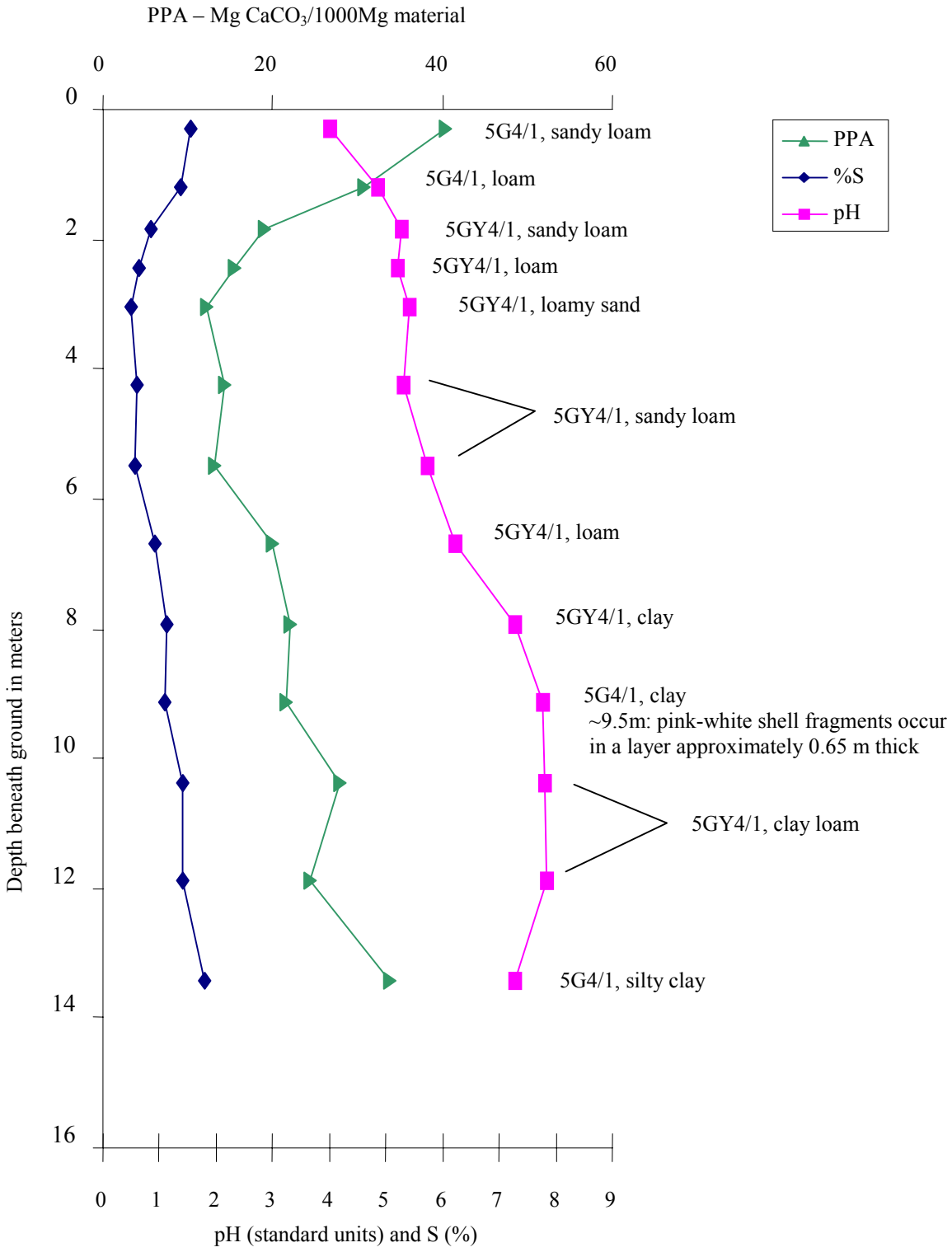

Figure 4.12. Profile showing potential peroxide acidity (PPA), %S, and pH versus depth, with Munsell colors and sediment textures noted, for a deep boring between the exit ramp from 295S to 360W and the cloverleaf from 360W to 295S, Hanover County, Virginia.

site most closely represents a natural weathering profile. For all profiles, the strong correlation between PPA and %S is evident except for the base of Figure 4.12 where $CaCO_3$ is present. The upper portions of Figures 4.11 and 4.12 illustrate how pH values drop very low (< 4) as sulfidic materials are oxidized. This is not evident in Figure 4.10 and is at least partially due to liming of the surface. In Figures 4.11 and 4.12, oxidation-reduction transition zones are indicated by steadily increasing pH values. In Figure 4.11, the zone is minimally evident visually due to the relatively short weathering period. In Figure 4.12, which retains most of the natural weathering profile, the transition zone is readily apparent by color transition from brownish-gray to dark gray, and the presence of yellow jarosite and red iron oxide features. Where sediments are completely reduced below the water table, around 8 m, pH values tend to range between 6-8 and color is homogenously drab dark gray.

Conclusions

Within the study area, depth-rs values generally increased with elevation, although values were as shallow as 3 - 4 m for all elevations, and were much more variable at higher elevations. A model could not be developed by regression analysis to accurately and precisely predict depth-rs using landscape variables, which included elevation, slope, distance to streams, and surficial geology. Similarly, interpolation based on depth-rs from a subset of the well logs data was unsuccessful at predicting depth-rs for the remaining points. By grouping the data into seven elevation classes, depth-rs values were summarized to provide predictive value ranges Depth-rs from twenty-three validation points supported the use of these predictive ranges. Significant breaks in mean depth-rs among the elevation classes reflected local geomorphic differences. Classes 1 and 2, which represent floodplains, had a mean depth-rs of 7 m. Classes 3, 4, and 5, which represent incised drainages, had a mean depth-rs of about 11 m. Classes 6 and 7, which represent uplands, had a mean depth-rs of 15 m. Depth-rs became significantly more variable at elevations above 26 m, and values as low as 5 m were found at all elevations. The data may be further analyzed to predict the likelihood of encountering sulfidic sediments within specific excavation depths by evaluating the relative proportion of wells that have depth-rs below the specified value for each elevation class. Within the study area, road corridor excavation depths are typically less than 9 m. For this depth, there is a low risk of encountering sulfidic materials at

elevations greater than 47 m, a moderate risk at elevation between 41 – 47 m, and a high to very high risk at elevations below 41 m. Similarly, by evaluating the minimum, maximum, and mean depth-rs values for well logs within each represented soil map unit, soil risk factors may be assigned to those units. High-risk map units contained the following series: Augusta, Dogue, Caroline, Forestdale, Kenansville, Myatt Variant, and Pamunkey. Soil map units consisting of unspecified Udults, Ochrepts, and Fluvaquents also had a high risk. The elevation risk factor in conjunction with the soil risk factor accurately described the likelihood of encountering depth-rs at less than 9 m for 90% of 58 test points. All reduced sediment samples from locations throughout the study area contained high S levels, indicating that exposure of reduced Tertiary sediments should always be considered hazardous in terms of acid production.

References

Daniels, P. A. Jr., and E. Onuschak, Jr. 1974. Geology of the Studley, Yellow Tavern, Richmond, and Seven Pines quadrangles, Virginia. Vir. Div. of Mineral Resources. Report of Investigations 38. Charlottesville.

Dent, D. L. and L. J. Pons. 1995. A world perspective on acid sulfate soils. Geoderma. 67:263-276.

Hodges, R. L., G. Richardson, J. P. Sutton, J. E. Belshan, T. W. Simpson, W. S. Barnes, and J. E. Keys, Jr. 1980. Soil survey of Hanover County, Virginia. USDA. Washington, D.C.

Lin, C. and M. D. Melville. 1994. Acid sulphate soil-landscape relationships in the Pearl River Delta, southern China. Catena. 22:105-120.

Lin, C., M. D. Melville, and S. Hafer. 1995. Acid sulphate soil-landscape relationships in an undrained, tide-dominated estuarine floodplain, Eastern Australia. Catena. 24:177-194.

Madsen, H. B., N. H. Jensen, B. H. Jakobsen, and S. W. Platou. 1985. Mapping of potentially acid sulfate soils in Jutland, Denmark. Catena. 363-371.

Madsen, H.B. and N.H. Jensen. 1988. Potentially acid sulfate soils in relation to landforms and geology. Catena.

Pons, L. J., N. Van Breeman, and P. M. Driessen. 1982. Physiography of coastal plain sediments and development of potential soil acidity. p. 1 – 18. *In* J. A. Kittrick, D. S. Fanning, and L. R. Hossner (ed.) Acid Sulfate Weathering. Soil Sci. Soc. Am. Spec. Pub. 10, Madison, WI

Prokopovich, N. 1986. Engineering impacts of acid sulphate deposits in California. p. 49-58. *In* H. Dost (ed.) Selected papers of the Dakar symposium on acid sulphate soils. Pub 44. Int. Inst. For Land Reclamation and Improvement, Wageningen, The Netherlands.

Sobek, A. A., W. A. Schuller, J. R. Freeman, and R. M. Smith. 1978. Field and laboratory methods applicable to overburden and minespoils. U.S. E.P.A. Report EPA-600/2-78-054. Cincinatti.

Stone, Y, C. R. Ahern, and B. Blunden. 1998. Acid Sulfate Soils Manual. Acid Sulfate Soil Management Advisory Committee, Wollongbar, NSW, Australia.

van Holst, A. F., and C. J. W. Westerveld. 1973. Corrosion of concrete foundations in potential acid sulphate soils and subsoils in The Netherlands. p. 373-390. *In* H. Dost (ed.) Acid sulphate soils. Proc. Int. Symp. on acid sulphate soils, Wageningen, The Netherlands.13 – 20 August 1972. Pub. 18, Vol. II. Int. Inst. For Land Reclamation and Improvement, Wageningen, The Netherlands.

Valladeres, T. M. 1998. Estimating depth to sulfide-bearing sediments in the Maryland Coastal Plain: a pedo-geomorphic modeling approach. M.S. Thesis. Univ. Maryland, College Park.

Ward, L. 1984. Stratigraphy of outcropping Tertiary beds along the Pamunkey River – Central Virginia Coastal Plain. pp. 11 – 78. *In* L. W. Ward and Kathleen Krafft (ed.) Stratigraphy and paleontology of the outcropping Tertiary beds in the Pamunkey River, Virginia Coastal Plain – Guidebook for the Atlantic Coastal Plain Geological Association 1984 field trip: Atlantic Coastal Plain Geological Association.

Chapter 5

COMPARISON OF ACID ROCK DRAINAGE PREDICTION METHODS ON DIVERSE SULFIDIC MATERIALS

Introduction

Characterization of sulfidic materials prior to road construction allows for judicious planning which can significantly reduce the production and negative impacts of acid drainage. Accurate prediction of acid drainage has been the topic of much research, particularly with respect to mining. Test procedures are categorized as being either static or kinetic. Static tests are performed over a short and fixed time period. These tests create artificial weathering conditions to rapidly oxidize sulfides and determine the amount of acidity generated, or the "maximum potential acidity". Static tests are relatively quick, easy and inexpensive, but they do not account for differential acid-base reaction rates that significantly control net acid production in the field. Kinetic tests measure acid generation characteristics with respect to time. These tests may be designed to simulate field conditions in the laboratory or may be performed on-site. The drawbacks to kinetic tests are that they are more equipment intensive, they must be conducted over much longer time periods, and the procedures are not standardized. Results must be carefully interpreted with respect to the exact procedure utilized. While some techniques for predicting acid drainage are more commonly applied than others, there is no universal protocol for evaluating sulfidic materials. Furthermore, not all methods are suitable for all types of materials. Parameters such as mineralogy of the host material, grain-size and morphology of the sulfides will variably affect test results. Understanding the utility and limitations of different commonly utilized procedures allows for appropriate application of methods and interpretation of results.

Literature Review

Static tests use two basic approaches to estimate acid production. First, potential acidity may be indirectly estimated by determining percent S in a sample, assuming the S is in pyritic form, and applying stoichiometric equations to calculate the maximum amount of acidity that can be produced. Second, acid generation may be measured directly by oxidizing sulfidic samples and measuring the amount of acidity produced. The first approach is used in what is the most

commonly applied static test - Acid-Base Accounting (ABA). This technique was developed in the late 1960's at West Virginia University (Grube et al., 1973) and revised to a commonly referenced form by Sobek et al. (1978). Acid-base accounting balances the Maximum Potential Acidity (MPA) that can be generated by a material, expressed as a negative value, with the Neutralization Potential (NP) of that material, expressed as a positive value. This value is usually expressed in Mg of lime equivalence per 1000 Mg of material tested. The convention of using Mg/1000 Mg was adopted because it is equivalent to tons (English) of lime per acre furrow slice (6"). If the resulting value is negative the material should produce acidic water upon complete and kinetically balanced reaction. Positive results indicate water drainage will be alkaline.

The MPA of a sample is determined by calculations based on S content. Methods used for coal mine overburden analysis in the Appalachian region recommend using total-S, although other researchers suggest that sulfide-S is more appropriate (Kania, 1998). Total-S is usually measured using high-temperature furnace combustion such as a LECO Induction Furnace or Elementar Vario Max C-N-S Analyzer. Sulfide-S is usually determined through various S fractionation methods (Sobek et al., 2000) or by the chromium reducible sulfur procedure (Zhabina and Volkov, 1978; Canfield et al., 1986).

The NP of a sample represents carbonates and other acid neutralizers in a sample; however, negative NP values may occur when a sample contains weathering products, such as certain sulfate minerals, that produce acidity upon dissolution. Numerous procedures exist for determining NP. Many of these are variations of a basic method; the sample is reacted with a known quantity of acid, the base equivalency of the acid consumed is determined, and the value is converted to a calcium carbonate equivalent (CCE) neutralizing potential. Variations include the type and strength of acid used, test duration, and temperature. Other methods of determining carbonate content, such as CO_2 coulometry, and X-ray diffraction, have been proposed but are not in widespread use (Kania, 1998).

Some authors recommend a more mineralogical approach to ABA. Jennings et al. (1999) assert that characterization of complex mineral assemblages containing S compounds must consider not only the total quantity of S minerals present, but the specific mineralogy of the

compounds as well. These authors evaluated the response of common sulfide and sulfate minerals to oxidizing conditions, using H_2O_2, to evaluate relative amounts of acid generation. Similarly, Paktunc (1999) recommends a mineralogical approach to determination of neutralization potential. He asserts that while ABA works well for simple compositions, the tests may result in overestimation or underestimation of neutralization potential for more complex field samples. This author developed mineralogical constraint diagrams relating neutralization potential determinations to Ca, Mg, and CO_2 concentrations to serve as supplementary guides to improve interpretations of conventional tests.

Assumptions and associated limitations which need to be considered when interpreting standard ABA results include: i) all S in a sample will react to form acid; ii) all materials in the sample which consume acid during digestion in the lab will generate alkalinity in the field, iii) the reaction rate for the S will be the same as the dissolution rate for the neutralizing material; and iv) NP and percent S values below certain threshold levels do not influence water quality (Kania, 1998; Sobek et al., 1987). Furthermore, NP values will vary based on method. In the case of Sobek (1978), the exact procedure used is based on a subjective preliminary test that may lead to inconsistent results (Skousen et al., 1997). Researchers should acknowledge ABA limitations, and analyses may need to be modified as appropriate. Despite these limitations, years of extensive application indicate that the basic ABA method is an easy, fast, and useful tool for preliminary evaluation of potentially sulfidic materials (Sobek et al., 1987 and Sobek et al., 2000).

The second approach to determining acid potential, titration of acidity after oxidation of the sample, is used in various hydrogen peroxide (H_2O_2) methods. This method was introduced by Yoneda (1961) and various modifications have since been proposed to improve results (Barnhisel and Harrison, 1976; Finkelman, 1986; O'Shay et al., 1990). The basis of the method is that H_2O_2 oxidizes sulfides and generates sulfuric acid, which presumably will react with alkaline components if present. The net amount of acid produced is determined by final titration with NaOH. The most significant limitations of this procedure include: i) the assumption that all pyrite has reacted; ii) the assumption that all H_2O_2 has decomposed; and iii) the assumption that neutralization reactions will occur similarly in the field as under laboratory conditions.

Finkelman (1986) proposed two variations of the H_2O_2 procedure. First, he suggested that oxidizing a sample with hydrogen peroxide, then tracking pH change for 15 minutes, could estimate pyrite content. The rate of pH change is a function of the pyrite content. The results are interpreted by comparing the values with curves generated from standards with known pyrite contents. For more quantitative results, he proposed measuring the sulfate concentration of the reacted peroxide solution. Finkelman's procedures can be completed easily and rapidly in the field, yet despite these apparent advantages the methods are not in common use. Further evaluation of his procedures may be worthwhile.

O'Shay et al. (1990) proposed a modified method which appeared to improve results based on evaluation with standard pyrite samples. Modifications included finer grinding of the sample, removal of residual acidity, increasing the volume of H_2O_2, and incorporating Cu as a catalyst to decompose excess H_2O_2. These modifications appeared to significantly improve accuracy and consistency. Results of the modified method were compared to three methods used to calculate potential acidity based on total-S, pyritic iron, and non-sulfate S. The modified method produced the lowest acidity estimates, which the authors attribute to the nature of direct measurement rather than indirect measurement that may include non-acid producing forms of S or Fe, such as siderite. A study by Ammons and Shelton (1988) indicates a strong relationship between results obtained using the basic H_2O_2 method and total-S for unweathered sulfidic materials. This relationship was less pronounced for weathered samples.

In contrast to static tests, kinetic tests are designed to deal with the rates and mechanisms of reactions that result in acid rock drainage. These tests simulate weathering by cyclically exposing the sample to ambient conditions then leaching the sample. The effluent is collected and analyzed for pH, metal concentrations, and other parameters of interest. One advantage of kinetic tests is that the simulated rock drainage that can be analyzed with the same testing parameters as actual drainage from excavation sites. Nonetheless, interpretation of the results and extrapolation to the actual environment may be difficult. It is impossible to simulate in the laboratory the exact physical, chemical, and biological conditions that exist in the field environment. Furthermore, results of laboratory analyses will vary depending on controlled variables such as particle size, temperature, and timing of leaching cycles.

The three common forms of apparatus employed in kinetic studies include leaching columns, humidity cells, and soxhlet extractors. For column studies, a column is packed with material then leached, usually at least on a weekly basis, with distilled water or a simulated precipitation solution. The leachate is collected and analyzed. Column methods are described in detail in Stewart (1995) and Perry (1985). Humidity cells are designed to provide standard conditions for measuring acid generation by controlling air, temperature, moisture and microbes. The basic procedure involves filling a cell with crushed material, passing dry air over the sample, passing moist air over the sample, then washing the sample with a fixed volume of water and collecting the leachate for analysis. A single cycle is usually completed within one to two weeks. Both columns and cells are typically run for numerous weeks to years (Carrucio, 1968: Carrucio et al., 1977; Bradham and Carrucio, 1990).

Soxhlet extractors (Renton et al., 1988; Sobek et al., 1982) are less commonly used and provide a more aggressive weathering environment than leaching columns and humidity cells. The Soxhlet extractor consists of three parts – a water reservoir, an extraction column, and a condenser (Figure 5.1). The reservoir is filled with a known volume of water, the sample is placed in a cellulose thimble in the extractor, and the apparatus is set on a hot plate. As the water is heated, water vapor passes through a by-pass tube on the extractor to the condenser. The vapor liquefies and drips down onto the sample in the extractor. When the water level in the extractor nears the top of the thimble, it drains back into the reservoir by a siphon tube. By this method, the sample is continuously leached for a given time period, usually up to 24 hours, then the leachate is collected for analysis. The thimble is removed and placed in an oven for a given time period, usually up to two weeks, to reoxidize the sample. After the oxidation period the sample is leached again. In most studies, the leaching/oxidation cycle was repeated up to five times.

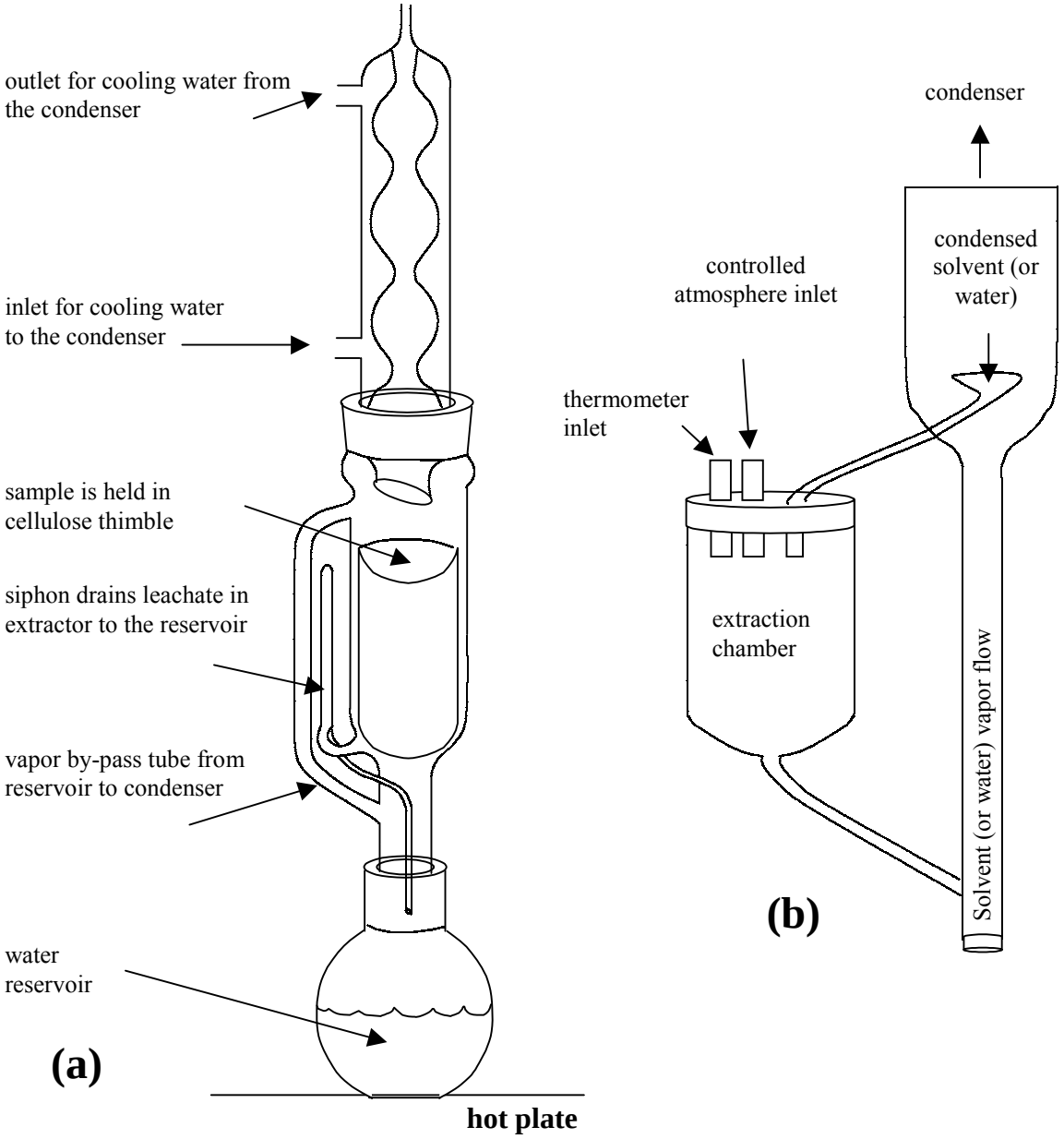

Figure 5.1.(a) Schematic diagram of Soxhlet extractor (redrawn from Renton et al., 1988). (b) Modified Soxhlet design with extraction chamber removed from upward path of refluxing solvent (redrawn from Sobek et al., 1982).

Few comparative studies exist on the use of Soxhlet extractors for predicting acid drainage; however, the results have been promising. Bradham and Carrucio (1990) compared three common kinetic methods – Soxhlet extractors, humidity cells, and column weathering – with field data to assess the accuracy of these tests. They determined that accuracy was greatest for humidity cells, then Soxhlet extractors, and least accurate for column weathering. However, this assessment was based only on characterizing drainage as overall acid versus alkaline and did not discuss specific levels of acidity or alkalinity, or other water quality parameters. Sobek et al. (1982) proposed a modification to the standard Soxhlet by moving the extraction chamber so as to reduce the temperature during extraction (Figure 5.1). Comparing pH, EC, SO_4, Fe and Mn levels in the effluent, they concluded that their modified Soxhlet improved simulated weathering and produced results more similar to those encountered in the field. Renton et al. (1988) compared leachate analyses from 4 leaching cycles using Soxhlet extractors with leachate from a small field-scale experiment that was exposed to natural weathering for almost 1 year. They rescaled the Soxhlet results to equate to the field results, and then derived a predictive model for acid generation based on the experimentally determined rate constant, the mass of the material and its S content, and time. To validate the model, a different sample was analyzed with Soxhlet extractors and the leachate results were used to calculate a rate constant. Application of the predictive model was successful in determining acid generation from a 350-ton backfill model. The model initially overestimated sulfate production, but after 230 days the predicted values were within 10% of the observed values, and by 260 days the predicted and observed values were equal. These authors suggested that the ultimate acid load may be predicted for any mass of potentially toxic rock material by observing sulfate levels in Soxhlet effluent over time.

Most procedures for evaluating acid production were developed for the analysis of coal overburden and mine soils (Sobek et al., 2000). Existing studies that evaluate potential acidity procedures generally involve application on a variety of one type of material, such a coal overburden with varying S or $CaCO_3$ contents. However, the question remains as to how these procedures perform for other types of sulfidic materials. The objective of this study was to evaluate the use and limitations of some existing potential acidity procedures on a diverse set of sulfidic materials.

Materials and Methods

Samples of sulfide-bearing shales, phyllites, slates, and coastal sediments were collected from acid roadcuts and excavation sites throughout the state of Virginia. Sample locations are described and illustrated in detail in Chapter 3. Rock samples were stored in plastic bags or cardboard containers. Subsamples of rock material were crushed to pass through an 80-mesh sieve then stored in paper envelopes. Unconsolidated sediment samples were placed in plastic bags, frozen on dry ice upon collection, and stored in a freezer to minimize oxidation prior to analysis. One week before analysis, sediment subsamples were spread out to air-dry. Approximately 50 g of the subsample were crushed to pass through an 80-mesh sieve then stored in paper envelopes. The remaining material was passed through a 10-mesh sieve then stored in cardboard boxes. All processed materials were stored at room temperature.

The potential peroxide acidity (PPA) procedure of Barnhisel and Harrison (1976) is currently the standard potential acidity procedure used to evaluate materials in the Soil Survey and Mined Land Reclamation Laboratory (SS+MLR) of the Crop and Soil Environmental Sciences Department at Virginia Tech. A number of tests were run to evaluate the utility and accuracy of this procedure. First, a series of standards containing known amounts of pyrite in a quartz matrix were tested for PPA to evaluate the extent of pyrite oxidation. The pyrite and quartz were both ground to pass through an 80-mesh sieve. For each standard, a small amount of pyrite was weighed out to 0.0001 g, and then brought up to a weight of approximately 1 g by adding quartz. Single samples of nineteen standards, ranging from 0.12 to 5.76% pyrite, were prepared immediately prior to analysis. Second, fifteen samples, randomly selected from the materials collected from acid roadcuts in Virginia, were run in duplicate. Third, thirty rock and sediment samples, randomly selected from the materials collected at acid roadcuts in Virginia, were re-tested for PPA after various time periods, ranging from 7 to 31 months, to determine the stability of air-dried samples stored at room temperature. Finally, single samples of two hundred and ninety-six rock and sediment samples (see Chapter 3) collected from acid roadcuts in Virginia were tested for PPA.

The PPA method calls for initial analysis using a 5 g sample then, if the results are above a threshold (20 Mg $CaCO_3$/ 1000 tons), subsequent analysis on a 1 g sample. Due to the high

number of samples being processed, and knowing that the majority of samples contained significant amounts of sulfide, 1 g samples were routinely used. Results from this study are presented as pure calcium carbonate equivalence, or Mg $CaCO_3$/1000 Mg material, although the actual cited method expresses final results as 1.5 times this value to account for the use of agricultural lime as opposed to pure calcium carbonate, and to ensure conservative liming recommendations. The samples also were analyzed for total-S using an Elementar Vario Max CNS analyzer, and for qualitative presence of carbonates by the HCl "fizz test" (Sobek, et al., 1978).

Detailed characterization was completed on a subset of fourteen diverse samples, which are described in detail below and summarized in Table 5.1. This subset included eleven samples from Virginia and three samples from Brazil. Detailed locations for the Virginia samples are provided in Chapter 3. The samples were selected to represent different rock types, sediments of varying textures, and samples containing carbonate minerals. The samples were tested in duplicate for PPA by the standard method, and in triplicate for PPA after leaching with 0.5 N HCl to remove carbonates. Total-S was determined using triplicate samples. To determine sulfidic-S, a subsample was leached with 0.5 N HCl to remove sulfates, then S content was measured on the leached material. This method was modified from ASTM Method D2492, which uses 5N HCl. For ABA, two MPA values were calculated, one using total-S and one using sulfide-S. The NP was determined on duplicate samples by the method of Sobek et al., (1978). Correlation was used to compare PPA and ABA results. A multi-method total elemental analysis (Appendix C) was completed by XRAL Laboratories of Ontario, Canada, and whole sample mineralogy was determined using x-ray diffraction on powder mounts. To characterize the morphology of sulfide minerals, polished sections were prepared and observed using reflected light microscopy (Craig and Vaughan, 1994). For finer textured sediments and tailings, clay mineralogy was determined using x-ray diffraction on oriented clay mounts (Rich and Barnhisel, 1977).

Description of subset samples

stf1 – minimally weathered, underlying material collected at a depth of 15 – 30 cm from Mine Road in Stafford County. This roadcut was approximately 5 years old when the material was collected. Indications of intense acid sulfate weathering at this site included low soil pH

values, lack of vegetation, highly acidic road drainage, and iron staining and deterioration of concrete along this cut and an adjacent neighborhood. This roadcut exposes dark gray, graphitic, pyritic phyllite and slate of the Quantico Formation. The mineralogy consists mainly of quartz, with minor amounts of mica, kaolinite and pyrite and trace amounts of chlorite. The pyrite occurs as few, subhedral grains, approximately 0.1 mm x 0.1 mm. Trace amounts of pyrrhotite and chalcopyrite also are present.

stf4 – partially weathered surface material from the same location as Stafford 1. The mineralogy consists mainly of quartz and mica, with minor amounts of chlorite and pyrite. The pyrite occurs as corroded subhedral grains.

fl9 – partially weathered material collected from the surface of Rt-750 in Floyd County. This roadcut was most recently disturbed approximately 13 years prior to the time of sampling. Indications of acid sulfate weathering include prominent sulfate salt efflorescence along the roadcut surface, lack of vegetation, acidic drainage, and Fe- and Al-precipitates along a local streambed. This roadcut exposes the Ashe Formation of the Lynchburg Group. Locally the rock is mapped as Alum Phyllite, and consists of a steel-gray, fine-grained phyllite with pods of amphibolite and calcsilicate gneiss. This sample was collected from the amphibolite. The mineralogy consists mainly of quartz, chlorite and mica with trace amounts of feldspar, calcite, and pyrrhotite. The pyrrhotite occurs as polycrystalline lamellar aggregates.

fl19 – partially weathered material collected from the surface of Rt-8 in Floyd County. This roadcut consists of similar material described for fl9, and the sample is from the phyllite. The mineralogy consists mainly of quartz and mica with trace amounts of chlorite.

fc4 – minimally weathered sample of Marcellus Shale from a small VDOT quarry off Rt-600 in Frederick County. The mineralogy consists mainly of quartz, mica, and chlorite with trace amounts of feldspar and pyrite. The pyrite occurs as framboids, clusters of microcrystals, euhedral and subhedral grains, and anhedral masses dispersed throughout the sample.

wc4 – minimally weathered sample of Chattanooga shale from Rt-23 in Wise County. This roadcut was approximately 10 years old at the time of sampling. Indications of acid sulfate weathering include precipitation of sulfate salts on the roadcut surface, iron staining and concrete

deterioration along the base of the cut, and guardrail corrosion. The mineralogy of this sample consists mainly of quartz, with minor amounts of mica and trace amounts of feldspar, chlorite and pyrite. The pyrite occurs as framboids, and cluster of microcrystals, dispersed through the sample.

gas32 – previously undisturbed, reduced, sandy loam sediments, collected at 9.7 m (32 ft) depth, from a deep boring behind the Citgo gas station at the intersection of Rts 156 and 630 in Hanover County. These sediments are believed to be from the Chesapeake Group, which are Tertiary marine sediments. The mineralogy consists mainly of quartz, with minor amounts of mica and pyrite, and trace amounts of kaolinite and calcite. Pyrite occurs as framboids and clusters of microcrystals dispersed throughout the sample. Clay mineralogy consists mainly of mica, montmorillonite, hydroxy-interlayered vermiculite (HIV)/intergrade, and hydroxy-interlayered smectite (HIS)/montmorillonite intergrade, with minor amounts of kaolinite, vermiculite, and quartz, and trace amounts of feldspar.

mcv5-4 – undisturbed, reduced, loam sediments, collected at 1.2 m (4 ft) depth from a deep boring between the cloverleaf and exit ramp in the northwest section of the I-295/360 interchange near Mechanicsville in Hanover County. These sediments are from the Calvert Formation of the Chesapeake Group. Indications of acid sulfate weathering include very low soil pH, lack of vegetations, yellow jarosite mottles, iron-staining and concrete deterioration along drainage ditches, and acid drainage. The mineralogy consists mainly of quartz, with minor amounts of mica and feldspar, and trace amounts of chlorite and pyrite. The pyrite occurs as framboids dispersed throughout the sample. Clay mineralogy consists mainly of HIS/montmorillonite intergrade, montmorillonite, and mica, with minor amounts of HIV/intergrade, kaolinite, vermiculite, chlorite, quartz and feldspar.

mcv6-16 – same location as mcv5-4, but inside the cloverleaf.. Undisturbed, reduced, silt loam sediments from the Chesapeake Group were collected from a depth of 4.9 m (16 ft). The mineralogy consists mainly of quartz, with minor amounts of mica and feldspar, and trace amounts of kaolinite, pyrite and chlorite. The pyrite occurs as framboids and few weathered subhedral grains. The clay mineralogy consists mainly of montmorillonite, mica, and

HIS/montmorillonite intergrade, and HIV/intergrade, with minor amounts of chlorite and kaolinite, quartz, vermiculite, and feldspar.

gas16 – same location as gas32. Undisturbed, reduced, clay loam sediments from the Chesapeake Group were collected at a depth of 4.9 m (16 ft). The mineralogy consists mainly of quartz, mica and pyrite, with minor amounts of kaolinite. The pyrite occurs as framboids and clusters of microcrystals. The clay mineralogy consists mainly of mica, montmorillonite, HIV/intergrade, HIS/montmorillonite intergrade, with minor amounts of kaolinite, vermiculite, quartz and feldspar.

mcv6-28 – same location as mcv6-16. Undisturbed, reduced, clay sediments from the Chesapeake Group were collected at a depth of 8.5 m (28 ft). The mineralogy consists of quartz, with minor amounts of mica, and trace amounts of kaolinite, pyrite and chlorite. The pyrite consists of framboids dispersed throughout the sample. The clay mineralogy consists mainly of HIS/montmorillonite intergrade, montmorillonite, and mica, with minor amounts of HIV/intergrade, kaolinite, vermiculite, quartz, feldspar, and chlorite.

ni – tailings from a nickel mine in Brazil. The mineralogy consists mainly of kaolinite, with minor amounts of amphibole and pyrrhotite, and trace amounts of quartz and chlorite. The pyrrhotite occurs anhedral grains dispersed throughout the sample. The clay mineralogy consists mainly of kaolinite and mica, with minor amounts of HIV/intergrade, chlorite, quartz, feldspar, and gibbsite.

bass – acid sulfate soil from Brazil. The mineralogy consists mainly of quartz, with minor amounts of kaolinite and mica, and trace amounts of chlorite and pyrite. The pyrite occurs as framboids dispersed throughout the sample, and numerous subhedral grains. The clay mineralogy consists mainly of kaolinite and mica, with minor amounts of HIV/intergrade, and trace amounts of quartz, chlorite, and trace amounts of feldspar, and gibbsite.

gold – tailings from a gold mine in Brazil. The mineralogy consists mainly of quartz, with minor amounts of mica and feldspar, and trace amounts of kaolinite and pyrite. Pyrite occurs as few subhedral pyrite grains, small amounts of pyrite remaining in goethite pseudomorphs, and small amounts of chalcopyrite. Clay mineralogy consists mainly of mica,

montmorillonite, kaolinite, with minor amounts of quartz, HIS/montmorillonite intergrade, and trace amounts of feldspar and gibbsite.

Table 5.1. Identification of fourteen diverse sulfidic materials used for procedural comparisons.

Virginia			
sample	county	age of exposure*	geologic map unit (Rader and Evans, 1993)
stf1	Stafford	< 5 yrs	Quantico Formation (Ordovician)
stf4	Stafford	< 5 yrs	Quantico Formation (Ordovician)
fl9	Floyd	13 yrs	Alum phyllite (Proterozoic)
fl19	Floyd	< 10 yrs	Alum phyllite (Proterozoic)
fc4	Frederick	unknown	Millboro Shale (Devonian)
wc4	Wise	10 yrs	Chattanooga Shale (Mississippian/Devonian)
gas32	Hanover	0	Millboro Shale (Devonian)
mcv5-4	Hanover	0	Chesapeake Group (Tertiary)
mcv6-16	Hanover	0	Chesapeake Group (Tertiary)
gas16	Hanover	0	Chesapeake Group (Tertiary)
mcv6-28	Hanover	0	Chesapeake Group (Tertiary)
Brazil			
sample		description	
ni		nickel mine tailings	
bass		acid sulfate soil	
gold		gold mine tailings	

* approximate age of exposure, or time since most recent disturbance, at time of sampling

Soxhlet extraction analysis was evaluated for four samples (Table 5.2). The samples were selected to be i) the same or similar to materials from the subset of 14 samples that were characterized in detail, and ii) to represent roadcuts where acid drainage could be collected from the field for comparison. The applied method was similar to that described by Renton et al., (1988). Prior to analysis, subsamples were analyzed for total-S and PPA. Standard 123 mm Soxhlet extractors were used in triplicate for each sample. For each triplicate, 100 g of sample, crushed to less than 1 cm diameter fragments, were weighed into cellulose thimbles. A wad of cotton was placed over the sample to minimize splashing and channeling of the percolating leachate within the material. The thimbles were placed in the extractors, 300ml of distilled, deionized water were placed in the reservoir, and 50 ml of distilled, deionized water were poured into the thimbles to "pre-wet" the samples. The samples were leached for 24 hours, after which time the leachate was collected for analysis. The thimbles were placed in a tall-form beaker and transferred to a 105^{o} C oven for 14 days to reoxidize the sample. At the end of the reoxidation

period, the thimbles were returned to the extractors and leached again. The oxidation/leaching cycle was repeated 10 to 15 times. Each time the leachate was analyzed for pH, acidity, and S. The initial weight of S for each sample was calculated based on the initial sample weight and percent total-S. After each leaching the cumulative amount of S in the leachates was subtracted from the initial amount of S, and the percent S that presumably remained unreacted in the sample was calculated. For the first six leachings the leachate was analyzed for Al, Fe, Mn, Cu, and Zn concentrations.

Road drainage was collected from each of the sites represented by the Soxhlets on three occasions and analyzed for acidity, sulfate, Al, Fe, Mn, Cu, and Zn. For Floyd, Clifton Forge, and Mechanicsville water samples were collected from the outlet of culverts that drain the roadcuts. For Clifton Forge, additional samples were collected from a drainpipe that feeds leachate directly from the backfill into the culvert. For Mechanicsville, additional samples were collected from a shallow well installed at the base of the outcrop. For Stafford, water samples were collected at two locations, a few hundred feet apart, from a drainage ditch at the base of the outcrop.

Regression, correlation, and paired t-tests, were used to evaluate potential acidity procedures, and to model relationships. All statistical analyses were completed using MINITAB 13. Graphs were generated using MINITAB 13 and Microsoft Excel 2000.

Table 5.2. Samples used for Soxhlet extraction.

Sample (percentages by weight)	Geologic Map Unit
cf1-2 (100%)	Millboro shale (Devonian black shale)
mcv6D (50%) and mcv6C (50%)	Chesapeake group (similar to mcv5-4 and mcv6-16 from Table 5.1)
stf1 (100%)	Quantico slate
fl9 (40%), fl1-1 and 1-3 (each 30%)	Alum phyllite (similar to fl19 from Table 5.1)

Results and Discussion

Analysis of Sulfide Standards

To evaluate the extent of pyrite oxidation using the PPA method, nineteen 1 g samples containing known quantities of pyrite in a quartz matrix were tested. The results are presented in Table 5.3. Regression analysis indicated that S content is a strongly significant predictor of PPA ($r^2 = 0.977$, $p < 0.001$). While this result is expected, it is also necessary to compare the extent of acid generation to theoretical predictions. According to stoichiometric calculations, a sample containing1% S in pyritic form has an MPA of 31.25 Mg $CaCO_3$ /1000 Mg of material assuming that all of the pyrite completely reacts. To evaluate the extent of acid generation as compared to this theoretical maximum, PPA as a percentage of MPA was plotted as a function of sulfur content (Figure 5.2). The results were variable for sulfur levels up to about 0.9%, but at higher sulfur levels the extent of acid generation appeared to be fairly constant at 80% of MPA, and may have actually decreased slightly. Regression analysis indicated that for samples with less than 0.9% S, sulfur content was a poor indicator of the ratio PPA/MPA ($r^2 = 0.161$). However, for samples with greater than 0.9% S, sulfur content was a strongly significant predictor of PPA/MPA ($r^2 = 0.809$, $p < 0.001$). This result was likely a function of scale. For samples with low sulfur content, laboratory error during weighing or titration may be of the same order of magnitude as the predicted MPA. For this preliminary work, a constant sample size of 1 g was used for all the standards; however, the results would likely improve if larger samples (5 g recommended) were used for the low S standards. Using these data it was difficult to evaluate the extent of acid generation at the lower S levels; however, it appeared that at S levels ranging from 0.9% to 3.1% the amount of net acidity produced ranged from 75 – 90% of the predicted value. More extensive analysis would be necessary to precisely quantify this relationship, particularly at the lower S levels.

Analysis of Storage Time Effects on Potential Peroxide Acidity Procedure

To investigate the effect of storage time of dried samples at room temperature on PPA, thirty samples, run as single samples, were tested within 7 d after processing (PPA1t) and again after a time period ranging from 7 to 31 months (PPA2t; Figure 5.3) The PPA1t values ranged from 0.24 to 103.25 Mg $CaCO_3$/1000 Mg material with a mean of 27.15. The PPA2t values

Table 5.3. Percent sulfur and potential peroxide acidity (PPA) values for standards with known amounts of pyrite.

% pyrite	% S	PPA *Mg $CaCO_3$/1000 Mg material
0.11	0.06	2.19
0.17	0.09	0.96
0.42	0.22	5.98
0.47	0.25	4.66
0.49	0.26	5.89
0.83	0.44	12.47
0.98	0.52	20.82
1.32	0.70	15.62
1.34	0.71	25.01
1.79	0.95	27.24
2.06	1.09	30.80
2.47	1.31	37.29
2.64	1.40	38.13
3.04	1.61	42.72
3.09	1.64	45.87
3.74	1.98	50.03
3.90	2.07	49.81
4.74	2.51	59.24
5.75	3.05	73.55

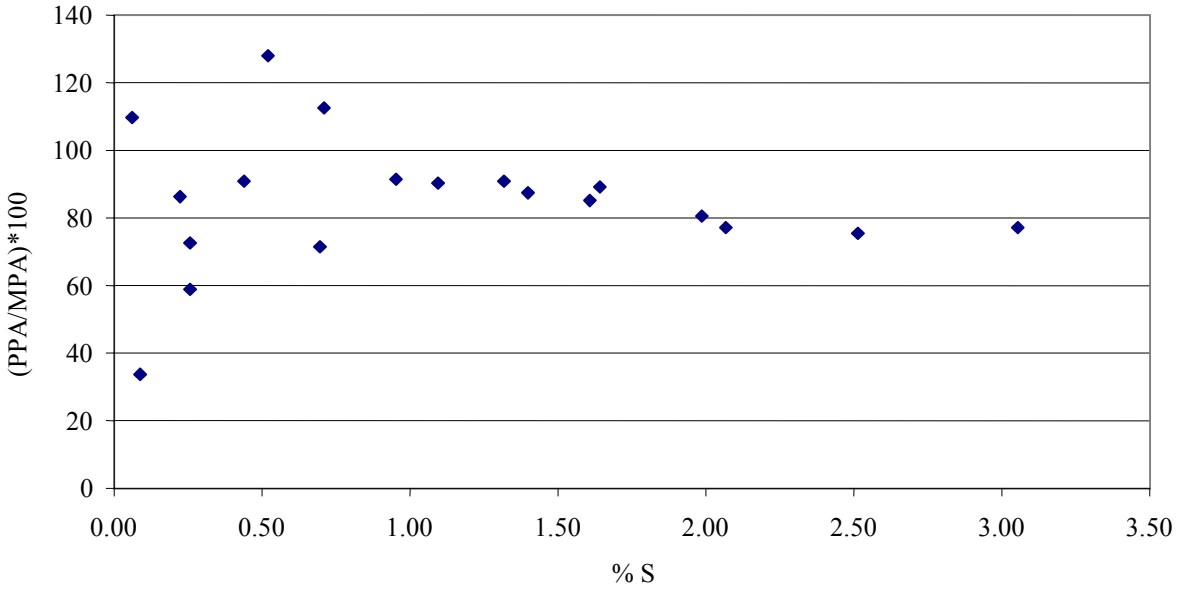

Figure 5.2. Potential peroxide acidity (PPA) expressed as a percentage of stoichiometric maximum potential acidity (MPA) versus sulfur content for nineteen standard samples.

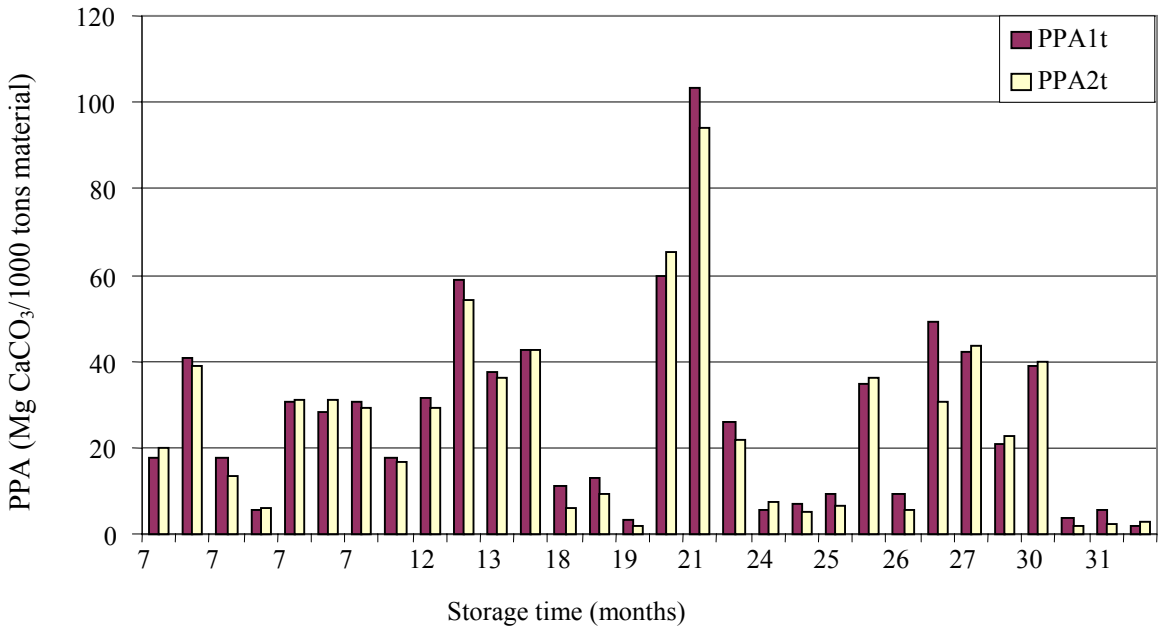

Figure 5.3. Comparison of potential peroxide acidity (PPA) values after various storage times. The initial determination is PPA1t and the second determination, after 7 to 31 months of storage time, is PPA2t.

ranged from 0.67 to 94.08 with a mean of 26.17. A paired t-test indicated that the two sets of PPA values were marginally different at $p = 0.076$. Most differences were less than ± 5 Mg $CaCO_3$/1000 Mg except for two outliers. For one outlier, both PPA values were extremely high (94 and 103) so although the absolute difference was much higher than the other samples, the relative difference was not. Furthermore, regression analysis indicated that the small changes in PPA values that did occur were not significantly related to either storage times [(PPA1t - PPA2t) = 0.61 + 0.0625(time); $R^2 = 0.044$] or %S [(PPA1t - PPA2t) = 0.481 + 0.46(%S); $R^2 = 0.046$). While the concern regarding storage time is that sulfides will oxidize and subsequent analyses will under-predict potential acidity, over one-third of the samples had higher values for PPA2t than PPA1t. One possible cause of differences between pairs of PPA measurements may be inadequate mixing of the sample prior to extraction of the subsample. Sulfide minerals are denser than most common soil minerals and tend to settle towards the bottom of their storage container. Therefore, the sample needs to be properly mixed each time a subsample is extracted. Another cause may be discrepancies in the exact laboratory procedure. In particular, as the titration

endpoint is approached, “pH drift” tends to increase. Consequently, determination of the endpoint is somewhat subjective and likely to vary among technicians. Although PPA ideally is determined on fresh samples, results from this investigation demonstrate that samples that have been dried and stored at room temperature for several months will still yield similar values to the original samples.

Analysis of Replication Using Potential Peroxide Acidity Procedure

Potential peroxide acidity is a time-consuming procedure, which makes the use of replicates prohibitive if large numbers of samples are to be analyzed. To evaluate the need for using replicates, 15 samples were run in duplicate (PPA1r and PPA2r) to determine consistency of results (Figure 5.4). The PPA1r values ranged from 0.11 to 90.40 Mg $CaCO_3$/1000 Mg material, with a mean of 17.26. The PPA2r values ranged from 0.09 to 87.00 with a mean of 17.29. The differences between PPA1r and PPA2r ranged from –2.0 to 3.4 with a mean difference of –0.037 and a standard deviation of 1.3. A paired t-test indicated that the means were not significantly different (p = 0.9). Therefore, consistency was very high between replicates and supported the use of single samples for the larger sample set (n = 296).

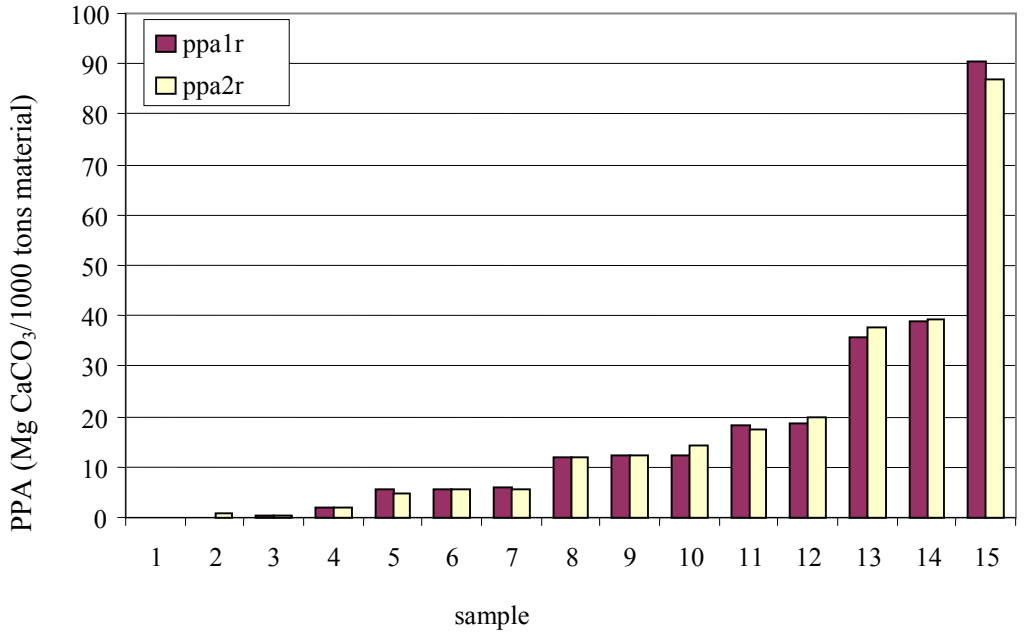

Figure 5.4. Potential peroxide acidity for duplicates (PPA1r and PPA2r) of fifteen samples.

Application Of Potential Peroxide Acidity Procedure On Diverse Sulfidic Materials

The PPA procedure was developed as a tool for overburden analysis in coal mining. However, sulfidic materials occur in numerous other geologic settings across the state of Virginia. As discussed earlier, theoretical predictions suggest that 1% S has an MPA of 31.25 Mg CaO_3 /1000 Mg if all of the pyrite in a sample is completely oxidized. In the absence of interfering factors, such as carbonates that neutralize acidity, %S and PPA should have a direct linear relationship. To investigate the relationship between %S and PPA for diverse sulfidic materials, 296 samples, run as single samples, were analyzed for total S, PPA, and presence of carbonates. Twenty-seven samples were eliminated after testing positive for carbonates. As expected, the remaining 269 samples showed strong correlation between PPA and %S ($r = 0.94$). Regression analysis on these samples resulted in residual values (predicted values – measured values) that are not normally distributed, rendering the regression invalid. Irregular distribution of residuals occurred dominantly with low S values. Removing samples that contain less than 0.25% S resulted in normal distribution of the residuals, supporting the use of regression analysis. Removal of these samples was justified since samples with less than 0.2% S would have little acid-producing potential. Regression analysis of the remaining samples indicated %S was a highly significant predictor of PPA and explained a large amount of the variability ($R^2 = 0.806$, $p < 0.001$). The regression equation and confidence intervals for PPA versus %S are shown in Figure 5.5.

Results from the combined analyses reported above, and from evaluation of pyrite standards, indicated that accuracy of PPA depended on the use of appropriate sample sizes. As suggested by the procedure, samples from low sulfur materials must be large enough to produce enough acidity that results will not be significantly affected by laboratory error, while samples from high sulfur materials must be small enough to allow complete reaction of the sulfides. Due to the large number of samples analyzed in this study, 1 g samples were routinely used for all samples. Results would likely improve if low- and high-S samples were re-tested with larger and smaller sample sizes, respectively.

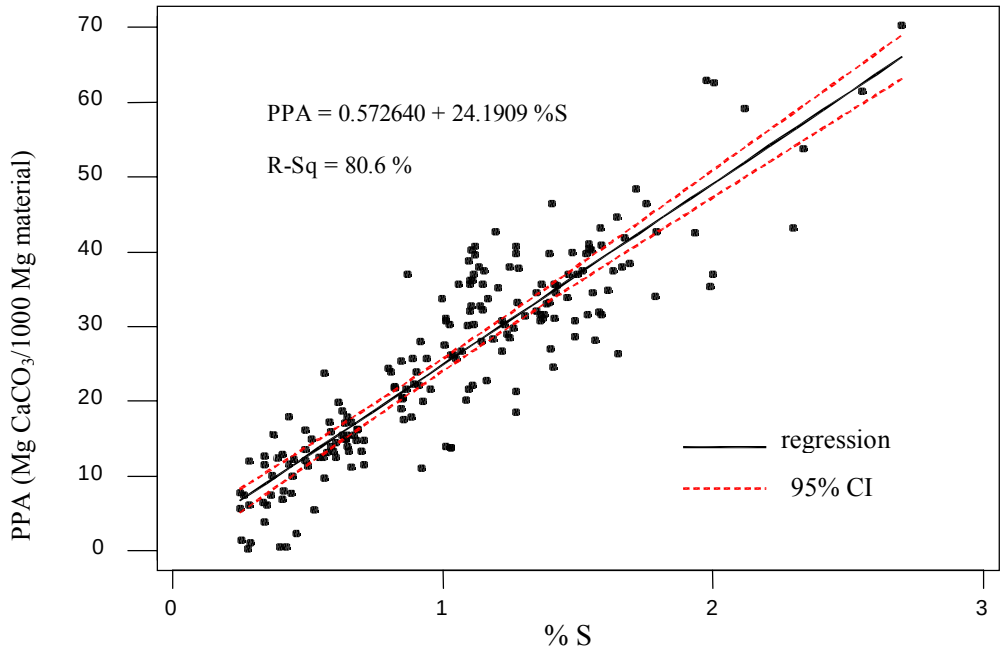

Figure 5.5. Regression analysis for potential peroxide acidity (PPA) and %S for samples with greater than 0.25% S.

To further investigate the relationship between S and PPA for different materials, the samples were divided into four groups based on general geologic classification: Coastal Plain sediments, slates, phyllites and shales. Samples containing carbonates were removed from analysis. Scatterplots of PPA and S for each group are shown in Figure 5.6. Overall, high correlations between S and PPA were found for slates, shales, and sediments (r = 0.99, 0.98, and 0.92 respectively). Phyllites had a poor correlation (r = 0.36). A closer look at the phyllite data revealed a high correlation (r = 0.88) between S and PPA for the 10 samples from the I-77 roadcut in Carroll County, but a poor, negative correlation (r = -0.14) for the samples collected at Rt-750 and Rt-8 in Floyd County. Again, although there were only a few samples, dividing the data by roadcut revealed that the 4 samples collected from Rt-8 had a poor, positive correlation (r = 0.45) whereas the 6 samples from the Rt-750 roadcut had a poor, negative, correlation (r = -0.34). This may be explained by the presence of sulfate precipitates, which were significantly more prominent at the Rt-750 roadcut than any other sampled roadcut. Compared to sulfides, sulfate precipitates produce less or no acidity, as would be expected. Although mineralogy was not completed on these samples, the presence of gypsum, which does not produce acidity, was

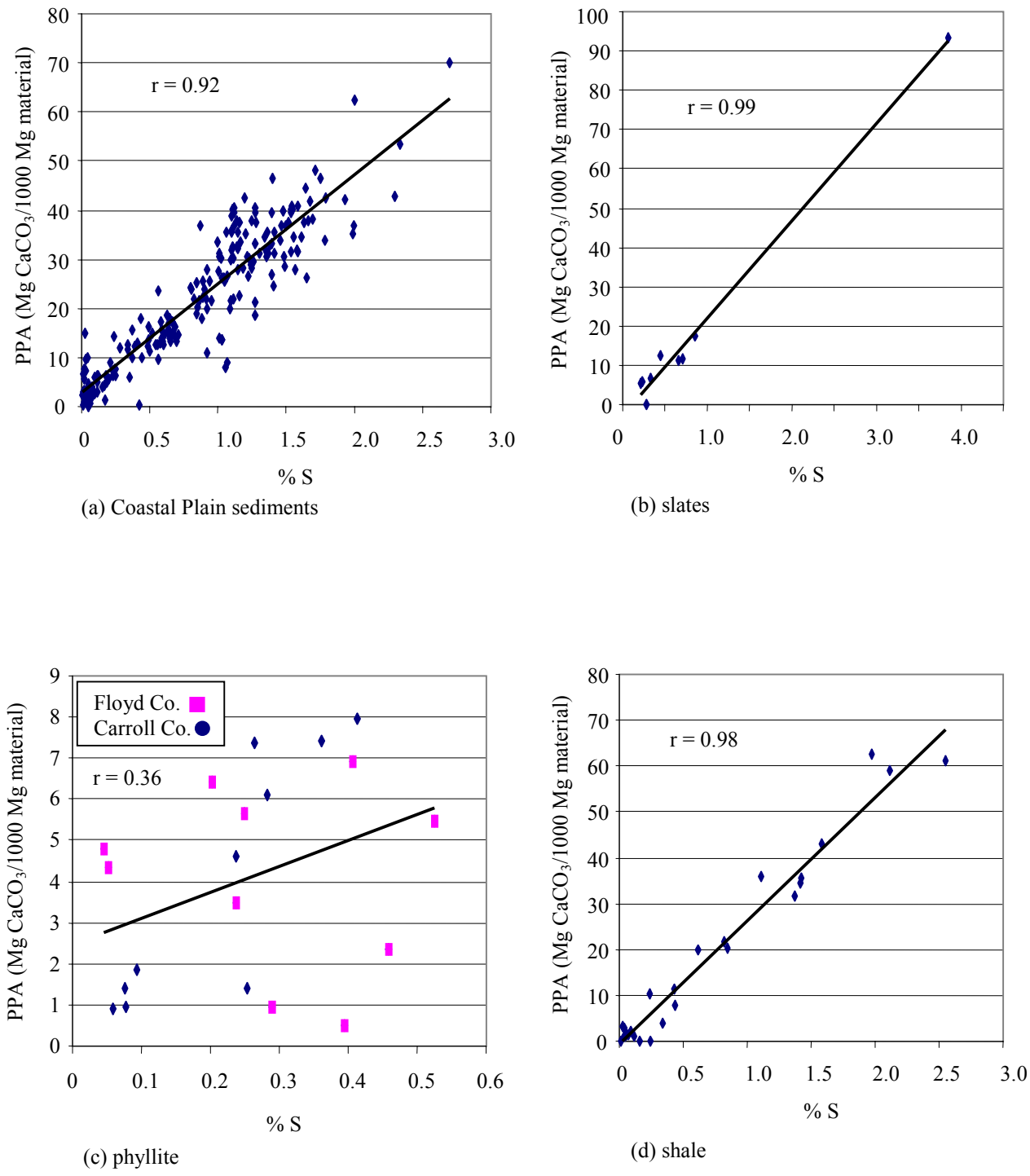

Figure 5.6. Simple correlation plots of potential peroxide acidity (PPA) versus % S for (a) Coastal Plain sediments, (b) slate, (c) phyllite, (d) shale.

confirmed for this location by x-ray analysis of a powder mount prepared from precipitate material that was scraped off of the roadcut surface. Furthermore, carbonates have been documented at this location. Some samples may contain low levels of carbonates which were not readily apparent by the "fizz test", but which could have noticeably affected PPA results since these were relatively low-acid producing materials.

Overall, the PPA procedure has proven to be a robust test, which may be applied to a wide variety of sulfide bearing geologic materials. Nonetheless, this procedure is somewhat time-consuming and expensive. With the current laboratory setup in the SS + MLR Laboratory, it takes a minimum of three days to process 15 samples at a cost of at least $12/sample just for materials. In comparison, S can be determined for over 60 samples in one day at about one-fourth of the cost. As indicated by regression analysis, in the absence of carbonates and certain sulfate minerals, S is a highly significant indicator of PPA and therefore may be used for initial evaluation of materials. Samples with high S (> 0.2%) may be further analyzed by other tests as necessary. When carbonates or sulfate minerals are present in a sample, S will overpredict PPA. This is an acceptable error since samples with high S will be re-assessed by further analysis. No causes are evident, other than laboratory error, which would result in an underestimation of PPA based on S. Therefore, S provides an adequate screening tool which could save considerable time and expense in the routine analysis of potentially acid materials.

Potential Peroxide Acidity and Acid-Base Accounting on Diverse Sulfidic Materials

In addition to PPA, a number of other tests may be used to evaluate the potential acidity of sulfidic materials. The most commonly applied static test is acid-base accounting (ABA), which, like PPA, was developed for overburden analysis in coal mining. To evaluate the application of these methods to different materials, a set of 14 samples representing diverse sulfidic materials were analyzed by PPA and ABA. All potential acidity values are expressed as Mg $CaCO_3$/1000 Mg material. Whole sample and clay mineralogy for these samples are described in Tables 5.4 and 5.5, pH and texture results are shown in Table 5.6, and sulfide mineralogy and morphology are described in Table 5.7.

Table 5.4. Mineralogy of whole sample by X-ray diffraction on powder mounts.

Sample	Mineralogy		
	Major (> 10%)*	Minor (3 – 10%)*	Trace (< 3%)*
fl19	quartz, mica		chlorite
gold	quartz	mica, feldspar	kaolinite
stf4	quartz, mica	chlorite	
mcv5-4	quartz	mica, feldspar	chlorite, pyrite
mcv6-16	quartz	mica, feldspar	kaolinite, pyrite, chlorite
mcv6-28	quartz	mica	kaolinite, pyrite, chlorite
gas16	quartz	feldspar, pyrite, mica	kaolinite, chlorite
fl9	quartz, chlorite, mica		feldspar
wc4	quartz	mica	feldspar, chlorite, pyrite
fc4	quartz	mica, chlorite	feldspar, pyrite
gas32	quartz	mica, pyrite	kaolinite
bass	quartz	kaolinite, mica	chlorite, pyrite
stf1	quartz	mica, kaolinite, pyrite	chlorite
ni	kaolinite	amohibole, pyrrhotite	quartz, chlorite

* ranges are approximate

Table 5.5. Clay mineralogy for < 2 mm fraction of sediments and tailings.

sample	% of mineral present									
	kaolinite	mica	gibbsite	feldspar	quartz	chlorite	vermiculite	HIV*/ Intergrade	mont-morillonite	HIS*/mica-montmorillonite intergrade
gold	20	50	1	1	7	0	0	0	20	3
mcv5-4	8	20	0	3	4	5	5	8	24	25
mcv6-16	6	20	0	3	5	6	5	10	28	18
mcv6-28	8	20	0	3	4	3	4	8	22	30
gas16	8	37	0	2	3	0	4	12	24	10
gas32	8	37	0	2	3	0	4	12	24	10
bass	72	10	2	2	3	3	0	8	0	0
ni	55	17	3	5	5	5	3	5	0	0

*HIV = hydroxy-interlayered vermiculite
**HIS = hydroxy-interlayered smectite

Table 5.6. Texture and pH for sediments and tailings.

sample	**pH in H_2O**	**pH in KCl**	**%sand**	**%silt**	**%clay**
gold	3.30	3.20	51	45	4
mcv5-4	4.01	3.7	45	37	18
mcv6-16	7.60	6.41	23	75	2
mcv6-28	7.68	6.82	27	31	42
gas16	3.85	3.45	37	36	27
gas32	7.35	6.82	71	17	12
bass	2.64	2.46	63	37	0
ni	3.75	3.46	81	18	1

Table 5.7. Sulfide mineralogy and morphology by reflected light microscopy for 14 samples used to compare potential acidity procedures.

sample	**Major sulfide mineralogy and morphology**	**Accessory minerals**
fl19	Few subhedral grains of pyrite about 0.1mm x 0.1 mm. Small pyrrhotite inclusions in sphalerite.	Sphalerite, trace amount of chalcopyrtie.
gold	Few pyrite grains ranging up to 1.5 mm x 1 mm. Subhedral grains of goethite pseudomorphs replacing pyrite with little pyrite remaining.	Trace amount of chalcopyrite.
stf4	Few, small, euhedral and subhedral grains of pyrite.	Chalcopyrite, covellite
mcv5-4	Framboidal pyrite dispersed throughout sample. Framboids are larger than 'bass' sample.	
mcv6-16	Framboidal pyrite dispersed through sample. Framboids are larger than 'bass' sample and less abundant than 'gas' samples. Few weathered subhedral pyrite grains.	
mcv6-28	Framboidal pyrite dispersed through sample. Framboids are larger than 'bass' sample.	
gas16	Framboidal pyrite dispersed through sample. Clusters of pyrite microcrystals with grains about 0.008mm in diameter. Clusters are about 0.16 mm x 0.25 mm, ranging up to 0.5 mm x 0.4 mm.	
fl9	Polycrystalline lamellar aggregates of pyrrhotite, drawn out parallel to foliation of the rock	Few anhedral masses of chalcopyrite
wc4	Framboidal pyrite and clusters of pyrite microcrystals dispersed through sample.	
fc4	Framboidal pyrite, clusters of microcrystals, euhedral and subhedral grains, and anhedral masses dispersed through sample.	
gas32	Framboidal pyrite and cluster of pyrite microcrystals are dispersed through the sample.	
bass	Framboidal pyrite heavily dispersed throughout sample. Framboids are mostly smaller than 0.004mm in diameter, but range up to about 0.012 mm in diameter. Numerous subhedral grains of pyrite about 0.004mm X 0.004 mm.	
stf1	Pyrite occurring in corroded subhedral grains.	Chalcopyrite
ni	Anhedral grains of pyrrhotite dispersed through sample. Grains are about 0.5 to less than 0.002mm in diameter.	Chalcopyrite, magnetitc, digenite

Tests that predict net potential acidity are primarily controlled by two factors – the amount of sulfides in a sample, which can produce acidity upon oxidation, and the amount of carbonates in a sample, which can neutralize all or some of the acidity. Results are affected to a lesser extent by the presence of sulfates, which may release some acidity upon dissolution. Therefore, in order to evaluate and compare the results of potential acidity tests on diverse sulfidic materials it is important to be familiar with the sulfide-S, sulfate-S, and carbonate characteristics of the samples (Figure 5.7). Total-S for the sample set ranged from 0.40 - 14.3% S, although all but two of the samples were below 3.0%. As a percentage of total-S, sulfate-S values ranged from 1 – 95%. However, as seen in Figure 5.7, only three samples (stf4, fl19, and gold) contained a significant proportion of sulfate (63 – 95% of total-S). These three samples also had the lowest total-S values (0.40 – 0.82%). Samples stf4 and fl19 had high proportions of sulfate-S because they are highly weathered compared to the other samples. For samples with S ranging from 1.36 – 2.83%, the sulfate-S proportions varied non-systematically from 12 – 28%. For the two samples with the highest total-S, the sulfate-S proportion was less than 1%. Only three samples, fl9, gas32, and ni tested positive for carbonates, showing weak effervescence by the "fizz test".

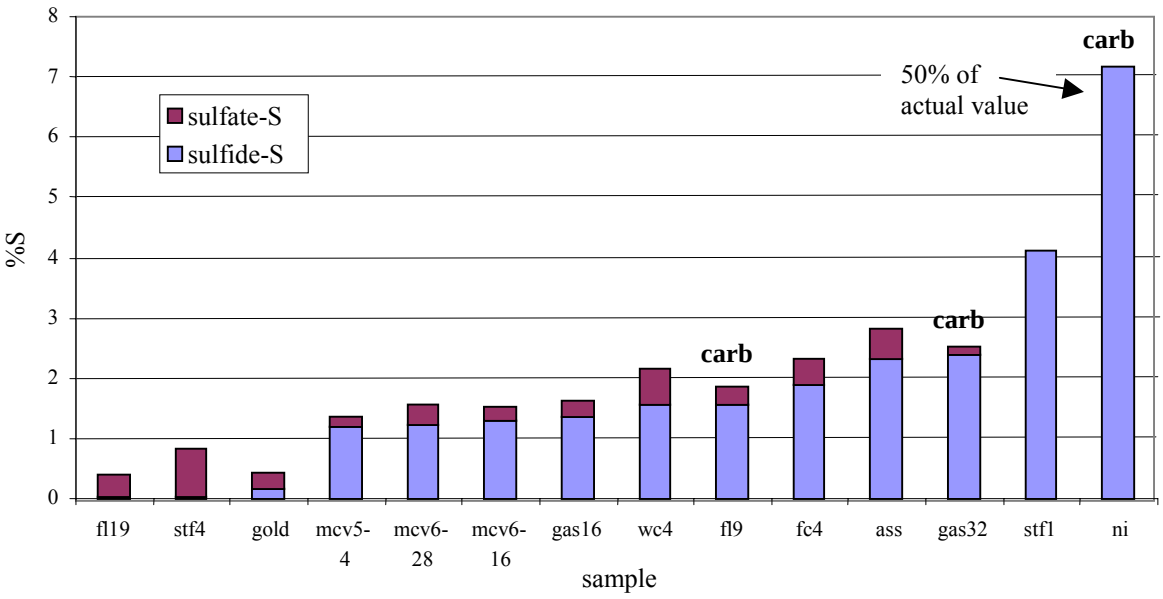

Figure 5.7. Sulfate-S, sulfide-S, and presence of carbonates (carb) for fourteen samples from diverse sulfidic materials.

Potential peroxide acidity results are also affected by the presence of carbonates, which will neutralize some or all of the acidity. Some authors (Grube, et al., 1971; O'Shay, et al., 1990) suggest that carbonates may unpredictably influence the amount of acidity being generated and therefore should be removed prior to peroxide analysis. Others (Barnhisel and Harrison, 1976) argue that since carbonates neutralize acidity in the field they should remain in the sample. To compare the difference between results with and without carbonate removal, the fourteen samples were tested for PPA after removal of carbonates by leaching the samples with 0.5 N HCl, and by the standard PPA method. PPA results are presented in Table 5.8 and illustrated in Figure 5.8. Two samples - gas32 and fl9 – showed noticeable increases in PPA after carbonate removal. This was expected since these were two of the three samples that tested positive for carbonates. The ni sample also tested slightly positive for carbonates, but it did not show a noticeable increase in PPA after carbonate removal. The low carbonate levels had little impact compared to the very high sulfide level. Four samples – stf4, wc4, bass, and fc4 - noticeably decreased in PPA after leaching with HCl, indicating that an acid-producing component was removed. This was likely due to the removal of sulfate weathering products, such as jarosite, that release acidity upon dissolution. The four samples that showed decreased PPA after leaching had the highest absolute values of sulfate-S. For the eleven non-carbonate containing samples a moderate correlation existed between percent sulfate-S and difference between PPA values before and after leaching with HCl ($r = 0.71$). Analysis of samples that have been leached to remove carbonates may underestimate PPA by removing acid-producing sulfate minerals. Furthermore, the presence of carbonates is easy to assess, and, if necessary, neutralization potential may be determined separately for carbonate-bearing samples. Therefore, PPA should be determined on samples that have not been leached with HCl.

In the following discussions on ABA and PPA (standard method) results, the ni sample is described separately because it is extremely different from the other samples. Acid-base accounting results are presented in Table 5.9 and illustrated in Figure 5.8. Acid-base accounting using total-S (ABA-TS) was highly correlated with ABA using sulfide-S (ABA-SS; $r = 0.98$). This result was expected since the only samples with significant proportions of sulfate-S have relatively low total-S values, while most of the remaining samples had sulfate-S proportions that varied within a relatively narrow range of values, and the two samples with the highest total S

Table 5.8. Potential acidity in Mg $CaCO_3$/1000 Mg material values by PPA.

sample	leached with 0.5 N HCl – 3 replicates				Standard – 2 replicates		
	1	2	3	average	1	2	average
stf1	98.3	90.1	98.2	95.5	103.2	94.7	99.0
stf4	0.2	1.0	1.9	1.0	17.5	19.7	18.6
gas32	63.7	61.7	68.0	64.4	41.4	45.2	43.3
gas16	38.2	37.7	38.7	38.1	40.9	39.0	39.9
fl9	24.2	22.6	22.4	23.0	17.5	13.3	15.4
fl19	1.7	3.8	3.2	2.9	5.4	6.0	5.7
mcv6-16	33.4	31.7	35.2	33.4	30.7	31.0	30.8
mcv6-28	34.0	31.4	35.5	33.6	28.4	31.2	29.8
fc4	48.3	48.9	50.8	49.3	59.0	54.1	56.6
wc4	37.7	36.4	40.5	38.1	60.0	65.4	62.7
ni	159.8	183.8	221.5	188.3	151.6	232.0	191.8
ass	55.1	50.6	53.2	52.9	66.7	73.4	71.2
gold	2.2	3.1	3.7	2.9	0.2	0.4	0.4
mcv5-4	31.3	31.2	29.7	30.7	30.6	29.2	29.9

Table 5.9. Potential acidity in Mg $CaCO_3$/1000 Mg material by ABA.

sample	%S	MPA*		NP**	ABA†	
		(TS‡)	(SS§)		(TS‡)	(SS§)
stf1	4.01	125.17	124.23	-3.08	128.25	127.31
stf4	0.82	25.75	1.22	-9.6	35.35	10.82
gas32	2.54	79.23	74.75	16.6	62.63	58.15
gas16	1.64	51.24	42.03	-8.7	59.94	50.73
fl9	1.87	58.51	48.84	21	37.51	27.84
fl19	0.40	12.43	1.06	-3.6	16.03	4.66
mcv6-16	1.52	47.46	40.31	2.6	44.86	37.71
mcv6-28	1.57	49.15	38.81	7.31	41.84	31.50
fc4	2.34	73.09	59.53	-15.17	88.26	74.70
wc4	2.15	67.16	48.59	-12.9	80.06	61.49
ni	14.27	445.94	442.18	4.5	441.44	437.68
ass	2.83	88.56	72.81	-33.3	121.86	106.11
gold	0.42	13.11	4.84	5	8.11	-0.16
mcv5-4	1.36	42.59	37.16	-8.9	51.49	46.06

* maximum potential acidity
** neutralization potential
† acid base accounting: ABA = MPA – NP
‡ TS = Total-S
§ SS = sulfide-S

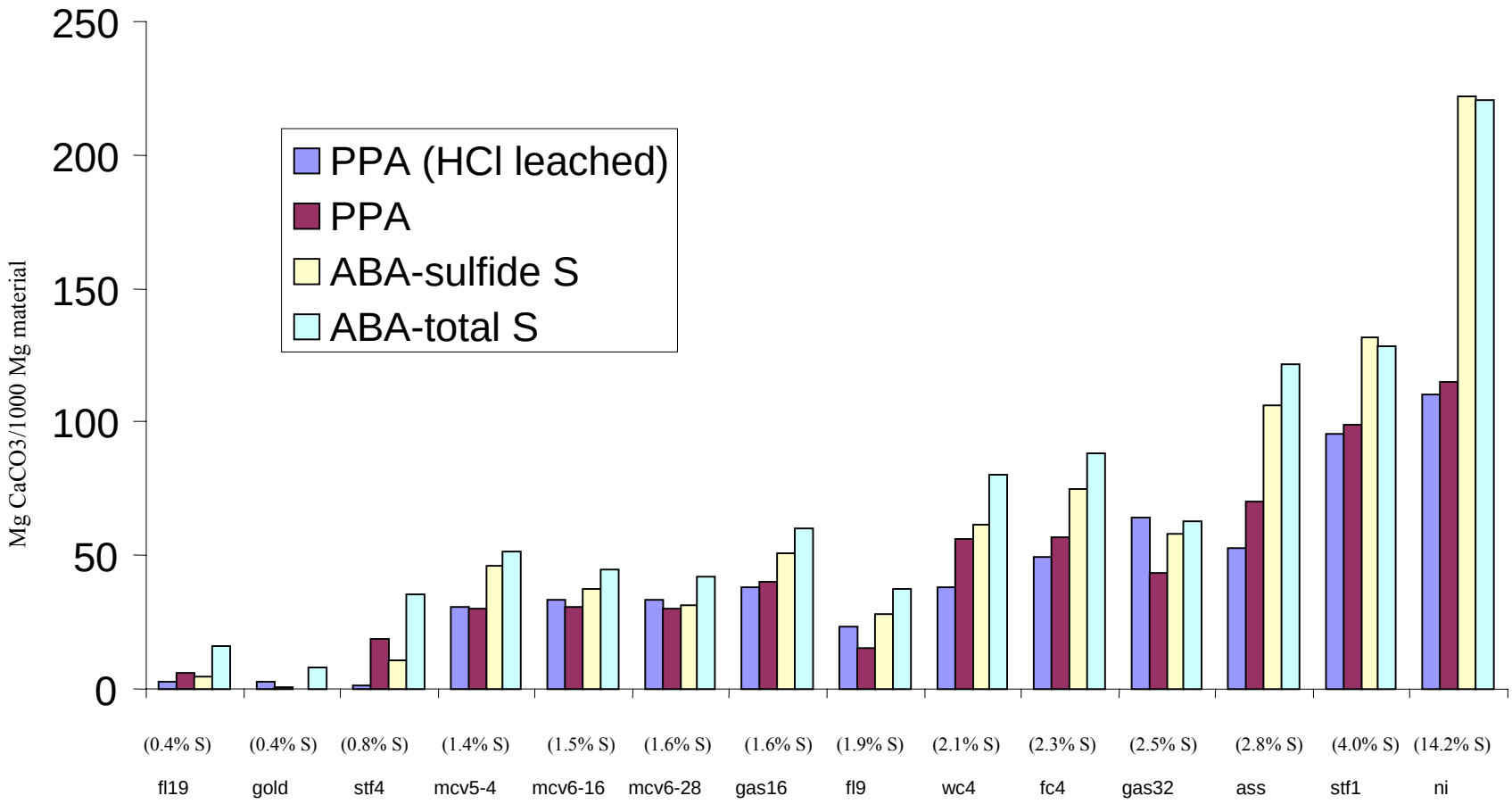

Figure 5.8. Results for potential acidity procedures on fourteen diverse samples arranged by increasing sulfur content, with %S indicated below each sample label. (Note: x-axis not to scale)

had very low proportions of sulfate-S. The PPA values were highly correlated with ABA-TS (r = 0.98) and ABA-SS (r = 0.98). The average difference between ABA-TS and PPA was 21.5 Mg $CaCO_3$/1000 Mg material, with a standard deviation of 11.5, and ABA-TS was higher for all samples. The average difference between ABA-SS and PPA was 11.2 Mg $CaCO_3$/1000 Mg material, with a standard deviation of 12.8, and ABA-SS is higher or almost equivalent to PPA for all samples. The differences between PPA values and ABA values were highly correlated with total sulfur (r = 0.850 for ABAss and 0.703 for ABAts).

The PPA and ABA results also may be compared by considering the ratio of PPA to ABA. The PPA/ABA-TS values ranged from 0.06 to 0.77 (Figure 5.9) and were moderately correlated with %S (r = 0.67). The three samples (fl9, stf4, and gold) which contained high proportions of sulfate-S account for three of the four lowest PPA/ABA-TS values (0.06 – 0.53). Two of the next lowest PPA/ABA-TS values had the highest absolute sulfate-S values (wc4 and bass). These results were expected because sulfates produce much less acidity than sulfide for a given %S, but ABA-TS calculates MPA as if all S was sulfidic. Therefore, MPA will be higher than PPA when noticeable amounts of acid-producing sulfate minerals are present in the sample. Furthermore, these sulfates will generate acidity during NP analysis and so they are accounted for twice in the ABA-TS calculation. Although the samples with the four lowest NP values also had the highest sulfate-S levels, overall a poor negative correlation (r = -0.42) was found between NP and sulfate-S for samples that did not contain carbonates.

The fourth sample with a low PPA/ABA-TS value, fl9, contained carbonates. Although carbonates may reduce the oxidation efficiency of H_2O_2 at pH values > 5.8, which will reduce PPA results, this was unlikely a factor for this sample as the final suspension pH was 3.1. Alternatively, the NP procedure for ABA may have underestimated the actual NP for this sample. The NP procedure proved to be difficult to complete without previous experience. For example, the procedure calls for heating the samples on a hot plate to near boiling, yet, it was difficult to determine if the samples were effervescing or beginning to boil. Thermometers kept in a few samples indicated that temperatures remained below 95^o C. Furthermore, the hot plates did not heat uniformly over the entire surface, making it difficult to maintain all samples at a

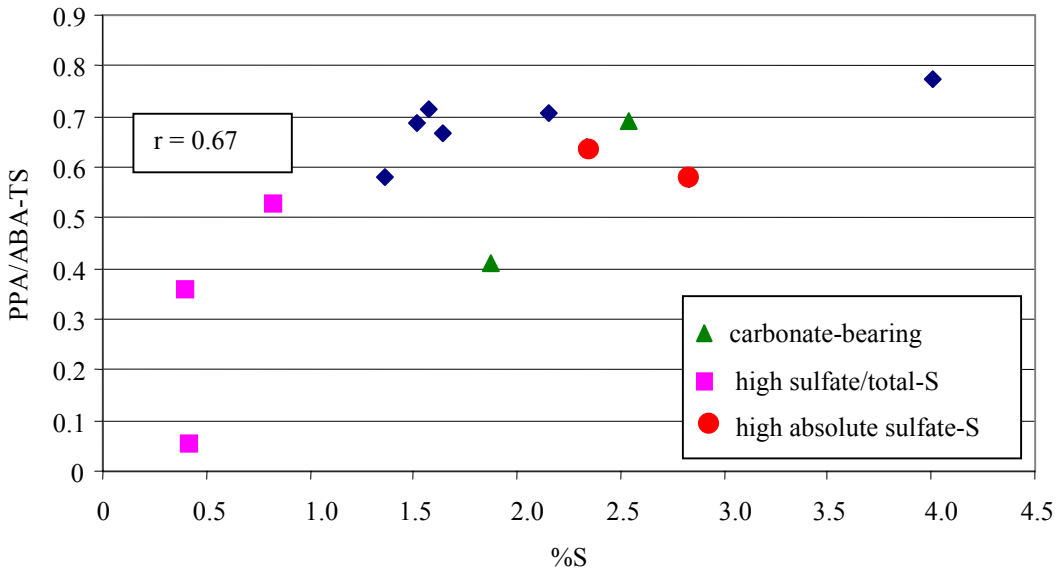

Figure 5.9. The ratio of potential peroxide acidity to acid-base accounting using total-S to calculate maximum potential acidity (PPA/ABA-TS) versus %S for fourteen samples of diverse sulfidic materials.

temperature near boiling without having some of them start to boil. Therefore, underestimation of NP may have resulted from laboratory error.

The remaining samples had PPA/ABA-TS ratio values ranging from 0.57 to 0.77. In comparison, PPA/ABA-SS values ranged from –2.9 to 1.7. As expected, the largest differences between PPA/ABA-SS and PPA/ABA-TS are for the high-sulfate samples. After removing the high-sulfate and carbonate-bearing samples, PPA/ABA-SS values ranged from 0.65 to 0.95. For the sample from the nickel mine tailings, ABA-TS was almost double PPA. The PPA values likely underestimate the potential acidity of this sample. Potential acidity increased by 80 Mg $CaCO_3$/1000 Mg material when the sample weight was decreased from 1.0 g to 0.19 g. Reduction in sample size, or increased H_2O_2 additions may further increase the potential acidity results.

Soxhlet Extractors

In comparison to static tests, simulated weathering procedures more closely approximate field conditions and allow analysis of change in materials and leachates over time. To evaluate the use of a kinetic test on diverse sulfidic materials, four samples were analyzed using Soxhlet extractors. After each leaching, S remaining in the solid material was calculated by subtracting the amount of S in the leachate from the amount of S in the initial solid sample. Plots of acidity and S remaining in the solid material versus time are shown in Figures 5.10 and 5.11, respectively. Following the initial leaching, three samples – Floyd, Clifton Forge, and Mechanicsville - exhibited exponential decline in remaining sulfur and acid production. The Stafford sample exhibited a linear decline in remaining sulfur, which corresponded to its relatively constant rate of acid production.

Soxhlet potential acidity values were calculated using the total amount of acidity generated by each sample. For Floyd, Clifton Forge, and Mechanicsville these values were equivalent to PPA values (Table 5.10). For Floyd and Mechanicsville, the values were noticeably lower than ABA-TS and slightly lower that ABA-SS. Acid-base accounting data were not available for Clifton Forge. By the final leaching, these three samples were producing low amounts of acidity; therefore, additional leachings would be unlikely to raise the potential acidity values by a significant amount. Replicate Soxhlet values were similar for these three samples. For Stafford, potential acidity based on Soxhlet acid generation exceeded the PPA value, but were lower than ABA values. Furthermore, this sample was still producing high amounts of acidity, which will noticeably increase the potential acidity value. Replicates for Stafford were similar, but more variable than the other three samples. The difference in potential acidity predictions mat be due to underestimation by the PPA method. This sample was just within the appropriate potential acidity range to justify the use of a 1 g sample; however, it is now apparent that a smaller sample may have yielded higher, more accurate, results.

Reaction rates may be compared qualitatively using Figure 5.10. Half-life values, the point at which 50% of the initial sulfur remains in the solid material, in terms of leaching cycle are reported in Table 5.10. The samples from Mechanicsville and Floyd appeared to react more rapidly than Clifton Forge and Stafford. These results may be explained by sulfide mineralogy,

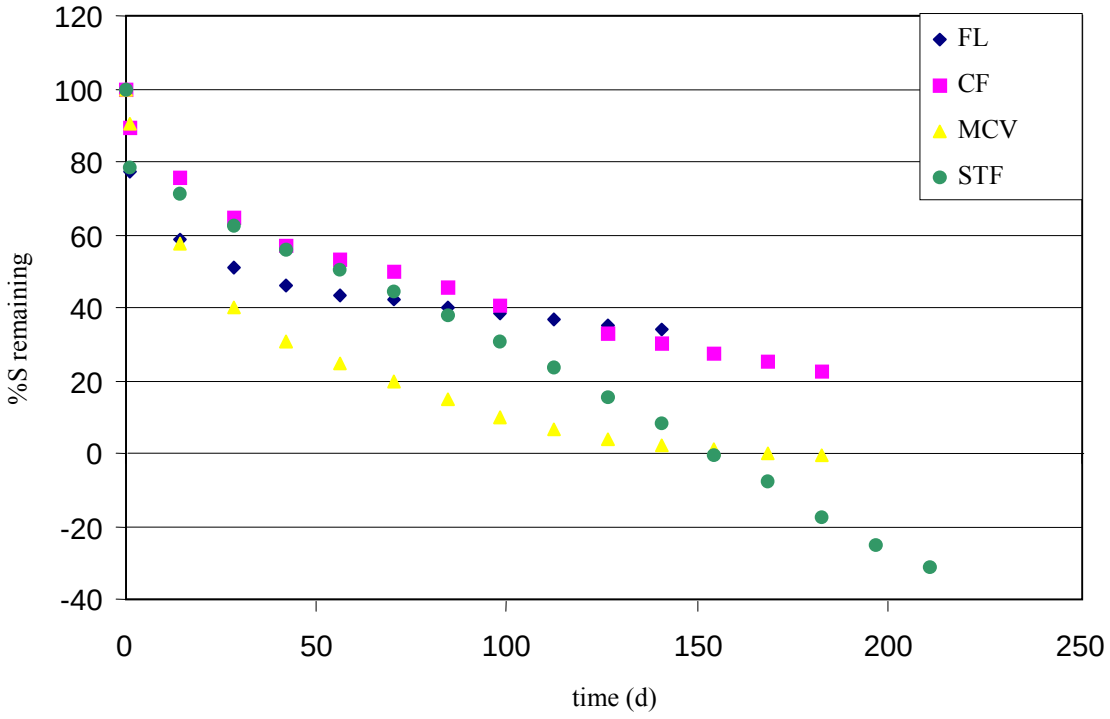

Figure 5.10. Percent S remaining in solid material after sequential Soxhlet runs as estimated by subtracting the amount of S (determined by ICP) in the leachates from the initial amount of total-S (determined using a CNS analyzer).

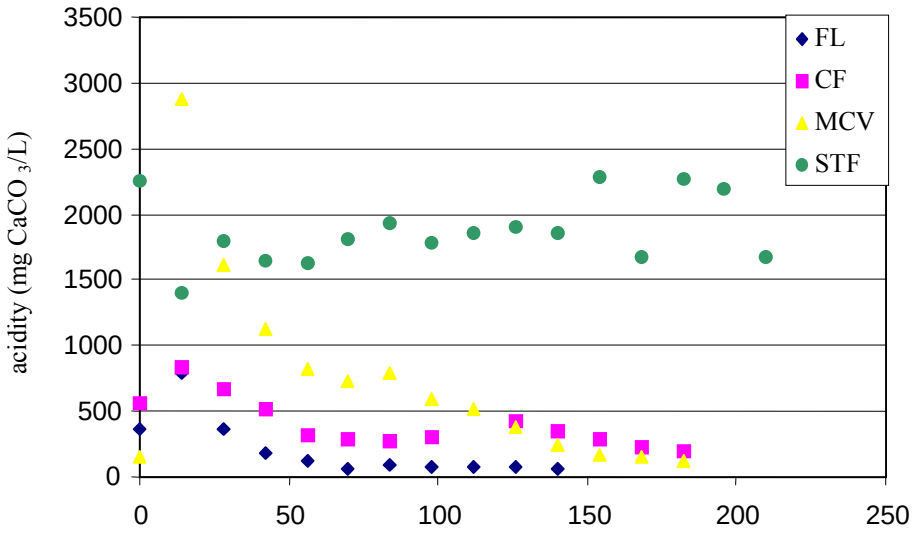

Figure 5.11. Acid production from Soxhlet extractors for sequential runs.

Table 5.10. Potential acidity and half-life for samples analyzed with Soxhlet extractors.

	Total acidity* (3 replicates)			Soxhlet potential acidity** (3 replicates)			PPA**	ABA-TS**	ABA-SS**	$t_{1/2}$†
sample	1	2	3	1	2	3				
Floyd	2247	2262	2190	7.9	7.9	7.7	7.8	24.6	13.9	3
Clifton Forge	4428	5532	5865	15.5	19.3	20.5	19.3	NA	NA	5-6
Mechanicsville	10611	10473	9660	37.1	36.6	33.8	36.8	46	38.42	2-3
Stafford	34342	24603	31476	120	86	110	89.7	128.25	131.74	6-7

* mg $CaCO_3$/L
** Mg $CaCO_3$/1000 Mg material
† t1/2 indicates approximate leaching cycle for which 50% of initial S remains in the solid phase.

morphology, and grain size. The Floyd sample was crushed phyllite containing sulfide primarily in the form of pyrrhotite, which reacts more rapidly than pyrite. The Mechanicsville sample consists of unconsolidated sediments with sulfide primarily in the form of framboidal pyrite, which reacts more rapidly than larger grains. The Clifton Forge sample was crushed shale with sulfide occurring as pyrite in framboids, clusters of microcrystals, and subhedral grains. Although the sulfide grain size was only slightly larger than the Mechanicsville sample, this material should react slower because the overall sample texture is significantly larger which limits exposure of sulfide surfaces to weathering. The Stafford sample consisted of crushed slate with sulfide occurring primarily as subhedral grains, which reacted more slowly than the finer grained sulfides found in the other three samples. Again, since this material consisted of crushed rock, sulfide weathering should be slower than for unconsolidated sediments.

For the Stafford and Mechanicsville samples the %S values appeared to drop below zero, which was likely the result of error in the initial sulfur determinations. The error appeared to be small for Mechanicsville, but significant for Stafford. Two factors account for error in the Stafford sample. First, sulfide distribution in the Stafford sample was highly variable and therefore it was difficult to accurately represent the large samples used in the Soxhlets with the small samples used in S determination. Second, although the technician in charge of the CNS analyzer (housed in the Forestry Department) advised the use of 1 g samples, it has become apparent that at high S levels (i.e. above 3.5%) the CNS analyzer may under-report S for that volume of sample. This is a new instrument and optimal procedures are still being established for the most efficient use of the machine. In future studies, the use of numerous smaller samples obtained from a well-mixed material may improve the accuracy of S estimation.

Comparison of road drainage with Soxhlet leachate

Geologic material at a given road cut may be variable and difficult to accurately represent with laboratory scale samples. Furthermore, many factors aside from rock type affect water quality at a specific location. Therefore, comparisons between leachate from the Soxhlet extractors and road drainage (Table 5.11) from the vicinity of the collection sites are semi-quantitative and intended to represent initial findings rather than definitive conclusions. For Floyd and Clifton Forge, road drainage values were based on three samples collected at the outlet of culverts draining the roadcuts. Samples collected from inside the Clifton Forge culvert were "pure" roadcut drainage and contained exceedingly high values for acidity and metals. To maintain consistency, these samples were eliminated from the analysis because none of the other sites had "pure" leachate collection areas. For Mechanicsville and Stafford, road drainage values were based on five samples.

The highest and lowest acidity values for road drainage samples, along with the average acidity values from the Soxhlet extractors, are illustrated in Figure 5.12. For Clifton Forge, Mechanicsville, and Stafford, average acidity for the Soxhlet extractors was calculated based on acidity values from all leachings. For Floyd, average acidity was based on the first seven leachings, as acidity values were constant for subsequent leachings. Average acidity for road drainage and average acidity from the Soxhlet extractors were highly correlated ($r = 0.98$).

Metal content was compared in a similar manner. For each sample, levels of Fe, Al, Mn, Cu, and Zn were summed to determine total metals (TM) values for each of the first 6 leachings. Since metal values were not available after the first 6 leachings, average TM values could not be calculated in the same manner as average acidity. However, regression analyses indicated significant relationships between TM and acidity for all samples (Table 5.12). Average TM values were predicted using these formulae with the average acidity values for the Soxhlet leachates. Figure 5.13 shows for each sample site the highest and lowest TM values for road drainage, along with average TM values from the Soxhlet extractors. Average TM for the road drainage and average TM from the Soxhlet extractors were highly correlated ($r = 0.98$). These results indicate that strong relationships do appear to exist between water quality from the

Table 5.11. Road drainage data, used for comparison with leachate from Soxhlet extractors, for four acid roadcuts (detailed locations are indicated in Chapter 3).

sample	pH	acidity (mg $CaCO_3$/L)	total metal (mg/L)*
FL4-1(1)	3.73	178	17
FL4-1(2)	2.48	232	34
FL4 1(3)	3.24	184	30
CF2-1	5.28	257	5
CFs1	2.74	318	62
CFs2	7.10	20	0.9
MCV1.1	3.16	226	3
MCV1.2	2.71	350	32
MCV1.3	2.62	336	1
MCV2.1	3.09	416	66
MCV2.2	3.91	258	39
STFn1	2.27	2070	597
STFn2	2.61	990	296
STFn3	2.47	1465	317
STFf1	2.36	1238	139
STFf2	2.70	935	238

*total metal value is sum of Al, Fe, Mn, Cu, and Zn

Table 5.12. Regression formulae to predict total metals (ppm) using acidity. Formulae were determined from first six leachings using Soxhlet extractors for four diverse samples.

sample	Regression formula*	R^2
Floyd	y = 0.18x – 12.4	0.98
Clifton Forge	y = 0.24x – 37.7	0.97
Mechanicsville	y = 0.29x – 27.9	0.98
Stafford	y = 1.36x – 1756	0.74

y = total metals (ppm) and x = acidity (mg $CaCO_3$/L)

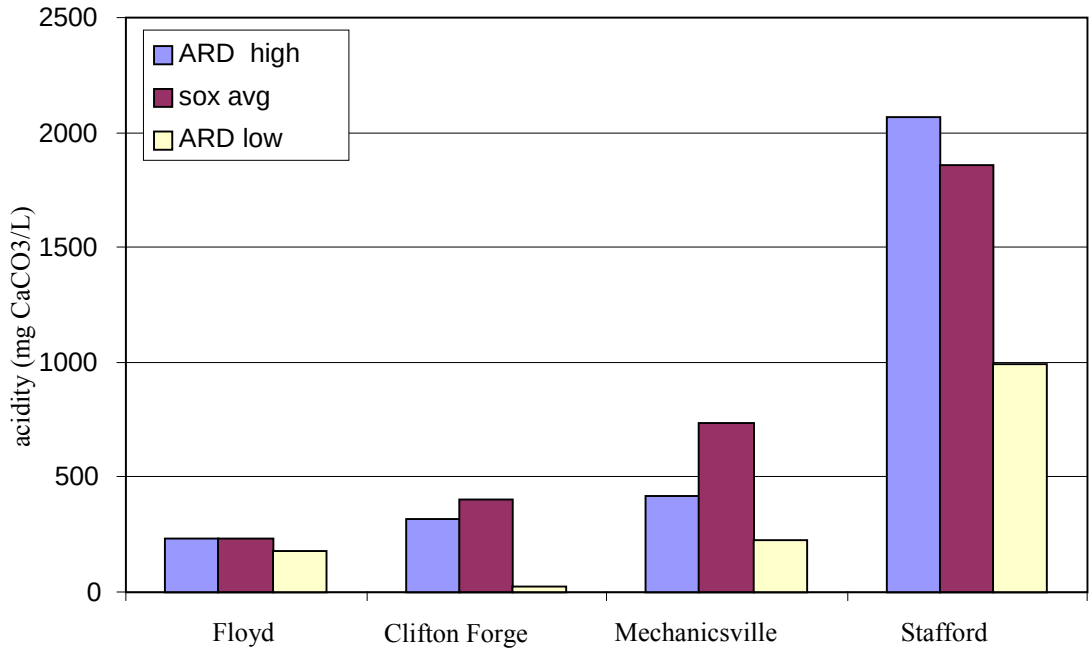

Figure 5.12. Comparison of average acidity from Soxhlet leachate (sox avg) with high and low acidity values from road drainage (ARD high and ARD low).

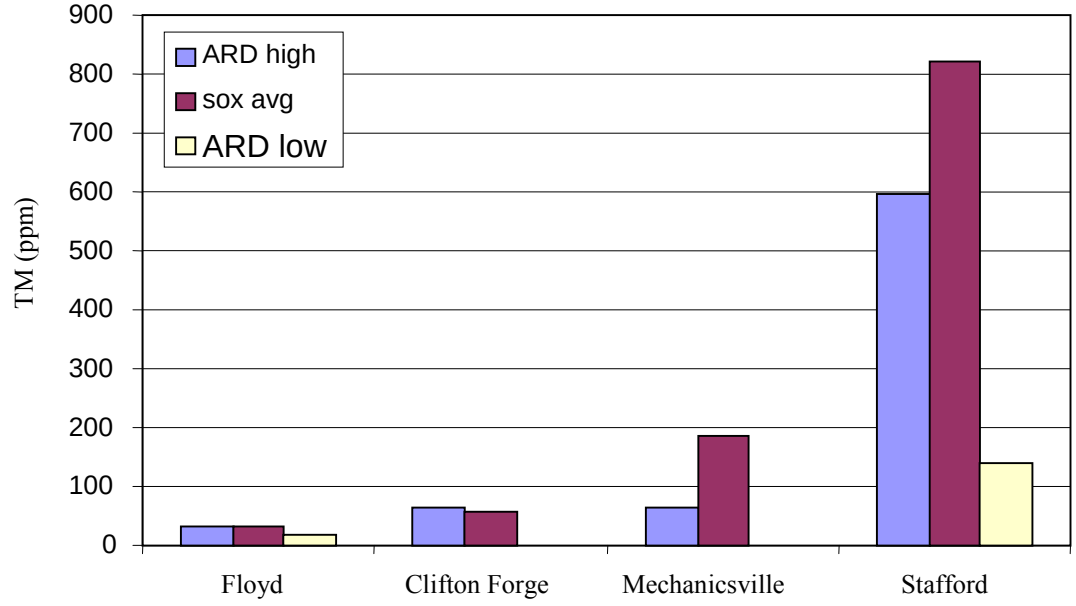

Figure 5.13. Comparison of average total metals (TM) from Soxhlet extractor leachate (sox avg) and high and low total metals values from acid road drainage (ARD high and ARD low).

Soxhlet extractors and from road drainage; however, a more detailed controlled study would need to be conducted to quantify the relationships.

Conclusions

Based on analyses from extensive applications, and comparison with a well documented kinetic test, PPA has proven to be a robust test for assessing potential acidity of diverse sulfidic materials. Appropriate sample size, as specified by the procedure, is critical for obtaining accurate results. In extreme cases, such as the nickel mine tailings that contained over 14% S, additional amounts of H_2O_2 may be necessary as well as smaller sample size. Some PPA methods recommend removal of carbonates prior to analysis. Routine carbonate removal is not recommended as this also may remove acid-producing sulfates and consequently underpredict acidity. If necessary, samples may be screened for carbonates using the "fizz test" and analyzed separately. Analyses comparing S and PPA indicated that S may serve as an adequate screening tool to evaluate materials that do not contain carbonates. Using S is preferable because the analysis is significantly less costly and time-consuming. Further analyses may then be completed only on high-S (> 0.2%) samples.

Results from PPA and ABA were highly correlated, with PPA yielding 0.6 to 0.95 the amount of acidity as predicted by ABA. A few explanations may account for the difference. First, whereas ABA is calculated on the assumption that sulfides will completely react, the PPA procedure appeared to oxidize only about 80% of the sulfides. This may have occurred because the sample size (1 g) was too large for some of the higher-S samples, resulting in under-prediction of PPA. Furthermore, the trace occurrence of other sulfide minerals, such as chalcopyrite and sphalerite, may erroneously increase ABA by overpredicting MPA based on S (using either total-S or sulfide-S); however, these minerals should have little effect on PPA. Third, NP for ABA may have been underestimated due to difficulty with the procedure. Soxhlet potential acidity was equivalent to PPA for three of four samples; however, PPA significantly underpredicted acid generation for the fourth sample, again indicating the importance of adequate sample size in PPA determination. Acidity and metal contents of road drainage were highly correlated with average acidity and metal contents of leachate from the Soxhlet extractors. Although these initial findings are based on a very small number of samples, they do suggest that

Soxhlet extractors may be a useful tool for evaluating long-term road drainage. Further research in this area would be worthwhile.

References

Ammons, J.T., and P.A. Shelton. 1988. A comparison of results from acid-base accounting vesus potential acidity measured by the rapid oxidation of weathered and unweathered soils containing pyrite. In: Mine Drainage and Surface Mine Reclamation Conf. Proc., Vol. 1, Pittsburgh, PA: US Bureau of Mines Information Circular 9183, pp. 206-209. Pittsburgh.

Barnhisel, R. I. and J. Harrison. 1976. Estimating lime requirement by a modified hydrogen peroxide potential acidity method. (Unpublished method for KY Agr. Ex. Sta., Soil Testing Laboratory) Lexington, KY.

Bradham, W. S. and F. T. Caruccio. 1990. A comparative study of tailings analysis using acid/base accounting, cells, columns, and Soxhlets. p. 19-25. *In* Procedings, 1990 Mining and Reclamation Conference and Exhibition, Charleston, WV. Amer. Soc. Surf. Mining and Rec. Lexington, KY.

Canfield, D. E., R. Raiswell, J. Westrich, C. Reaves, and R. Berner. 1986. Chemical Geology. 54:149-155.

Carrucio, F.T. 1968. An evaluation of factors affecting acid mine drainage production and the ground water interactions in selected areas of western Pennsylvania. P. 107-151. *In* Proc., 2nd Symp. Pn Coal Mine Drainage Research. Monroeville, PA. Bituminous Coal Research, Inc. Monroeville.

Carrucio, F. T., J. C. Ferm, J. Horne, G. Geidel, and B. Baganz. Paleoenvironment of coal and its relation to drainage quality. 1977. U.S. E.P.A Cincinatti.

Craig, J. R. and D. J. Vaughan. 1995. Ore microscopy and ore petrology. John Wiley and Sons, Inc., NY.

Finkelman, R. B.1986. Hydrogen peroxide oxidation: an improved method for rapidly assessing acid-generating potential of sediments and sedimentary rocks. Reclamation and Revegetation Research. 5:521-534.

Grube, W. E., Jr., R. M. Smith, R. N. Singh, and A. A. Sobek. 1973. p. 134-152. Characterization of coal overburden materials and minesoils in advance of surface mining. *In* Research and applied technology symposium on mined-land reclamation. Bituminous Coal Research, Inc. Monroeville, PA.

Jennings, S. R., D. J. Dollhopf, and W. P. Inskeep. 1999. Acid production from sulfide minerals using hydrogen peroxide weathering. Applied Geochemistry. 15:235-243.

Kania, T. 1998. Laboratory methods for acid-base accounting: an update. p. 6-1 to 6-9. *In* K. B. C. Brady, M. W. Smith, and J. Schueck (ed.) Coal mine drainage prediction and pollution prevention in Pennsylvania. Dept. of Env. Protection. Harrisburg.

O'Shay, T., L.R. Hossner, and J.B. Dixon. 1990. A modified hydrogen peroxide method for determination of potential acidity in pyritic overburden. J. Environ. Qual. 19:778-782.

Paktunc, A.D. 1999. Mineralogical constraints on the determiniation of neutralization potential and prediction of acid mine drainage. Env. Geo. 39:2:103-112.

Perry, E. F. 1985. Overburden analysis: an evaluation of methods. P. 369-375. *In* 1985 Nat. Symp. on Surface Minnig, Hydrology, Sedimentology, and Reclamation, Univ. KY. Lexington, KY.

Renton, J. J., T. Rymer, and A. H. Stiller. 1988. A laboratory procedure to evaluate acid producing potential of coal associated rocks. Mining Sci. and Tech. 7:227.

Rich, C. I. And R. I. Barnhisel. 1977. Preparation of clay samples for x-ray diffraction analysis. P. 797-808. *In* J. B. Dixon and S. B. Weed (ed.) Minerals in soil environments. Soil Sci. Soc. of Am. Madison, WI.

Skousen, J. G., J. Renton, H. Brown, P. Evans, B. Leavitt, K. Brady, L. Cohen, and P. Ziemkiewicz. 1997. Neutralization potential of overburden samples containing siderite. J. of Env. Qual. 26(673-681).

Sobek, A.A., W.A. Schuller, J.R. Freeman, and R.M. Smith. 1978. Field and laboratory methods applicable to overburden and minespoils. U.S. E.P.A. Report EPA-600/2-78-054.

Sobek, A. A., M. A. Bambenek, and D. Meyer. 1982. Modified Soxhlet exctractor for pedogenic studies. Soil Sci. Soc. Am. J. 46(6): 1340-1342.

Sobek, A.A., L.R. Hossner, D.L. Sorensen, P.J. Sullivan, and D.F. Fransway. 1987. Acid-base potential and sulfur forms. Reclaiming Mine Soils and Overburden in the Western United Stantes. Soil Conservation Society of America, Ankeny, IA. p. 233-258.

Sobek, A.A., J.G. Skousen and S.E. Fisher, Jr.. 2000. Chemical and physical properties of overburdens and minesoils. p. 77-104 *In:* R.I. Barnhisel et al. (Eds.). Reclamation of Drastically Disturbed Lands. American Soc. Agron. Monograph No. 41, Madison WI.

Stewart, B.R. 1995. The influence of fly ash additions on acid mine drainage production from coarse coal refuse. Ph.D. Dissertation. Virginia Polytechnic Institute and State Univ., Blacksburg.

Sullivan, L.A., R.T. Bush, D. McConchie, G. Lancaster, P.G. Haskins, and M.W. Clark. Comparison of peroxide-oxidisable sulfur and chromium-reducible sulfur methods for determination of reduced inorganic sulfur in soil. Aust. J. Soil Res. 37:255-65.

Yoneda, S. 1961. Studies on polder soils in Japan. XVI. Rapid method for determining oxidizable sulfur and change of soil reaction of sea muds and polder soils. Soil Sci. Rep., Faculty Agric. Okayama Univ. 17:39-46.

Zhabina, N.N., and I.I. Volkov. 1978. A method of determination of vaious sulfur compounds in sea sediments and rocks. Environmental Biogeochemistry: Methods, Metals, and Assessment. Vol. 3. 735-745.

Chapter 6

SUMMARY AND CONCLUSIONS

Excavation through sulfidic geologic materials during road construction has resulted in ARD-related problems at numerous discrete locations across Virginia. Failure to establish vegetation on low pH road banks, and acid drainage to surface waters, causes local environmental problems. Degradation of construction materials may necessitate road repairs, which can be time-consuming, costly, and a nuisance to travelers. These problems can be minimized, and even prevented, by incorporating sulfide hazard analysis into the pre-design stage of highway construction. Evaluating the likelihood of encountering sulfidic materials can decrease exposure of problematic materials. When exposure cannot be avoided, proper characterization of the material allows for immediate application of appropriate remediation procedures.

Two studies were conducted to assist VDOT with evaluating the likelihood of encountering sulfidic materials. First, geologic materials from existing acid roadcuts across the state were identified and characterized to develop a state-wide sulfide hazard rating map. Sulfide occurrence is a function of geologic setting. If sulfides are identified in numerous rock samples from a specific geologic formation, then the entire formation may be considered as "at risk" for containing sulfides. On a state-wide scale, delineation of potentially acid materials is best accomplished by identifying the boundaries of sulfide-bearing formations using the Geologic Map of Virginia. Geologic formations associated with acid roadcuts were characterized by PPA and S, and grouped into four categories based on potential acid-producing severity: i) the Tabb Formation in the Coastal Plain (PPA $\leq$ 6 Mg $CaCO_3$/1000 Mg; S $\leq$ 0.2%), ii) the Lynchburg Group of the Ashe Formation in the Blue Ridge (PPA $\leq$ 18; S $\leq$ 2.0%), iii) Chesapeake Group and Lower Tertiary deposits in the Coastal Plain, and Millboro, Marcellus, and Chattanooga shales, and the Needmore Formation in the Valley and Ridge (PPA $\leq$ 60; S $\leq$ 2.6%), and iv) Quantico slate in the Piedmont (PPA $\leq$ 99; S $\leq$ 3.9%). Additional sulfide-bearing formations were identified through a geologic literature review, and were indicated on the map, although the acid-producing severity of these materials has not been evaluated. Where planned highway

corridors intersect the specified formations, detailed geologic sampling should be conducted to identify the presence, extent, and nature of sulfidic materials. Unfortunately, the most troublesome sulfide forms are fine-grained, and as such they are not readily apparent in hand specimens and they often remain undocumented. Therefore, the state-wide sulfide hazard rating map presented in this dissertation may be considered to be the first approximation of a dynamic database that can be amended by future studies. All future road corridors passing through known risk zones should be tested for S with depth and PPA as indicated and appropriate.

The second study was conducted to develop a procedure for evaluating depth to sulfidic sediments in the Coastal Plain. Sulfides appear to be ubiquitous in formations of the Cheasapeake Group and Lower Tertiary deposits, which occur at variable depths throughout the Coastal Plain. A study area near Richmond, Virginia was evaluated using landscape parameters, including elevation, slope, distance to streams, and mapped soil type, and data from well logs to estimate depth to sulfidic sediments. Within the study area a number of variables control depth to reduced sediments, including factors that control the thickness of overlying Quaternary sediments, and weathering processes that control the reducing environment in which sulfides are stable. Due to the complexity of these interacting factors, a model could not be developed for precisely predicting depth to sulfidic sediments based on landscape parameters. However, it was determined that the likelihood of encountering sulfidic sediments within a given depth for a specific location was related to geomorphic surface, which can be represented by elevation, and mapped soil type.

Since excavation in the sulfide depth study area is generally within 9 m from the ground surface, the data were evaluated with respect to this depth. To assign risk factors based on elevation, the data were divided into seven elevation classes. Risk factors were designated based on the proportion of wells with depth-rs < 9 m as follows: i) greater than 50% is a very high risk, ii) 25 - 49% is a high risk, iii) 11 – 24% is a moderate risk, and iv) less than 11% is a low risk. Similarly, to assign soil risk factors, the data were divided by soil map unit. For soil map units with at least five data points, risk factors were assigned based on the proportion of wells with depth-rs < 9 m as follows: i) greater than 25% is a high risk, ii) 11 – 25% is a moderate risk, and iii) less than 11% is a low risk. For soil map units with fewer than five data points, risk factors

were assigned based on mean depth-rs as follows: i) ≤ 9 m is a high risk, ii) 10 to 19 m is a moderate risk, and iii) > 19 m is a low risk. Evaluating the elevation risk factor in conjunction with the soils risk factor successfully predicted whether or not sulfidic sediments would be encountered for 90% of 58 test points. By re-evaluating the well log data, and appropriately re-assigning the elevation and soil risk factors, this process could be repeated for other excavation depths. Furthermore, this method could be applied to evaluate other areas in the Coastal Plain.

Sulfide oxidation reactions occur rapidly to generate acidity within weeks of exposure. The extent of ARD can be minimized by immediate application of remediation procedures, which require proper characterization of potential acidity. The current standard procedure of the SS&MLR Laboratory is PPA. This procedure was developed for overburden analysis for coal mine operations, and it's applicability to other diverse sulfidic materials remained in question. Extensive application of the PPA procedure, in comparison with other potential acidity procedures, indicated that PPA is a robust test for assessing the potential acidity of diverse sulfidic materials. For samples that did not contain carbonates, PPA results were highly correlated to S, indicating that S can be used as a quick, inexpensive screening tool to identify samples requiring further analysis. Samples may be screened for carbonates using the "fizz test". The practice of removing carbonates prior to PPA analysis is not recommended as this procedure also removes jarosite and other sulfates, which may produce noticeable amounts of acidity upon dissolution. In comparison to other potential acidity tests, PPA yielded 0.6 to 0.95 the amount of acidity as ABA for 14 diverse samples, and equivalent amounts of acidity as Soxhlet extraction for 3 out of 4 samples. Differences were greatest for high-S samples (> 3%) and were likely due to the use of a sample size (1 g) that was larger than the recommended amount (0.2 g). Although the procedure recommends beginning with a 5 g sample and sequentially using smaller samples as necessary, the 1 g sample size was appropriate for the majority of samples. Use of a 1 g sample is justified when sulfides are suspected; however, subsequent analysis of a larger or smaller sample may be necessary. Comparison of average acidity and metal contents of leachate from the Soxhlet extractors were highly correlated with average acidity and metal contents of road drainage, indicating that Soxhlet extractors may be a useful tool for evaluating long-term road drainage. However, these results were based on a very small number of samples and further research in this area would be worthwhile.

Sulfidic materials exist in various geologic and geomorphic settings across Virginia. Where sulfidic materials are likely to occur, as indicated by the state-wide sulfide hazard rating map, detailed sampling and characterization of materials can minimize ARD-related problems. Sulfide hazard analysis, including the extent and nature of problematic formations, should be considered an essential step in the pre-design stage of highway construction and other earth-disturbing activities.

Appendix A

Survey form distributed to VDOT district environmental managers to identify possible acid sulfate roadcuts.

Acid Sulfate Materials Inventory Form

Please fill this form out as completely as possiblefor each potential occurrence of acid sulfate geologic/soil conditions on your District. Partially completed forms are "ok" as long as items one through four are fully documented! Thanks for your help.

1a. District: _____ 1b. Person making report: _____

2. Contact's phone number and best time to call: _____

3. Location of possible acid sulfate materials: _____

_____

(Please attach a map of the site which would allow us to find it without you!)

4. Symptoms or evidence that led you to submit this report _____

_____

5. Have you ever specially treated this area? If so, how? Examples would be heavy liming, rip-rap, revegetation mats, replaced guardrails, etc…

_____

_____

6. Geologic formation estimated or mapped (circle one) at this location:

_____

7. What is the date of original and last disturbance or treatment of this area?

Original disturbance: _____ Most recent disturb. or treatment: _____

Please fill out a copy of this form for each site that you identify and return it to:
W. Lee Daniels, Dept. of Crop and Soil Env. Sci., Va Tech, Blacksburg, VA, 24061-0404

Appendix B

Soil profile descriptions from undisturbed material at the top of acid-sulfate roadcuts.

Floyd County

Profile: FL6
Location: Floyd County, rt 750 south end of roadcut
Approximate series classification:
Vegetation: grass, primary succession
Parent material: Alum phyllite
Slope: 25% (shoulder slope)
Aspect: 120^{o} (ESE)
Described by: Zenah Orndorff and Chris Jage

A – 0 to 14 cm; dark grayish brown (10YR4/2) loam; micaceous; 25% rock fragments (weathered phyllite); very strongly acid; diffuse boundary.
AC – 14 to 32 cm; dark grayish brown (10YR4/2) loam; micaceous; 50% rock fragments (weathered phyllite); very strongly acid; abrupt boundary.
C – 32 to 42 cm; dark grayish brown (10YR4/2) sandy loam; micaceous; 70% rock fragments (weathered phyllite); very strongly acid.
Cr – 42 to 62 cm; very dark grayish brown (10YR3/2) sandy loam; few reddish yellow (7.5YR6/8) mottles; micaceous; 80% rock fragments (weathered phyllite); very strongly acid.

Profile: FL7
Location: Floyd County, rt 750, middle of roadcut
Approximate series classification:
Vegetation: grass, primary succession
Parent material: Alum phyllite, residuum
Slope: 5% (ridge top)
Aspect: 100^{o} (ESE)
Described by: Zenah Orndorff and Chris Jage

A – 0 to 8 cm; dark brown (10YR3/3) silt loam; 35% rock fragments (weathered phyllite); extremely acid.
Bw – 8 to 34 cm; brown (10YR4/3) silt loam; 20% rock fragments (weathered phyllite); very strongly acid.
CB – 34 to 47 cm; dark grayish brown (10YR4/2) loam; 30% rock fragments (weathered phyllite); very strongly acid.
C1 – 47 to 62 cm; dark yellow brown (10YR4/4) clay loam; 40% rock fragments (weathered phyllite); very strongly acid.
C2 – 62 to 98 cm; dark grayish brown (10YR4/2) sandy loam; 60% rock fragments (weathered phyllite); strongly acid.

C3 – 98 to 114 cm; dark grayish brown (10YR4/2) sandy loam; 45% rock fragment (weathered phyllite); very strongly acid.
C4 – 114 to 155 cm; very dark grayish brown (2.5Y3/2) sandy loam; 20% rock fragments (weathered phyllite); very strongly acid.

Profile: FL8
Location: Floyd County, rt-750, north end of roadcut
Approximate series classification:
Vegetation: mixed hardwoods and pines
Parent material: Alum phyllite, residuum
Slope: 19%
Aspect:340^{o} (NNW)
Described by: Zenah Orndorff and Chris Jage

A – 0 to 14 cm; dark brown (10YR3/3) silt loam; 15% rock fragments (weathered phyllite); extremely acid.
AB – 14 to 29 cm; dark grayish brown (2.5Y4/2) silt loam; 10% rock fragments (weathered phyllite); extremely acid.
BC – 29 to 40 cm; dark grayish brown (2.5Y4/2) silt loam; 20% rock fragments (weathered phyllite); extremely acid.
Cr – 40 to 43 cm; dark grayish brown (2.5Y4/2) silt loam; 80% rock fragments (weathered phyllite); extremely acid.

Profile: FL21
Location: Floyd County, rt 8 (between rts 750 and 705), northbound lane
Approximate series classification: n.d.
Vegetation: grass
Parent material: Alum phyllite
Slope: 53% (side slope) Aspect: 280^{o}, WNW
Described by: Zenah Orndorff and Chris Jage

A – 0 to 14 cm; dark brown (7.5YR3/4) sandy loam; 30% rock fragments (weathered phyllite); very strongly acid; abrupt boundary.

Cr – 14 - 34 cm; brown (7.5YR4/2) loamy sand; 40% rock fragments (weathered phyllite); medium acid.

Highland County

Profile: HC26
Location: Highland County, rt-250, middle of roadcut.
Approximate series classification:
Vegetation: mixed hardwoods
Parent material: shale residuum/sandstone colluvium
Slope: 44%
Aspect:100^{o} (ESE)
Described by: Zenah Orndorff and Chris Jage

Oi – 8 to 3 cm
Oe – 3 to 0 cm
A – 0 to 2 cm; black (10YR2/1) sandy loam; 20% shale fragments; extremely acid.
Bw – 2 to 12 cm; yellowish brown (10YR5/6) sandy loam; 35% shale fragments; extremely acid.
C – 12 to 28 cm; brownish yellow (10YR6/6) loam; 35% shale fragments; extremely acid.

Profile: HC 27
Location: Highland County, rt-250, about 30 m west of HC26
Approximate series classification:
Vegetation: mixed hardwoods
Parent material: shale residuum and sandstone colluvium
Slope: 40%
Aspect: 120^{o} (SE)
Described by: Zenah Orndorff and Chris Jage

Oa – 2 to 0 cm.
A – 0 to 16 cm; very dark grayish brown (10YR3/2) loamy sand; extremely acid.
BA – 16 to 35 cm; brownish yellow (10YR6/6) sandy loam; 6% shale fragments; extremely acid.
Bw – 35 to 53 cm; olive yellow (2.5Y6/6) loam; 2% shale fragments; extremely acid.
BC – 53 to 65 cm; brownish yellow (10YR6/6) clay loam; 2% shale fragments; extremely acid.
C1 – 65 to 83 cm; red (2.5YR5/8) and brownish yellow (10YR6/6) clay; 2% shale fragments; extremely acid.
C2 – 83 to 107 cm; light reddish gray (2.5YR7/1) and red (2.5YR4/8) silty clay; 10% shale fragments; extremely acid.
C3 – 107 to 120 cm; light reddish gray (2.5YR7/1) and red (2.5YR4/8) silty clay; 5% shale fragments; extremely acid.
C4 – 120 to 140 cm; very dark gray (10YR3/1) and strong brown (7.5YR4/6) loam; 65% shale fragments, very strongly acid.

Profile: HC 28
Location: Highland County, northwest end of outcrop
Approximate series classification:
Vegetation: primary succession shrubs and hardwoods
Parent material: shale residuum and sandstone colluvium
Slope: 65%
Aspect: 140^{o} (ESE)
Described by: Zenah Orndorff and Chris Jage

Oi – 3 to 0 cm.
A – 0 to 5 cm; very dark grayish brown (10YR3/2) sandy loam; 20% shale fragments; extremely acid.
Bt – 5 to 35 cm; yellowish brown (10YR4/4) loam; 30% shale fragments; extremely acid.
C1 – 35 to 52 cm; light yellowish brown (10YR6/4) silt loam; 60% shale fragments; very strongly acid.
C2 – 52 to 66 cm; light yellowish brown (10YR6/4) clay loam; 50% shale fragments; very strongly acid.
C3 – 66 to 99 cm; light yellowish brown (10YR6/4) and light gray (10YR7/1) clay loam; 50% shale fragments; very strongly acid.
C4 – 99 to 115 cm; very dark gray (10YR3/1) and light gray (10YR7/1) clay loam; 75% shale fragments; very strongly acid.

Profile:HC64
Location: Highland County, rt 250, east end of roadcut, east side of first ridge
Approximate series classification: Weikert
Vegetation: mixed hardwoods and pines, some weedy vegetation
Parent material: shale residuum
Slope:58%
Aspect: 110^{o} ((ESE)
Described by: Zenah Orndorff, Phil Cobb, and Brian Jones

A – 0 to 5 cm; very dark grayish brown (10YR3/2) silt loam; moderate fine granular structure; 20% rock fragments, clear smooth boundary.
BA – 5 to 16 cm; dark brown (10YR3/3) silt loam; weak granular structure; 25% rock fragments; clear wavy boundary.
Bw1 – 16 to 30 cm; very dark grayish brown (10YR3/2) silt loam; weak moderate subangular blocky structure; many very pale brown (10YR7/3) silt coatings on rock fragments; 45% fine shale gravel to coarse shale channers; gradual diffuse boundary.
BC – 30 to46 cm; brown (10YR4/3) silt loam; weak coarse subangular blocky structure to massive; many very pale brown (10YR7/3) silt coatings on rock fragments; 60% fine shale gravel to coarse shale channers; gradual wavy boundary.
R – 46 cm; black shale.

Profile:HC65
Location: Highland County, rt 250, east end of roadcut, middle of first ridge
Approximate series classification: Weikert
Vegetation: mixed hardwoods and pines, some weedy vegetation
Parent material: shale residuum
Slope:10% locally, overall 15%
Aspect: 200^{o} (SSW)
Described by: Zenah Orndorff, Phil Cobb, and Brian Jones

O – 2 to 0 cm; pine needles, leaves, twigs.
A – 0 to 4 cm; grayish brown (10YR5/2) silt loam; moderate fine granular struture; 10% fine shale gravel, clear smooth boundary.
EB – 4 to 22 cm; yellowish brown (10YR5/6) silt loam; moderate fine to medium granular structure; very pale brown (10YR7/4) and yellowish brown (10YR5/6) silt coatings and few yellow (10YR7/6) and red (2.5YR3/4) stains on rock fragments; 25% shale fragments; irregular boundary.
R – 22 cm; fractured black shale; very pale brown (10YR7/4) and yellowish brown (10YR5/6) silt coatings on rock fragments

Profile:HC66
Location:Highland County, rt 250, east end of roadcut, west edge of first ridge (sideslope)
Approximate series classification: Berks
Vegetation: mixed hardwoods, some weedy vegetation
Parent material: shale residuum
Slope:24%
Aspect: 270^{o} (W)
Described by: Zenah Orndorff, Phil Cobb, and Brian Jones

A – 0 to 4 cm; very dark grayish brown (10YR3/2) silt loam; moderate fine granular structure; 20% fine shale fragments; clear smooth boundary.
E – 4 to 20 cm; dark yellowish brown (10YR4/4) silt loam; moderate fine granular structure; 10% fine shale fragments; clear wavy boundary.
EB – 20 to 26 cm; dark yellowish brown (10YR4/4) silt loam; weak subangular blocky structure; very pale brown (10YR7/4) silt coatings on rock fragments; 20% shale fragments; clear wavy boundary.
Bw – 36 to 64 cm; dark yellowish brown (10YR4/4) silt loam; common very pale brown (10YR7/3) silt coatings and common gray (10YR6/1) redoximorphic features on rock fragments; 35% shale fragments; gradual wavy boundary
CB – 64 to 82 cm; dark brown (10YR3/3) silt loam; few very pale brown (10YR7/3) silt coatings and common gray (10YR6/1) redoximorphic features on rock fragments; 40% shale fragments, diffuse irregular boundary.
Cr – 82 to 112 cm; fractured black shale; few very pale brown (10YR7/3) silt coatings, common gray (10YR6/1) redoximorphic features, and yellow (10YR7/6) staining on rocks fragments.

Profile: HC67
Location: Highland County, rt 250, east end of roadcut, west edge of first ridge
Approximate series classification:
Vegetation: mixed hardwoods
Parent material: shale residuum
Slope: 28% (toeslope)
Aspect: 220^{o}
Described by: Zenah Orndorff, Phil Cobb, and Brian Jones

A – 0 to 6 cm; very dark grayish brown (10YR3/2) silt loam; 10% shale fragments; clear smooth boundary.
BE – 6 to 19 cm; very dark grayish brown (10YR3/2) silt loam; very pale brown (10YR7/3) silt coatings on rock fragments; 25% shale fragments; gradual wavy boundary.
Cr – 19 to 40 cm; fractured shale; very pale brown (10YR7/3) silt coatings on rock fragments.

Profile: HC68
Location: Highland County; rt 250, drainage way past west side of eastern ridge
Approximate series classification: Ross
Vegetation: dense hydrophilic plants
Parent material: shale residuum
Slope: 5%
Aspect: 160^{o} (SSE)
Described by: Zenah Orndorff, Phil Cobb, and Brian Jones

Ap – 0 to 7 cm; very dark grayish brown (10YR3/2) silt loam; weak subangular blocky structure parting to moderate granular structure; clear smooth boundary.
Btg1 – 7 to 22 cm; dark gray (10YR4/1) and dark yellowish brown (10YR3/6) silty clay loam; moderate subangular blocky structure; few black (10YR2/1) Mn stains on rock fragments; 15% sandstone gravels and cobbles.
Btg2 – 22 to 74 cm; dark gray (10YR4/1) and dark yellowish brown (10YR3/6) silty clay; weak subangular blocky structure; few black (10YR2/1) Mn stains on rock fragments; 15% sandstone gravels and cobbles.

Profile: HC69
Location: Highland County; eastern edge of middle ridge (side slope)
Approximate series classification: Weikert
Vegetation: mixed hardwoods
Parent material: shale residuum
Slope: 63%
Aspect: 80^{o} (E)
Described by: Zenah Orndorff, Phil Cobb, and Brian Jones

A – 0 to 6 cm; brown (10YR4/3) silt loam; moderate granular structure; 5% shale fragments; clear smooth boundary.
Bw – 6 to 21 cm; dark brown (10YR3/3) silt loam; weak subangular blocky rock controlled structure; gradual wavy boundary.
Cr – 21 to 25 cm; dark brown (10YR3/3); thin (< 1 mm) white calcite veins evident in shale fragements; clear irregular boundary.
R – 25 cm; shale

Profile: HC71
Location: Highland County; eastern edge of middle ridge (shoulder slope)
Approximate series classification: Gilpin
Vegetation: mixed hardwoods
Parent material: shale residuum
Slope: 36%
Aspect: 120^{o} (E)
Described by: Zenah Orndorff, Phil Cobb, and Brian Jones

A – 0 to 4 cm; brown (10YR4/3) silt loam; moderate granular structure; 10% fine shale fragements; clear smooth boundary.
EB – 4 to17 cm; yellowish brown (10YR5/4) silt loam; weak granular to subangular blocky structure; 5% fine shale fragments; clear smooth boundary.
Bt1 – 17 to 35 cm; yellowish brown (10YR5/6) silt clay loam; weak subangular blocky structure; 10% fine shale fragements; clear wavy boundary.
Bt2 – 35 to 53 cm; dark yellowish brown (10YR4/6) silty clay loam; weak subangular blocky structure; common pale brown (10YR6/3) silt coatings on rock fragments; 10% shale fragments; clear wavy boundary.
BCt – 53 to 64 cm; dark yellowish brown (10YR4/6) silty clay loam; massive structure; few very pale brown (10YR7/3) silt coatings on rock faces; 25% shale fragments; gradual irregular boundary.
Cr – 64 to 98 cm; dark yellowish brown (10YR4/6); few very pale brown (10YR7/3) silt coatings on rock faces.
R – 98 cm; shale.

Profile: HC72
Location: Highland County; middle of middle ridge (narrow rounded ridgetop)
Approximate series classification: Gilpin
Vegetation: mixed hardwoods
Parent material: shale residuum
Slope: 2%
Aspect: ---
Described by: Zenah Orndorff, Phil Cobb, and Brian Jones

O – 2 to 0 cm; pine needles, leaves.
BE – 0 to 12 cm; dark yellowish brown (10YR4/4) loam; weak subangular blocky structure; 2 to 10% fine shale gravel.
Bt1 – 12 to 26 cm; dark reddish brown (5YR3/3) and dark yellowish brown (10YR4/6) silty clay loam; moderate subangular blocky structure; 2 to 10% fine shale gravel.
Bt2 – 26 to 57 cm; dark yellowish brown (10YR4/4), strong brown (7.5YR5/6), and brownish yellow (10YR6/6) silty clay loam; moderate subangular blocky structure; 2 to 10% shale fragments.
BCt – 57 to 70 cm; dark yellowish brown (10YR4/4) and strong brown (7.5YR5/6) clay loam; weak subangular blocky structure; 5 to 10% shale fragments.
BC – 70 to 85 cm; dark yellowish brown (10YR4/4) and strong brown (7.5YR5/6) loam; weak subangular blocky structure; 20% fine shale gravel.
Cr1 – 85 to 96 cm; yellowish red (10YR4/6), strong brown (10YR4/6), and few black (5YR2.5/1) shale fragments.
Cr2 – 96 to 106 cm; black (5YR2.5/1) shale fragments.
Cr3 – 106 to 135 cm; dark yellowish brown (10YR5/6) shale fragments.

Hanover County

Profile: MCV7
Location: Hanover County, bw. cloverleaf of 360W to 295S and exit ramp from 295S to 360W (south end of cloverleaf)
Approximate series classification: Kenansville
Vegetation: mixed hardwoods, blackberries
Parent material: Pleistocene sand and gravel overlying Eastover formation
Slope: 20%
Aspect: 355^{o} (NW)
Described by: Zenah Orndorff and Bob Hodges

Ap – 0 to 35 cm; yellowish red (5YR5/6) sandy loam.
Bt – 35 to 98 cm; yellowish red (5YR5/8) sandy loam.
BC – 98 to 141 cm; strong brown (7.5YR5/6) sandy loam; 2% quartz pebbles.
C1 – 141 to 190 cm; reddish yellow (7.5R6/6) sandy loam; 2% quartz pebbles.
C2 – 190 to 237 cm; brownish yellow (10YR6/6) loamy sand.
C3 – 237 to 310 cm; pale yellow (5Y8/3) samd.
C4 – 310 to 360 cm; strong brown (7.5YR5/6) sandy loam; 2% quartz pebbles.
C5 – 360 to 386 cm; pale yellow (5Y8/2) loamy sand.
C6 – 386 to 474 cm; yellow (2.5Y7/6) and olive yellow (2.5Y6/6) loamy sand.
C7 – 484 to 506 cm; strong brown (7.5YR5/6) and dark brown (7.5YR4/4) sandy loam; 15% quartz gravel. Auger refusal at 506 cm likely due to ironstone overlying Eastover.

Profile: MCV8
Location: Hanover County, bw. cloverleaf of 360W to 295S and exit ramp from 295S to 360W (north end of cloverleaf)
Approximate series classification:
Vegetation: pines
Parent material: Pleistocene sand and gravel overlying Eastover formation
Slope: 10%
Aspect: 200^{o} (SW)
Described by: Zenah Orndorff and Bob Hodges

Fill – 0 to 60 cm.
Bt – 60 to 70 cm; strong brown (7.5YR5/8) clay loam.
BC1 – 70 to 102 cm; red (2.5YR4/8) and light reddish brown (2.5Y7/3) silty clay loam.
BC2 – 102 to 136 cm; pale red (2.5Y7/2), light red (7.5YR6/8), and red (2.5YR4/6) clay.
BCg – 136 to 188 cm; strong brown (7.5YR5/8) and pale yellow (2.5Y8/3) silty clay loam.
CBg – 188 to 239 cm; light gray (5Y7/2) silty clay loam; dark red (10R3/6) coatings on ped faces.
C1 – 239 to 286 cm; light gray (5Y7/2) and strong brown (7.5YR5/8) silty clay loam.
C1g – 286 to 330 cm; pale olive (5Y6/3) loam.
C2 – 330 to 356 cm; light gray (5Y7/2) and strong brown (7.5YR5/8) loam.
C3 – 356 to 390 cm; light brownish gray (10YR6/2) and strong brown (7.5YR5/8) loam; Ultra acid.
C2g(1) – 390 to 510 cm; light brownish gray (10YR6/2) loam; Ultra acid. (PPA ~ 36 Mg $CaCO_3$/1000 tons)

Profile: MCV10
Location: Hanover County, off shoulder of exit ramp from 295S to 360W.
Approximate series classification:
Vegetation: pines and mixed hardwoods
Parent material: Pleistocene sand and gravel overlying Eastover formation
Slope: 7%
Aspect: 334^{o} (NNW)
Described by: Zenah Orndorff, Steve Nagle, and Ronnie Alls

Ap – 0 to 14 cm; yellowish brown (10YR5/6) sandy loam.
E – 14 to 64 cm; brownish yellow (10YR6/6) loamy sand.
Bt1 – 64 to 80 cm; strong brown (7.5YR5/6) sandy clay loam; 20% quartz gravel.
Bt2 – 80 to 322 cm; strong brown (7.5YR5/8) and pale yellow (2.5Y7/3) silty clay loam.
BCg – 322 to 386 cm; pale yellow (2.5Y7/3) and reddish yellow (7.5YR6/8) loam.
Cg(1) – 386 to 609 cm; dark greenish gray (5GY4/1) loam. Ultra acid. (PPA ~ 36 Mg $CaCO_3$/1000 tons).

Appendix C

Elemental analysis of fourteen diverse sulfidic samples from Virginia and Brazil used for procedures comparison (Chapter 5).

	Au	Pd	Pt	Na2O	MgO	Al2O3	SiO2	P2O5	K2O	CaO	TiO2	MnO	Fe2O3	Rb	Sr	Y	Zr	Nb	Ba	LOI	Sum
Scheme Code	MEXFA*			MEXXRF**																	
Analysis Unit	ppb			%										ppm						%	
Detection Limit	5	1	10	0.01	0.01	0.01	0.01	0.01	0.01	0.01	0.001	0.01	0.01	2	2	2	2	2	20	0.01	0.01
Sample																					
stf4	7	15	<10	0.17	0.9	15.7	57.3	0.24	3.65	0.53	0.902	0.23	11.4	160	106	38	212	19	662	8.9	100.1
stf1	49	<1	<10	0.29	1.73	17.5	58.5	0.19	3.95	0.18	0.974	0.03	8.93	191	42	34	215	19	786	7.75	100.1
gas32	8	<1	<10	0.18	2.27	7.87	64.9	0.14	4	1.33	0.695	0.03	13	140	109	26	617	14	195	5.9	100.5
gas16	14	<1	<10	0.52	0.98	11.4	73.7	0.11	2.11	0.29	0.894	0.02	4.77	120	73	39	566	18	320	5.25	100.2
fl 9	15	11	<10	1.87	2.79	18.4	54.9	0.43	3.74	3.08	0.584	0.22	7.21	150	135	39	130	19	822	5.5	98.9
fl 19	12	<1	<10	1.55	2.02	23.7	55.1	0.18	3.36	0.7	0.853	0.22	6.76	126	148	36	195	20	692	5.9	100.5
mcv6-16	8	<1	<10	0.84	1.67	13.8	67.9	0.09	2.84	1	0.942	0.03	6.01	141	132	35	429	18	475	5.3	100.5
mcv6-28	5	<1	<10	0.61	1.71	12.2	70.1	0.11	2.4	1	0.983	0.02	5.56	129	122	34	602	19	389	5.25	100.2
fc4	7	25	11	0.54	1.29	16.4	63.7	0.06	3.43	0.1	0.881	0.02	5.94	162	92	35	184	16	1300	7.6	100.2
wc4	5	19	<10	0.39	1.13	19.1	59.2	0.05	4.25	0.12	0.852	<0.01	4.93	228	84	34	180	19	595	10.3	100.4
ni	47	296	488	<0.01	13	1.32	22.4	0.04	0.1	0.9	0.192	0.17	41.4	5	6	6	20	<2	<20	11.5	91.6
bass	7	<1	<10	0.11	0.43	16.6	64	0.02	0.82	0.13	0.805	0.01	4.86	51	28	22	368	19	248	12.3	100.2
gold	24	<1	<10	0.15	1.25	19.1	60.2	0.02	5.46	0.08	1.107	0.07	6.75	190	33	35	269	18	713	5.95	100.3
mcv5-4	<5	15	26	1.04	1.21	11	73.7	0.04	2.38	1.08	1.004	0.03	4.71	109	144	31	755	17	516	3.8	100.2
DUP-1	<5	<1	10	0.17	0.9	15.7	57.4	0.24	3.67	0.53	0.903	0.23	11.4	160	105	37	211	19	662	8.8	100.1
DUP-13	20	<1	<10	0.15	1.25	19	60.1	0.02	5.46	0.08	1.104	0.07	6.71	192	32	34	268	18	712	6.05	100.2

*MEXFA = NiS fire assay (analysis with inductively coupled plasma mass spectrometry)
**MEXXRF = x-ray fluorescence spectrometry

	Sn	Be	B	V	Co	Ni	Cu	Zn	Ge	Mo	Ag	Cd	Pb	Bi	S
Scheme Code	MEXXRP†	MEXICP‡													MEXLEC§
Analysis Unit	ppm	ppm													%
Detection Limit	2	0.5	10	10	1	1	0.5	0.5	10	1	0.2	1	2	5	0.01
Sample															
stf4	5	3.8	112	143	31	81	39.2	133	<10	6	<0.2	<1	25	10	3.71
stf1	4	2.6	112	168	13	16	13.5	92.3	<10	10	<0.2	<1	25	10	0.77
gas32	3	2.7	213	144	7	22	1.8	65.8	<10	10	0.4	<1	9	<5	2.2
gas16	3	1.7	90	108	14	29	9.9	86.4	21	3	<0.2	<1	11	16	1.56
fl 9	4	4.1	<10	63	10	14	35.2	195	<10	<1	<0.2	<1	34	9	1.58
fl 19	4	4.4	74	94	10	15	11.5	158	<10	<1	<0.2	<1	34	<5	0.18
mcv6-16	4	2.2	93	116	14	28	14	91	<10	5	0.3	<1	18	<5	1.49
mcv6-28	4	2	84	112	8	28	12.7	91.5	11	7	0.2	<1	13	<5	1.49
fc4	6	3.3	157	321	28	108	58.3	61.3	<10	27	<0.2	<1	36	9	2.44
wc4	5	3.3	153	775	14	97	69.1	324	<10	55	1	7	34	7	2.28
ni	6	6.7	15	83	753	42560	4960	158	<10	2	1.1	<1	17	<5	15.2
bass	3	1.5	<10	91	20	125	31	62.6	<10	<1	0.8	<1	24	13	2.31
gold	5	3.6	70	141	13	37	27.5	134	<10	<1	<0.2	<1	13	<5	0.57
mcv5-4	4	1.7	61	93	10	30	10.9	72.4	<10	<1	0.4	<1	13	7	1.24
DUP-1	6	3.6	93	142	30	79	38.1	132	<10	6	<0.2	<1	23	9	3.77
DUP-13	4	3.8	71	137	12	36	26.1	139	<10	<1	<0.2	<1	14	<5	0.57

† MEXXRP = x-ray flourescence
‡ MEXICP = inductively coupled plasma mass spectrometry
§ MEXLEC = Leco combustion

	Sc	Cr	As	Se	Br	Sb	Cs	La	Ce	Nd	Sm	Eu	Tb	Yb	Lu	Hf	Ta	W	Th	U	Sc
Scheme Code	MEXNA***																				
Analysis Unit	ppm																				
Detection Limit	1	2	1	3	1	0.2	1	0.5	3	5	0.1	0.2	0.5	0.2	0.05	1	1	3	0.5	0.5	1
Sample																					
stf4	15	82	4	<3	<1	0.3	16	51.9	103	17	9.2	1.9	1.7	4.1	0.57	7	<1	8	14.7	5.1	15
stf1	18	97	19	<3	<1	<0.2	6	42.2	90	29	7.5	1.7	0.9	4.2	0.49	6	<1	5	8.3	2.9	18
gas32	9	146	17	5	2	0.3	3	45.4	123	50	9.4	0.9	1.3	3.2	0.41	15	2	<3	14.2	5	9
gas16	10	69	11	<3	3	0.6	6	38.4	97	44	10.2	1.6	0.9	3.5	0.41	12	2	3	10.9	3	10
fl 9	15	34	<1	<3	<1	<0.2	4	50.4	113	83	9.7	0.9	1.5	4.3	0.44	4	1	<3	8.3	0.6	15
fl 19	18	44	<1	4	<1	0.4	5	71.8	157	42	12.2	2.2	1	5.5	0.62	5	<1	3	16.7	4.3	18
mcv6<16	12	78	10	<3	4	0.5	5	38.7	89	31	7.4	1	1.9	3	0.39	9	1	3	10.2	5.9	12
mcv6<28	11	52	13	3	5	0.7	4	39.6	104	25	7.3	1	0.5	3.1	0.34	12	2	<3	10.9	5.5	11
fc4	16	77	21	<3	<1	4.1	11	38	76	40	6.4	1.1	0.7	3.6	0.48	4	2	<3	11.5	5.7	16
wc4	16	91	35	<3	2	9	16	41.2	79	23	6.7	1	1.7	3.4	0.46	5	<1	3	12.5	11.8	16
ni	6	4000	16	6	<1	0.4	<1	2.5	24	8	0.5	<0.2	2.1	0.6	0.05	1	<1	<3	<0.5	<0.5	6
bass	11	67	8	4	4	0.2	<1	36.5	97	5	6.1	1.7	1.3	2.3	0.34	10	<1	3	18.1	3.5	11
gold	18	94	630	<3	4	0.5	6	53.7	120	38	8.5	0.9	1.6	4.2	0.54	6	<1	8	16.7	5.7	18
mcv5<4	11	77	11	4	3	0.2	2	38.6	83	15	7.6	0.6	0.7	2.9	0.34	17	2	5	10.6	4	11
DUP<1	16	78	4	<3	<1	0.3	17	52.1	100	13	9.8	1.8	1.7	4.4	0.59	7	<1	9	14.8	5.8	16

***MEXNA = neutron activation analysis

VITA

Zenah Wilson Orndorff

An experiment in hybridization, I was born October 30, 1968 to a globetrotting engineer, Ken Wilson, and his Lebanese wife, Odette Sifri Wilson. After attending public school through the 9th grade, I transferred to the illustrious Baldwin School for young ladies – their efforts were of questionable success. Making a break for the big city, I attended the Johns Hopkins University, in scenic downtown Baltimore, under the protective wing of my big brother Dwight. Attempting to become the first person to major in every possible subject, a month before graduation I finally settled on Natural Sciences with a minor in Writing Seminars. During this time I met my future husband, Wil Orndorff, and discovered the joys of crawling around dark, muddy holes in the ground. The summer after graduation I worked as an intern at the Smithsonian Environmental Research Center – an idyllic Chesapeake resort funded by taxpayers' money. After a grueling summer of hiking, canoeing, and constructing displays, I began work as a science teacher at the Sandy Spring Friends School in Sandy Spring, Maryland. Weekdays were spent teaching, developing educational materials, and sorting out the love lives of middle schoolers. Weekends were spent rambling about the central Appalachians, caving and hiking. During the summer of 1991 I attended a Virginia geology field course for earth science teachers run through Radford University. Those four weeks convinced me that I needed to come to Blacksburg. In 1992, Wil and I married and we both started graduate programs at Virginia Tech. Nine years, two children, and two degrees later we have no intention of leaving.